

AD-A048 230

AEROSPACE CORP EL SEGUNDO CALIF CHEMISTRY AND PHYSICS LAB F/G 20/7  
REACTIVE SINGLE COLLISION STUDIES WITH METAL ATOMS OR METAL HAL--ETC(U)  
NOV 77 R R HERM F04701-77-C-0078

UNCLASSIFIED

TR-0078(3970-10)-2

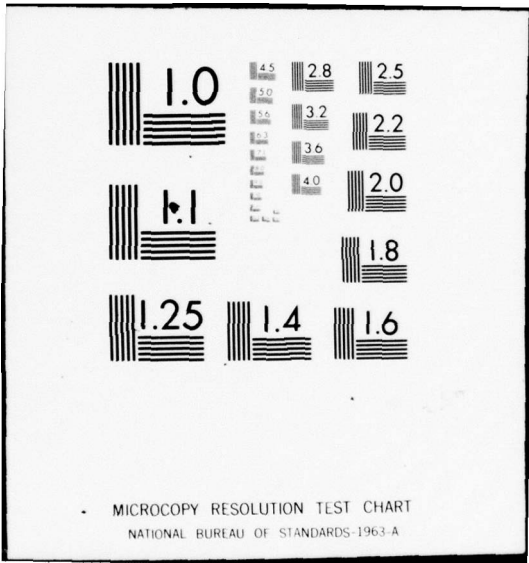
SAMSO-TR-77-209

NL

1 of 2

ADA048 230







13

AD A 0 4 8 2 3 0

# Reactive Single Collision Studies with Metal Atoms or Metal Halides

Chemistry and Physics Laboratory  
The Ivan A. Getting Laboratories  
The Aerospace Corporation  
El Segundo, Calif. 90245

14 November 1977

Interim Report

DDC  
RECEIVED  
DEC 28 1977  
F


Prepared for  
SPACE AND MISSILE SYSTEMS ORGANIZATION  
AIR FORCE SYSTEMS COMMAND  
Los Angeles Air Force Station  
P.O. Box 92960, Worldway Postal Center  
Los Angeles, Calif. 90009

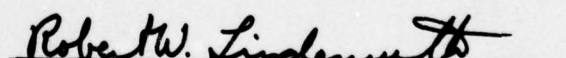
AD No. \_\_\_\_\_  
DDC FILE COPY

This interim report was submitted by The Aerospace Corporation, El Segundo, CA 90245, under Contract No. F04701-77-C-0078 with the Space and Missile Systems Organization, Deputy for Advanced Space Programs, P. O. Box 92960, Worldway Postal Center, Los Angeles, CA 90009. It was reviewed and approved for The Aerospace Corporation by S. Siegel, Director, Chemistry and Physics Laboratory. Lieutenant A. G. Fernandez, SAMSO/YCPT, was the project officer for Advanced Space Programs.


This report has been reviewed by the Information Office (OI) and is releasable to the National Technical Information Service (NTIS). At NTIS, it will be available to the general public, including foreign nations.

This technical report has been reviewed and is approved for publication. Publication of this report does not constitute Air Force Approval of the report's findings or conclusions. It is published only for the exchange and stimulation of ideas.

  
A. G. Fernandez, 1st Lt, USAF  
Project Officer

  
Robert W. Lindemuth, Lt Col, USAF

FOR THE COMMANDER

  
LEONARD E. BALTZELL, Col, USAF  
Asst. Deputy for Advanced  
Space Programs

18 19 REPORT DOCUMENTATION PAGE		READ INSTRUCTIONS BEFORE COMPLETING FORM	
1. REPORT NUMBER	2. GOVT ACCESSION NO.	3. RECIPIENT'S CATALOG NUMBER	
SAMSO-TR-77-209 ✓			
4. TITLE (and Subtitle)		5. TYPE OF REPORT & PERIOD COVERED	
REACTIVE SINGLE COLLISION STUDIES WITH METAL ATOMS OR METAL HALIDES.		Interim rept. ✓	
7. AUTHOR(s)		6. PERFORMING ORG. REPORT NUMBER	8. CONTRACT OR GRANT NUMBER(s)
Ronald R./Herm		TR-0078(3970-10)-2 ✓	F04701-77-C-0078 new
9. PERFORMING ORGANIZATION NAME AND ADDRESS		10. PROGRAM ELEMENT, PROJECT, TASK AREA & WORK UNIT NUMBERS	
The Aerospace Corporation El Segundo, Calif. 90245 ✓			
11. CONTROLLING OFFICE NAME AND ADDRESS		12. REPORT DATE	
Space and Missile Systems Organization Air Force Systems Command Los Angeles, Calif. 90009 ✓		14 Nov 1977	
14. MONITORING AGENCY NAME & ADDRESS (if different from Controlling Office)		13. NUMBER OF PAGES	15. SECURITY CLASS. (of this report)
		117	Unclassified
16. DISTRIBUTION STATEMENT (of this Report)		15a. DECLASSIFICATION/DOWNGRADING SCHEDULE	
Approved for public release; distribution unlimited			
17. DISTRIBUTION STATEMENT (of the abstract entered in Block 20, if different from Report)		DDC RECEIVED DEC 28 1977 F	
18. SUPPLEMENTARY NOTES			
19. KEY WORDS (Continue on reverse side if necessary and identify by block number)		409 383	
Alkali Atoms Alkali Halides Metal Atoms Reactive Scattering Molecular Beams			
20. ABSTRACT (Continue on reverse side if necessary and identify by block number)			
Molecular beam studies at low energy (typically $\leq 100$ kJ/mole) of reactive scattering of metal atoms, metal dimers, or metal halides from a variety of halide molecules are reviewed. Studies of vibrationally inelastic scattering of alkali halides are also reviewed.			



## PREFACE

I was fortunate to enter this field practically from its conception as a graduate student under Prof. D. R. Herschbach. I was equally fortunate to participate in it to its present stage of maturity because of the dedication of an excellent group of graduate students who studied under me at the University of California at Berkeley and Iowa State University: D. D. Parrish, S. M. Lin, C. A. Mims, B. L. Earl, L. C.-H. Loh, L. A. Gundel, C. M. Shollen, R. Behrens, Jr., A. Freedman, and T. P. Parr. I am also indebted to the USAEC and later USERDA for support of this work over a ten year period.

ACCESSION	
NTIS	<input checked="" type="checkbox"/>
DDC	<input type="checkbox"/>
UNIMPROVED	<input type="checkbox"/>
DISTRIBUTION/AVAILABILITY CODES	
/or SPECIAL	
A	

## CONTENTS

PREFACE . . . . .	1
I. Introduction . . . . .	9
II. The Molecular Beam Approach . . . . .	13
II.A. Beam Sources . . . . .	14
II.B. Detection of Scattered Species . . . . .	16
III. The Variety of Reactive Scattering Measurements . . . . .	23
III.A. Product Recoil Angle and Energy Distributions . . . . .	23
III.B. Dependence upon Reactant Quantum States . . . . .	35
III.C. Dependence upon Product Quantum States . . . . .	41
IV. Results for Different Chemical Systems . . . . .	45
IV.A. Scattering of Alkali Halide Molecules . . . . .	46
IV.B. Reactive Scattering of Alkali Atoms . . . . .	55
IV.C. Alkali Dimer plus Various Halides . . . . .	71
V. Closing Remarks . . . . .	64
REFERENCES . . . . .	79

PRECEDING PAGE BLANK-NOT FILMED

## FIGURES

1.	Schematic diagram of a product magnetic deflection slotted disk velocity analysis apparatus (viewed from above) used to study reactions of Li atoms with halogen-containing compounds . . . . .	115
2.	LAB $\leftrightarrow$ CM coordinate systems velocity vector transformation diagram for the collision of A and B to give C and D . . . . .	116
3.	LAB angular distributions measured by surface ionization with a sensitized filament (K + KBr) and desensitized filament (K) for the scattering of K from HBr . . . . .	117
4.	The upper panel shows three sets (i.e., dash, solid, and dot-dash curves) of collision-energy-independent product recoil angle and energy CM distributions which fit (solid curve) the measured LAB Bal product angular distribution data points from the Ba + CH <sub>3</sub> I reaction . . . . .	118
5.	CM polar contour map of $\partial^3 \sigma / \partial^2 \omega \partial w$ (assumed energy independent) for scattering for KI from crossed beams of K and I <sub>2</sub> . . . . .	119
6.	Contours show plots of constant LiO ( $X^2\Pi$ ) product flux in the LAB coordinate system from the Li + NO <sub>2</sub> reaction . . . . .	120
7.	Different curves show P(E') functions obtained by fitting different $\partial^3 \sigma / \partial^2 \omega \partial w$ expansion functions to LiX product LAB recoil velocity spectra measurements for the Li + CH <sub>3</sub> NO <sub>2</sub> , CCl <sub>4</sub> , and CH <sub>3</sub> I reactions . . . . .	121
8.	LAB angular distributions (normalized to unit peak heights) of reactively scattered KI or KCl for reactions of K with orientated (a) CH <sub>3</sub> I, (b) t-BuI, (c) CHCl <sub>3</sub> , and (d) CF <sub>3</sub> I. . . . .	122
9.	The open circles show measured non-reactive scattering of K from CCl <sub>4</sub> transformed into the CM system . . . . .	123
10.	Alkali iodide CM product recoil momentum distributions normalized to the same peak heights . . . . .	124
11.	Schematic depiction of a possible "double rebound" mechanism to account for forward KI scattering in the K <sub>2</sub> + CH <sub>3</sub> I reaction . . . . .	125

## TABLES

I.	Abbreviations of Different Experimental Techniques . . . . .	95
II.	Vibrationally Inelastic Collisions of Alkali Halides . . . . .	97
III.	Reactive Scattering of Alkali Halides . . . . .	98
IV.	Metal Atoms plus Halogen Molecules . . . . .	100
V.	Metal Atoms plus Organic Halides . . . . .	103
VI.	Metal Atoms plus Inorganic Polyhalides . . . . .	107
VII.	Metal Atoms plus Hydrogen Halides . . . . .	109
VIII.	Alkali Dimers plus various Halides . . . . .	111
IX.	Non-alkali Metals plus Various Oxides . . . . .	113
X.	Miscellaneous Alkali Dimer Reactions . . . . .	114

PRECEDING PAGE BLANK-NOT FILMED



## I. Introduction

The Bull and Moon (1954) study of the  $\text{Cs} + \text{CCl}_4$  reaction and Taylor and Datz (1955) study of the  $\text{K} + \text{HBr}$  reaction represent the earliest successful observations of product formation in molecular beam reactive scattering. The subsequent early era of neutral molecular beam reactive scattering experiments continued to be dominated by observations of alkali halide formation in reactions of alkali atoms with compounds containing halogens because of the sensitivity and selectivity of the hot filament surface ionization detector. More recently, implementation of advances in vacuum and mass spectrometry technologies has freed the field of this initial preoccupation with alkali and alkali halide chemistry and has vastly extended its chemical scope. Nevertheless, studies of alkali and alkali halide chemistry continue to comprise a significant fraction of the effort in this field despite the full blossoming of the "non-alkali era". This continuing interest is partially due to the ability of simple collision models to simulate the observed reaction features (at least qualitatively) and correlate them with electronic structure for some of the reaction systems. The conceptual simplicity and directness of the molecular beam approach continues to make it the most versatile single tool available to the modern experimental collision dynamacist who wishes to determine the dependence of the reaction cross section on detailed parameters (quantum states) of reactant and products. Reactions of alkali atoms continue to provide the chemical arena for the widest implementation of the various beam techniques. For this reason, the remainder of this chapter is organized so as to first briefly introduce the general beam concept. This is followed by a discussion of the different types of detailed molecular beam measurements which have been reported and their current experimental limitations. Particular experimental studies may be cited here as illustrations. The final section is then devoted



to discussions of the behaviours which have been reported for the different chemical systems. The emphasis here is on the qualitative reaction features rather than detailed quantitative numbers because this chapter provides an ideal format for celebrating the wide variety of reaction mechanisms which are encountered in the alkali and alkali halide reactions.

It is important to define the scope of the chapter at the outset because of the enormity of the literature of this field. In general, discussion is confined to relatively modest (typically  $\lesssim 100$  kJ/mole) energies in the collision partners and to the absence of electronic excitation in either reactants or products because these topics are covered in other chapters. Elastic and rotational inelastic collisions (i.e., "soft" collisions) of the alkali halides are excluded, whereas vibrational inelastic and reactive collisions of the alkali halides are included. Elastic and inelastic scattering of alkali atoms are excluded unless these observations pertain to possible reactions between the same collision partners. In this regard, "quenching" of glory undulations in the energy dependent total scattering cross section [e.g., Helbing and Rothe (1968)] are not discussed, and no attempt was made to insure a complete literature review of studies of the reactive attenuation of the wide-angle elastic differential cross section. Reactive collisions of alkali atoms with compounds containing halogens are discussed in detail as are similar reactions producing alkali oxides, nitrites, cyanides, etc. Reactions of alkali dimers and of other metal atoms with these same reagents are included in order to assess the extent to which the chemistry of these species resembles that of the alkali atoms. Related chemical studies of alkali dimer reactions with hydrogen or alkali atoms and of reactions of other metals atoms with various oxides are not discussed because it was felt that these systems are outside of the subject matter encompassed by the title of this volume.

An attempt has been made to cite all relevant experimental studies which appeared in archival journals through the first quarter of 1977. Theoretical results or unpublished experimental studies are cited only where they are especially relevant to the discussion. No attempt has been made to cite all relevant review articles. The following reviews have proven especially useful in preparing this chapter: Farrar and Lee (1974); Fluendy and Lawley (1973); Gowenlock, et. al. (1976); Greene, et. al. (1966); Greene and Ross (1968); Grice (1975); Herschbach (1961); Herschbach (1965); Herschbach (1966); Herschbach (1973); Kinsey (1972); Polanyi (1972); Ross and Greene (1970); Steinfeld and Kinsey (1970); Toennies (1974); and Zare and Dagdigian (1974).

## II. The Molecular Beam Approach

Conceptually, the molecular beam approach is simple and direct. A beam of atoms or molecules is generated by any of a variety of techniques and allowed to collide with a second reagent in either a crossed beams or beam plus scattering cell mode of operation; the scattered species are subsequently detected. Any number of selectors or analyzers may be inserted between the beam source and detector in order to determine the dependence of the collision cross section on reactant (E) or product (E') relative translational energies or quantum states of internal motion. The experimental reality is, of course, that any such selector or analyzer typically represents a significant reduction in scattered intensity. The essence of molecular beam kinetics is the observation of scattered species which represent the *unrelaxed distribution* produced by a single bimolecular collision process. Experimentally, this is achieved by insuring that the product of density and time of interaction of the collision partners within the intersection volume defined by intersecting beams or the scattering cell be sufficiently small that the probability of any bimolecular process is low so that two or multiple collision processes are totally inconsequential. For the same reason, the ambient background pressure must be sufficiently low that the mean free path within the vacuum chamber exceeds its physical dimensions. Finally, cryogenic vacuum chamber walls, beam modulation and phase sensitive detection, and other experimental techniques must be combined in order to insure that no species which has struck a wall of the vacuum chamber will be recorded as a scattering event.

The crossed beams and beam plus scattering cell modes of operation are both acceptable provided that these steps are taken to insure single collision conditions. Beam plus scattering cell measurements have been common in ion-molecule reaction studies,

even in determinations of product angular distributions. The majority of studies discussed here, however, have used the crossed beams mode although scattering cells have been used quite often in laser induced fluorescence (LIF) studies. It should be noted that resolution in incident collision energy suffers in the beam plus scattering gas mode of operation. An extreme example of the influence of this effect was provided by the contrasting thresholds for charge transfer ionization in collisions of alkali atoms with  $\text{Br}_2$  [Rothe and Fenstermaker (1971)].

#### II.A. Beam Sources

Since molecular beam source technology is carefully discussed in chapter 2 of this volume, only a few relevant points need to be made here. Alkali atom beams have typically been obtained from two chamber effusive ovens where the temperature of the first chamber determines the pressure within the source. The second chamber is maintained at a higher temperature in order to eliminate or at least reduce the alkali dimer concentration in the beam. The alkali atoms also have a fortunate electronic structure in that there are no metastable electronic states which can be thermally populated; this can lead to problems in interpreting results in studies with vapors of some other metals. Beams of alkali halides and of other metals which may require high temperature to produce sufficient vapor pressures have often been obtained from single chamber effusive sources so that the importance of dimer impurities in the beam varies widely with the chemical system. It is totally inconsequential for the alkaline earths, for example, because of the weak binding in the dimers. On the other hand, beams of alkali halides may contain appreciable dimer. The increasing use of nozzle beams, at least with reactants which have appreciable room temperature vapor pressure, also raises the problem of possible dimerization or condensation in the expansion process. For example,



Gonzalez Urena et. al (1975) report the observation of K and Rb condensation reactions with  $\text{CH}_3\text{I}$  clusters; similar observations of  $\text{Br}_2$  condensation on  $\text{Cl}_2$  or  $\text{NH}_3$  clusters are reported in Behrens et. al (1975). In general, however, this does not appear to have been a problem in any of the studies reviewed here. Foreman et. al (1972a) have also exploited this phenomenon of dimerization in a nozzle expansion to produce intense beams of homonuclear alkali dimers. They made use of the magnetic deflection technique discussed below to eliminate the residual alkali atoms from the expanded beam.

The distributions over velocity and internal energy within the beam are important in the energy balance equation for the scattering process and in the transformation of the data from the laboratory (LAB) to the center-of-mass (CM) coordinate system. Since this is discussed in detail in Chapter 2, only a few succinct observations are noted here. "Effusive" beam sources which are used in scattering studies are seldom at the true effusive limit so that a thermal velocity distribution is not obtained although the distribution over internal energy states is probably approximately Boltzman. Deviations from the Boltzman velocity distribution which are observed are usually small and take the form of a depletion of the slower particles from the beam [see, for example, Sholeen and Herm (1976a)]. The cross beam in many of the reactive scattering experiments has been obtained from a multichannel array source. In this case, deviations from a thermal speed distribution are somewhat more pronounced [see, for example, Rulis and Bernstein (1972) and Sholeen and Herm (1976a)]. Vibrational degrees of freedom are probably still described by the thermal source distribution; there may be minor cooling of rotational degrees of freedom, although the data on this is scanty at best [Rulis and Bernstein (1972)]. Rotational and translational temperatures within an expanded nozzle beam are typical relatively low, and the beam speed distribution is shaply peaked. It is usually a

reasonable approximation to assume a thermal distribution over vibrational degrees characteristic of the source. In the case of alkali dimers from a nozzle expansion, however, the best available evidence indicates substantial vibrational relaxation as well [Sinha, et.al. (1973)], and this introduced slight uncertainty in the interpretation of some reactive scattering studies with alkali dimers [Whitehead and Grice (1973)].

## II.B. Detection of Scattered Species

### II.B.1. Surface Ionization Detection

The ionization of alkali atoms at a hot tungsten surface has been known since the early work of Langmuir [see, for example, Langmuir and Kingdom (1925)] and exploited as an efficient (sometimes approaching 100%) detector of alkali atoms (M) and alkali halides (MX) since the early days of molecular beam research [see, for example, Fraser (1937)]. However, this was not a practical detection technique for molecular beam studies of chemical reactions until the work of Datz and Taylor (1956) pointed out that Pt and 12% Pt-8% W alloy surfaces could ionize M with considerably higher efficiencies than MX and made possible the first crossed beams study of the K + HBr reaction by Taylor and Datz (1955). Early attempts to study reactions of M with halogen molecules by this differential surface ionization technique were sometimes erratic, however, until Touw and Trischka (1963) pointed out that M/MX ionization efficiency ratios were markedly different on 92% Pt-8% W hot surfaces which had previously been exposed to butane (desensitized toward MX) versus oxygen (sensitized toward MX). Most molecular beam studies of reactions of sodium, potassium, rubidium, or cesium atoms or dimers with compounds containing halogens have, in fact, employed this simple differential surface ionization technique, and a representative sample of derived MX scattering distributions

have been confirmed by the independent magnetic deflection technique in Herm, et.al (1964) and Gordon, et.al. (1968). The MX signal is determined by differential surface ionization as the difference between signals read on a surface with comparable M and MX efficiencies (W, Re, sensitized Pt or 92% Pt-8% W) and on a desensitized Pt or 92% Pt-8% W surface after normalization to equal M sensitivities on the two surfaces. Despite its wide use, however, there are some problems with the technique which should be noted in order to better define its limitations. Both M and MX produce an  $M^+$  surface ion signal so that the technique is insensitive to the identity of X. Product channel ratios in reactions of alkali atoms with interhalogens are still unknown, for example, except for indirect inferences provided by such studies as Moulton and Herschbach (1966). Desensitized surfaces also exhibit some sensitivity to MX, and Gillen and Bernstein (1970) demonstrated that this sensitivity increases with increasing internal excitation of MX. The effect is small, however, and shouldn't seriously distort product recoil energy measurements. Because the technique requires the difference of two signals, it cannot be used very close to the M beam where the non-reactively scattered M greatly exceeds the reactively scattered MX. For this same reason, it cannot be used to study reactions with very small total reaction cross sections. Finally, its chemical scope is limited. Studies of reactions with some oxidizing gases (e.g.,  $NO_2$ ) are impractical because of concurrent sensitization of the Pt filament [Herm and Herschbach (1970)]. It cannot be used for the study of reactions of non-alkali metals; it is impractical for the study of Li atom reactions [Parrish and Herm (1968)].

### II.B.1.a Product Magnetic Deflection

Figure 1 shows a schematic diagram of a magnetic deflection-slotted disk velocity analysis apparatus which was employed in a study of reactions of Li atoms with  $\text{NO}_2$  and a variety of halogen-containing molecules [Sholeen and Herm (1976a) and (1976b), Sholeen, *et. al.* (1976), and Behrens, *et. al.* (1976b)]. It is included here as an example of a modern apparatus for the study of reactive scattering of alkali atoms and, more specifically, to illustrate the product magnetic deflection technique which was deployed by Parrish and Herm (1968), (1969), and (1971) in order to circumvent some of the problems of differential surface ionization. An early molecular beam apparatus for reactive scattering measurements provided for singly differential measurements in that a product angular distribution was measured. All reported product angular distributions have been obtained with machines which provided for rotation of the source assembly relative to the detector assembly, although the new approach of fourier transform doppler spectroscopy might render this provision unnecessary in some cases in the future [Kinsey (1977)]. In the particular apparatus shown in Fig. 1, the source assembly was mounted on a platform which could be rotated relative to a fixed detector assembly, but the alternate arrangement is often preferable. The next generation of such machines incorporated one of the selectors or analyzers discussed in Section III in order to permit doubly differential measurements. More recently, use of two such devices makes possible triply differential measurements [e.g., Gillen, *et. al.* (1971)]. Figure 1, for example, includes both a slotted disk velocity selector (SDVS) (J) and inhomogeneous deflecting electromagnet (E). A mechanical beam chopper (O) with associated light cell (G) and phototransistor (R) for phase sensitive detection and an electron multiplier (B) are typical of modern techniques deployed to enhance signal-to-noise. A homogeneous electromagnet (C) mass



spectrometer system was also employed in this particular apparatus in order to separate the weak  $\text{Li}^+$  surface ion signal from the copious  $\text{K}^+$  background due to potassium impurities in the surface ionization filament (A).

In general, an atom or molecule in a magnetic or electric field,  $\vec{X}$ , will experience an energy shift,  $W = W(X)$ . If the field is spatially inhomogeneous, this will produce a force on the particle given by

$$\vec{F} = \mu_e \vec{\nabla}X \quad (1)$$

where  $\mu_e = -\partial W/\partial X$ , the effective moment in the direction of the field gradient, is independent of the field strength only in the case of a first order Zeeman or Stark interaction. A particle moving with a kinetic energy,  $E$ , along a coordinate perpendicular to  $\vec{\nabla}X$  will be displaced at the detector plane by

$$\vec{s} = l_X (l_X + 2 l_F) \mu_e \vec{\nabla}X/4E \quad (2)$$

in terms of the length of the field ( $l_X$ ) and distance from the end of the field to the detector ( $l_F$ ). Equation (2) is the basis of both magnetic and electric deflection techniques which are described in a number of monographs on molecular beam experiments [e.g., Fraser (1937) or Ramsey (1956)]. In the high field hyperfine Paschen-Bach limit (i.e., above a few thousand Gauss), for example,  $\mu_e$  for an alkali atom in the  $^2S_{1/2}$  ground state is approximately  $\pm \mu_0$ , in terms of the Bohr magneton,  $\mu_0$ . In a simple deflecting field such as the conventional "two wire" design [Ramsey (1956)] employed in Fig. 1, thermal energy alkali atoms may be deflected several mm towards the pole gaps for reasonable

field lengths and easily achieved field gradients, thereby removing them from a well-collimated beam. On the other hand,  $\mu_e/\mu_o \approx 10^{-3}$  for alkali dimers or alkali halides in their singlet spin ground electronic states so that these molecules are effectively undeflected upon traversing the same magnetic field. Thus, Foreman, et. al. (1972a) employed this technique to prepare a pure beam of alkali dimers ( $M_2$ ), and a couple of laboratories have employed it as an alternate surface ionization detection scheme in order to separate non-reactively scattered M from reactively scattered MX. In addition, Sholeen and Herm (1976a) managed to confirm the production of both ground state LiO ( $X^2\Pi$ ) and excited state LiO ( $A^2\Sigma$ ) from the Li + NO<sub>2</sub> reaction because  $\mu_e \approx +\mu_o$  for a  $^2\Sigma$  state whereas  $\mu_e$  assumes many values (dependent on the total angular momentum quantum number) which are typical much less than  $\mu_o$  for a  $^2\Pi$  state by virtue of strong coupling of the spin to internal molecular motions.

#### II.B.2. Electron Bombardment Ionization-Mass Spectrometer Detection

The extension of molecular beam studies of neutral reactions to include reagents other than the alkali atoms, dimers, or alkali halides was achieved by the introduction of an electron bombardment ionizer-mass spectrometer detection system in place of the conventional surface ionization detector. The reader is referred to Lee, et. al. (1969) for details of the design of such an apparatus. However, a couple of points should be noted. The surface ionization detector responds to the incident flux. Even the most efficient electron bombardment ionizers in use as molecular beam detectors have ionization efficiencies which are orders of magnitude less than unity, however, so that their detection efficiency varies inversely with the velocity with which a particle traverses the ionization region. Thus, they measure particle number density rather than flux density. Flux or number density measurements are equally valid in angular distribution studies, but

the proper detector response function must be included in the subsequent interpretation of the data. The bond energies of the alkali halide positive ions,  $\text{MX}^+$ , are relatively weak and vary widely with the particular species under consideration so that electron bombardment ionization of MX typically produces extensive fragment into  $\text{M}^+ + \text{X}$ . Thus, Sholeen and Herm (1976a) have pointed out that the chemical scope of surface and electron bombardment ionization detectors complement rather than compete against one another.

### II.B.3. Laser Induced Fluorescence Detection

Laser induced fluorescence has recently proven to be a powerful new molecular beam detection technique; it is reviewed in Zare and Dagdigian (1974). It can be very sensitive and provides unparalleled details on reaction energy partitioning by virtue of its ability to excite individual rovibronic transitions in simple product molecules. Its chemical scope is, however, generally limited to studies of simple product molecules which exhibit well-understood electronic transitions in the appropriate spectral range. It is, for example, an ideal detector for mono-halides or oxides of the alkaline earths. In contrast, it is less well-suited to studies of the alkali halides whose unpredissociated excited states are weakly bound and only partially characterized. As presently deployed, it is also a number density detector. This can lead to some minor ambiguities in quantitative energy partitioning measurements where the product angular distribution is unknown, although the seriousness of this problem depends upon the kinematics of the particular chemical system under study.

III. The Variety of Reactive Scattering Measurements  
III.A. Product Recoil Angle and Energy Distributions  
III.A.1. The LAB and CM Coordinate Systems

In crossed beams experiments, particles A and B collide in the LAB coordinate system with velocities  $\vec{v}_A$  and  $\vec{v}_B$ . The angular distribution of some scattered particle C (which would be the same as A or B in the case of elastic or inelastic scattering) is typically measured as a function of scattering angle,  $\Theta$ , in the plane defined by  $\vec{v}_A$  and  $\vec{v}_B$ . The kinetic energy of particle motion in the LAB system contains the (dynamically) uninteresting  $(m_A + m_B) C^2/2$  constant of the motion, where m's denote particle masses and  $\vec{C}$  is the velocity of the center of mass of the collision partners (the centroid vector). Thus, only the remaining kinetic energy is available to influence the collision dynamics as relative collision energy,

$$E = \mu g^2/2 \quad (3)$$

in terms of the reactant reduced mass,  $\mu$ , and relative collision velocity,  $\vec{g} = \vec{v}_A - \vec{v}_B$ .

The central data analysis problem in molecular beam kinetics is the transformation of the measurements from the LAB coordinate systems into the center-of-mass (CM) coordinate system. The nature of this transformation is illustrated graphically for the common case of perpendicular intersecting beams by the velocity vector transformation diagram (sometimes denoted a "Newton diagram") shown in Fig. 2 for the  $A + B \rightarrow C + D$  collision which depicts  $\vec{v}_A$ ,  $\vec{v}_B$ , and  $\vec{C}$  originating from the origin of the LAB coordinate system. This diagram illustrates that scattering of particle C at some angle  $\Theta$  with velocity  $\vec{v}_C$  in the LAB would correspond to scattering through an angle  $\theta$  with recoil velocity  $\vec{w}_C$  in the CM.



Several points relevant to typical beam experiments can be made in relation to this diagram. The second scattered particle (D in Fig. 2) is seldom measured because such measurements contain no new information conceptually. In practice, measurements of distributions for both particles would provide a refreshing check on the data analysis procedure. Since there can be no net linear momentum in the CM system, the dashed lines in Fig. 2 indicate that  $\vec{v}_D$  can be calculated from a measurement of  $\vec{v}_C$ . Thus, the final translational energy for the scattered particles is also determined by a measurement of  $\vec{v}_C$ . This in turn determines the total internal excitation of the scattered species,  $W'$ , by the energy balance equation for the scattering process,

$$E' + W' = E + W + \Delta D_0 \quad (4)$$

where  $\Delta D_0$  is the exoergicity in the event of a reactive process and primes refer to scattered species. For any given collision between species in specific quantum states  $E'$  may, of course, assume only discrete values allowed by Eq. (4). Owing to the close spacing of internal energy levels in  $C + D$  and the relatively poor (at best) experimental resolution in  $E$  and  $E'$ , however,  $w_C$  and  $E'$  are almost always treated as continuous variables in the data analysis. The scattering in the CM system must exhibit cylindrical symmetry about  $\vec{g}$  because the distribution in impact parameters for the collision possesses this symmetry. Although no such symmetry exists in general in the LAB distribution owing to distortions introduced by the transformation Jacobian, this CM symmetry implies that no new information is conceptually to be obtained by measuring the LAB scattering distribution out of the plane defined by the intersecting beams. Although such measurements would be a refreshing experimental check, they are difficult and are seldom attempted. Only a couple of examples have appeared in the reactive scattering literature for special reasons [e.g., Kwei, *et. al.* (1970), Gersch and Bernstein (1972). Kinsey, *et. al.* (1976)].

Details of the transformation equations embodied in Fig. 2 are given in Warnock and Bernstein (1968). Laboratory measurements of the dependence of the scattered intensity of C on  $\vec{v}_C$  for the collision of two beams with well-defined initial velocities could be directly inverted to obtain the corresponding scattering distribution in the CM system. However, such ideal experimental resolution is seldom practical. It has not, for example, been achieved in any of the studies reviewed in this chapter. In crossed beams studies, it is generally adequate to regard the directions of beam motion as well defined and to consider only the distributions over scalar beam speed, i.e.  $\rho_A(v_A) dv_A$  is the number density of particles within beam A with speeds between  $v_A$  and  $v_A + dv_A$ . Then, the number of particles of C scattered per second into LAB solid angles  $\Omega$  to  $\Omega + d\Omega$  with recoil speeds of  $v_C$  to  $v_C + dv_C$  is given by

$$I(\Theta, v_C) = \kappa \iint_0^\infty g \left( \frac{\partial^3 \sigma}{\partial^2 \omega \partial w_C} \right) \left( \frac{v_C^2}{w_C^2} \right) Y(v_C) \rho_A(v_A) \rho_B(v_B) dv_A dv_B \quad (5)$$

in terms of a detector response function  $Y(v_C)$  and proportionality constant  $\kappa$  which depends on the ionization efficiency and interaction volume defined by the intersecting beams. Equation (5) is, of course, evaluated in terms of the energy balance Eq. (4) and transformation equations embodied in Fig. 2; the  $v_C^2/w_C^2$  factor in Eq. (5) is the Jacobian of this transformation. The corresponding total scattered angular distribution is given simply by

$$I(\Theta) = \int_0^\infty I(\Theta, v_C) dv_C \quad (6)$$

The object of angular distribution measurements in the LAB is, of course, to infer the form of the CM differential scattering cross section,  $\partial^3\sigma/\partial^2\omega \partial w_C$ , as a function of CM recoil speed  $w_C$  and solid angle,  $\omega$ , centered on the scattering angle,  $\theta$ , defined in Fig. 2. It may, of course, also depend parametrically on the relative collision energy as well as internal quantum states of reactants and products. Equations (5) and (6) indicate that LAB measurements of the distribution in recoil angle and speed,  $I(\Theta, v_C)$ , or just the total distribution in angle,  $I(\Theta)$ , contain information on  $\partial^3\sigma/\partial^2\omega \partial w_C$ . A broad spectrum of data analysis procedures has been employed in the literature, ranging from crude qualitative arguments about the displacement of the  $I(\Theta)$  distribution relative to the angular distribution of  $\vec{C}$  to non-linear least squares fits of polynomial expansions of  $\partial^3\sigma/\partial^2\omega \partial w_C$ ; these are discussed in the following sections.

The molecular beam technique is ideally suited to the determination of the dependence on various parameters of relative values of the CM differential scattering cross section,  $\partial^3\sigma/\partial^2\omega \partial w_C$ , the total CM scattered angular distribution,

$$\partial^2\sigma/\partial^2\omega = \int_0^\infty (\partial^3\sigma/\partial^2\omega \partial w_C) dw_C, \quad (7)$$

the in-plane CM scattered angular distribution,

$$\partial\sigma/\partial\theta = 2\pi \sin\theta \quad \partial^2\sigma/\partial^2\omega, \quad (8)$$

or the final product recoil energy probability density distribution,

$$P(E') = \left[ \int (\partial^3\sigma/\partial^2\omega \partial w_C) d^2\omega / \int (\partial^3\sigma/\partial^2\omega \partial w_C) d^2\omega dw_C \right] (\partial w_C / \partial E'). \quad (9)$$

However, determination of the absolute differential reactive cross section or total reaction cross section,

$$\sigma = \iint (\partial^3 \sigma / \partial^2 \omega \partial w_C) d^2 \omega dw_C, \quad (10)$$

is more difficult. In this sense, the molecular beam kinetics approach complements the conventional kinetics approach which is specifically designed to measure absolute collisional rate constants. A direct molecular beam determination of absolute cross sections requires a knowledge of the absolute value of  $\kappa$  in Eq. (5); the first example of such a study for a reaction producing neutral product molecules is the recent report of Aniansson, et. al. (1974) on the  $K + RbCl \rightarrow KCl + Rb$  reaction.

A couple of indirect methods have also been used to infer absolute total reaction cross sections from molecular beam kinetics studies [reviewed in Steinfeld and Kinsey (1970)]. One is based on an optical potential model interpretation of the attenuation of the wide-angle elastic scattering in chemically reactive systems; it is discussed later in this section. The second method is based upon a comparison of the absolute intensities of narrow-angle elastic scattering and of reactive scattering in the same chemical systems as measured in the same apparatus. Since the absolute narrow-angle differential scattering cross section is known or can be calculated from the long-range electrostatic, inductive, and dispersive contributions to the pair potential, this method does not require an absolute measurement of  $\kappa$  but does require a knowledge of the relative detection efficiencies for non-reactive versus reactive scattering. Conceptually, this method should be able to provide accurate determinations of total reaction cross sections. In practice, most studies which have employed it have only poorly resolved the shape of  $\partial^3 \sigma / \partial^2 \omega \partial w_C$



so that it is difficult to assess the quantitative reliability of the total reaction cross sections which are reported. Nevertheless, values which have been obtained by this technique should typically be quantitatively reliable to within a factor of two, and relative comparisons between related chemical systems should be more reliable.

### III.A.2. Product Recoil Angular Distribution Measurements

Early reactive scattering studies were largely confined to measurements of product angular distributions, often with crossed beams which both exhibited thermal speed distributions. Measurements of this sort are sometimes referred to as "primitive angular distributions" in the more recent literature. Figure 3 shows the first product angular distribution ever reported; it also illustrates the use of the differential surface ionization technique to study the  $K + HBr \rightarrow KBr + H$  reaction. This particular reaction is an example of a class of reactions involving hydride molecules with special kinematic constraints which arise because the detected product is much heavier than the undetected H (or D) product. Thus, the heavy KBr product of this reaction can acquire only relatively small CM recoil velocity,  $w_{KBr}$ , even for appreciable values of the recoil energy. This implies that the measured LAB product angular distribution contains practically no information on the CM differential cross section because the LAB distribution should be approximately the same as the angular distribution of  $\vec{C}$  for the collisions which lead to reaction. In their original study, Taylor and Datz (1955) pointed out that this implied that the shape of the measured LAB product angular distribution usually contained information on the dependence of the total reaction cross section on relative collision energy,  $\sigma(E)$ , within this approximation of negligible CM recoil speed. This is true because the angular distribution of  $\vec{C}$  is dependent on  $\sigma(E)$  except in the special case of two thermal beams with  $T_B/T_A = m_B/m_A$ . Their original collision energy distribution functions were sub-

sequently corrected in Datz, et. al. (1961). Information on the  $\sigma(E)$  dependence for the K + HBr [Taylor and Datz (1955), Datz et. al. (1961)], K + HCl [Odiorne and Brooks (1969)], and Ca, Sr, and Ba + HI [Mims, et.al. (1972)] reactions have been obtained by this technique, although agreement between measured LAB product angular distributions and calculated centroid angular distributions has not been good unless corrections were made for deviations of the actual beam speed distributions from the ideal thermal distribution.

Primitive product LAB angular distribution measurements for other reaction systems where the product mass ratio is not so extreme do provide information on the CM  $\partial^3\sigma/\partial^2\omega\partial w$  via the convolution integral [Eq. (6)], although the information content of a given measurement varies widely with the chemical system. Figure 4 shows a primitive BaI product angular distribution from the Ba + CH<sub>3</sub>I reaction reported by Lin, et. al. (1973b). This is a typical product LAB angular distribution in that it shows a single peak with little other structure. It provides information on  $\partial^3\sigma/\partial^2\omega\partial w$  to the extent that it is broader than and displaced away from the distribution in centroid vectors shown as the dashed curve in the lower panel of Fig. 4.

All data analyses based on primitive LAB angular distributions alone have had to assume an uncoupled CM distribution function, i.e. that  $\partial^3\sigma/\partial^2\omega\partial w$  can be expressed as some function of recoil angle,  $\theta$ , times some function of recoil speed,  $w$ . Data analyses in the very early studies were very qualitative. The preference for backward or forward scattering in the CM was indicated by a displacement of the LAB product angular distribution to larger or smaller  $\theta$  values than the centroid angular distribution. (Unless otherwise noted, backscattering will refer throughout this chapter to a  $\theta = 180^\circ$  event wherein the metal atom reverses direction as a result of the collision; forward scattering

refers to the opposite limit of  $\theta = 0^\circ$  and no change in metal atom direction. This definition will be extended later in discussing reactions involving two metal atoms.) In a similar way, a "characteristic" product recoil energy was estimated from the position of the peak in the LAB angular distribution and the nominal velocity vector transformation diagram, although this "characteristic"  $E'$  was sometimes misleading because the insidious effect of the transformation Jacobian was not appreciated in the early work. More quantitative insight was provided by the introduction of the "single recoil energy approximation" (SRE) wherein a delta function dependence on CM product recoil speed was assumed, the transformation Jacobian was included in the LAB  $\rightarrow$  CM transformation, and convolution over beam speed distributions were sometimes included or rendered unnecessary by the use of a velocity selected beam. The upper panel in Fig. 4 illustrates the real information content of a primitive product LAB angular distribution. The data can be fit by product recoil energy distributions which vary from the very broad to the unrealistically narrow SRE assumption by altering the breadth of the corresponding CM product angular distribution. Thus, these measurements typically define the CM product angular distribution semi-quantitatively, but the insight into the product recoil energy is more qualitative. In fact, the uncertainty in inferred CM recoil functions may be even worse than is depicted in Fig. 4 for experiments which employ broad beam speed distributions because the LAB  $\rightarrow$  CM transformation is then dependent on the sometimes uncertain form of  $\sigma(E)$ .

Nevertheless, much valuable chemical insight has been and will continue to be obtained from these primitive LAB angular distribution measurements. The magnitude of the observed product signal determines the total reaction cross section at least semi-quantitatively. Differentiation between different possible products which is possible with

an electron bombardment ionizer-mass filter or laser induced fluorescence detector is often interesting. The qualitative or semi-quantitative insight into the CM recoil functions can be quite interesting, especially in identifying trends within a family of related reactions. Moreover, these measurements can quantitatively determine dependences of the CM recoil functions on other parameters such as collision energy in favorable systems where much is already known about the quantitative form of these CM recoil functions from other detailed studies. Examples of this quantitative approach are provided by the recent collisional energy dependent studies of the reactions of  $\text{Rb} + \text{CH}_3\text{I}$  [Gonzalez Urena and Bernstein (1974)] ,  $\text{K} + \text{CH}_3\text{I}$  [Rotzoll, et.al. (1975)] , and  $\text{K} + \text{Br}_2$  [van der Meulen, et.al. (1975)].

### III.A.3. Product Recoil Velocity Measurements

Resolution of quantitative features of  $\partial^3 \sigma / \partial^2 \omega \partial w$  is much improved when the LAB distribution in recoil angle and speed is measured by interposing a speed analyzer between the beam collision volume and detector (e.g., Fig. 1) . Both slotted disk velocity selectors (SDVS) and time-of-flight (TOF) analyzers have been used for this purpose. The reader is referred to other review [e.g., Fluendy and Lawley (1973)] for details of these devices. In both devices, a slit cut on the circumference of a rotating disk is employed to transmit scattered particles for a short burst of time,  $\Delta t$ . The number of particles with a particular speed  $v = L/t$  is determined after an elapsed time  $t$  by means of an analyzer which is situated a distance  $L$  from this entrance disk.

In the case of TOF analysis, for example, this analyzer is simply the scattered intensity detector, and the speed distribution is obtained from the measured distribution in detector arrival times by



$$I(v) = I(t) (L/v^2). \quad (11)$$

In practice, the  $I(v)$  distribution should be derived by deconvoluting the gate function ( $\Delta t$ ), detector length, and detector time response function from the measured  $I(t)$  function. One potential disadvantage of this technique is that the  $L/v^2$  Jacobian in Eq. (11) causes the  $I(t)$  spectrum to heavily favor high velocity events. However, this is offset by the fact that the resolution ( $\Delta v/v = \Delta t/t$ ) can be varied during the experiment simply by changing the analyzer disk rotation frequency. Another advantage of TOF analysis is that the entire velocity spectrum is scanned so rapidly that slow drifts in beam intensities are inconsequential. Another disadvantage to the current TOF analysis techniques which are in use is the low duty factor (typically a few percent) produced by the relatively small number of slits on the analyzer disk which are used in order to avoid severe "wrap around" corrections for overlap between fast molecules from one pulse and slow molecules from a previous pulse. This can be improved by cross-correlating the detector time response with a random or pseudo-random TOF pulsing function.

In practice, however, the SDVS has proven to be a more attractive alternate method. Here, the analyzer situated a distance  $L$  from the pulsing disk is simply another disk of the same radius and slit sequence. These disks are affixed to the same rotating shaft, but corresponding slits are slightly displaced so that only molecules are transmitted which have the proper velocity to arrive at the final slit during the time period when it has rotated into the open position. Inclusion of intermediate disks to prevent transmission of harmonics of the design velocity permits a duty factor which is only slightly less than 50% [Hostettler and Bernstein (1960)]. Kinsey (1966) describes a geometric procedure for locating these intermediate disks, although other schemes have also been employed. Both

SDVS and TOF analyzers should generally be calibrated, often against a known Boltzman speed distribution; Grosser (1967), however, has described a self-calibrating SDVS. The SDVS transmitted velocity is directly proportional to the rotational frequency of the shaft. The resolution,  $\Delta v/v$ , is determined by the original design, is independent of  $v$ , and can't be varied during an experiment.

Bernstein and his co-workers have reported an elegant set of studies wherein an SDVS was employed to prepare a velocity selected beam of alkali atoms and a second SDVS was used to analyze the reactively scattered alkali halides. The speed distribution in the unselected cross beam was relatively unimportant because the characteristic speeds from a room temperature effusive source are generally smaller than the atom speed; it was, however, included in the data analysis via the convolution integral in Eq. (5). Results of their studies are cited in Section IV for different chemical systems. As an illustration of the details which can be resolved, however, Fig. 5 shows a CM contour plot of  $\partial^3 \sigma / \partial^2 \omega \partial w$  for the scattering of KI from crossed beams of K and I<sub>2</sub> which is reported in Gillen, et. al. (1971). These workers actually determined  $\partial^3 \sigma / \partial^2 \omega \partial w$  for several E, but the effect of changing E was small and Fig. 5 shows their composite energy independent map.

However, many of the reported measurements of LAB recoil velocity spectra of scattered species have employed broad "quasi-thermal" speed distributions in both beams. This may reduce the resolution attainable in  $\partial^3 \sigma / \partial^2 \omega \partial w$ , although the extent of the "kinematic blurring" implicit in Eq. (5) varies widely with the chemical system. For example, Fig. 6 shows LAB contours of constant LiO flux from the Li + NO<sub>2</sub> reaction which were obtained in the apparatus shown in Fig. 1 by Sholeen and Herm (1976a). Fifty percent of the centroid vectors which define the origin of the CM coordinate system terminate within the cross hatched area. This illustrates that the kinematic blurring due

to the broad beam speed distributions is not too severe in this case because the cross hatched area comprises only a small fraction of the total in-plane LAB recoil velocity space where appreciable LiO flux was measured.

Most modern experimental measurements use numerical data analysis techniques in order to correct for the influence of the beam speed distributions on the type of LAB measurement shown in Fig. 6. Siska (1973), for example, has described a promising iterative technique for inverting Eq. (5). However, it appears to require a prior smoothing of the data which makes it difficult to objectively appraise the data's true information content. Alternately, a number of laboratories have employed a polynomial [e.g., Gillen, *et. al.* (1971), Riley and Herschbach (1973), Sholeen and Herm (1976a)] or other functional expansion of  $\partial^3 \sigma / \partial^2 \omega \partial w$  and optimized parameters via a least squares fit of Eq. (5) to product LAB recoil velocity measurements. Use of different  $\partial^3 \sigma / \partial^2 \omega \partial w$  expansion functions sometimes provides insight into which CM recoil features are unequivocally determined by the measurements. For example, Fig. 7 shows the P (E') curves evaluated in this way by fitting product recoil velocity spectra measured in the apparatus shown in Fig. 1 for reactions of Li with CH<sub>3</sub>NO<sub>2</sub>, CCl<sub>4</sub>, and CH<sub>3</sub>I [Sholeen and Herm (1976b)]. These results are discussed in Section IV. They are included here to illustrate that the use of different expansion functions generally provide similar P (E') functions. However, the uncertainty in the quantitative form of P (E') may still be significant for the case of an especially unfavorable ratio of the masses of detected and undetected products (e.g., Li + CH<sub>3</sub>I → LiI + CH<sub>3</sub>).

### III.B. Dependence upon Reactant Quantum States

The determination of  $\sigma(E)$  for the case of severe kinematic constraint (i.e.,  $K + HBr \rightarrow KBr + H$  and related reactions) with crossed thermal beams was discussed above. Beyond this special case, numerous studies have determined the dependence of collision probability on  $E$  by the use of an SDVS on one of the beams or by exploiting the sharp speed distribution produced by a nozzle or seeded nozzle expansion. In principle a simple variable temperature effusive source or the ineffectual relaxation of vibrational degrees of freedom in a nozzle expansion source makes possible a separate assessment of the role of  $E$  and thermally distributed internal reactant states in promoting a particular collision process. Examples of some of the studies of this sort are provided by Sloane, *et. al.* (1972), Freund, *et. al.* (1971), Bennewitz, *et. al.* (1971), and Mariella, *et. al.* (1973). However, the true elegance of the molecular beam kinetics approach is its ability to deploy a variety of specific selectors for particular quantum levels.

#### III.B.1. Electric Deflection

The deflection of an alkali halide or other polar molecule with dipole moment  $\mu_e$  in a  $1\Sigma$  electronic state in a inhomogeneous electric field,  $\vec{\mathcal{E}}$ , is discussed in detail in other chapters of this volume. Since the rotational angular momentum is perpendicular to the polar axis, the first order projection of the dipole moment onto the direction of  $\vec{\mathcal{E}}$  time averages to zero. However, a second order effective dipole component survives, i.e.

$$\mu_e = \mu_e \left( \mu_e \mathcal{E} / E_r \right) \frac{J(J+1) - 3 M_J^2}{(2J-1)(2J+3)} \quad (J \neq 0) \quad (12)$$



in terms of the rotational energy ( $E_r$ ), quantum number ( $J$ ), and projection quantum number ( $M_J$ ), all of which should be primed if the technique is being used to analyze scattered products rather than select reactants. Mosech, *et. al.* (1975) have discussed various molecular beam analyzer techniques based on the behavior given in Eq. (12). It is well known that states for which  $J(J+1) - 3M_J^2 < 0$  will undergo sinusoidal trajectories about the field axis in an electrostatic quadrupole field so that molecules in a particular state which enter with the proper velocity on the axis of the field will be refocused onto the axis after a characteristic distance. Stolte, *et. al.* (1975) were able to exploit this refocussing to achieve a sufficiently intense CsF beam to determine that rotational energy is less effective than translational energy in promoting the endoergic  $K + \text{CsF} \rightarrow \text{KF} + \text{Cs}$  reaction. In addition, Bromberg, *et.al.* (1975) have described the production of a beam of CsF in a specific rotational, vibrational, and translational state by the molecular beam electric resonance method described in the following subsection; with some technical improvements, the intensity should be adequate for reactive scattering studies.

In contrast to the alkali halides, polar symmetric top molecules suffer a first order Stark effect interaction. This arises because the projection of the rotational angular momentum vector onto the body-fixed polar symmetry axis may assume only the integer values of  $K\hbar$  where  $|K| \leq J$ . The resultant first order time averaged projection of the dipole moment onto the direction of  $\vec{E}$  is given by

$$\mu_e = -\mu_e K M_J / J(J+1). \quad (13)$$

In a classical picture of precessing angular momentum vectors, this implies that the molecular symmetry axis precesses about the direction of  $\vec{E}$ . Thus, electric deflection may be used to align the symmetric top molecular symmetry axis at an average inclination

angle of  $\cos^{-1} (KM_J/J (J + 1))$  with respect to the incoming direction of a second reactant beam so as to experimentally study the "steric effect" in a reactive or non-reactive collision, i.e. the dependence of the collision probability on this inclination angle.

Brooks, et. al. (1969) and Beuhler and Bernstein (1969) give details of this molecular beam scattering technique. Jones and Brooks (1970) point out that the same technique may be applied to asymmetric tops in favorable cases. A hexapole field provides the optimal refocussing geometry in the case of the first order interaction given by Eq. (13). Since this geometry orientates the molecules with respect to the local radially-directed field direction, a transition to a weaker two pole field is necessary in order to adiabatically rotate the molecules into the LAB alignment. A simple reversal of polarity on this terminal field serves to reverse the alignment direction in the LAB. Distribution over K, M, and J rotational quantum numbers as well as beam speed distributions all contribute to broaden the distribution in inclination angles and to increase the deconvolution problem in the quantitative analysis of the collisional steric effect. Results on different chemical systems are cited in Section IV. However, Figure 8 is included here as an illustration of the variety of chemical behavior which is observed. It is ironic that oblate tops (e.g.  $\text{CHCl}_3$ ) are easier to align experimentally because thermal population favors higher K states, but the interesting chemical behaviors have been observed with the prolate tops.

### III.B.2. Other State Selectors in Use

The broad spectral range currently available with lasers makes possible potential laser excitation of specific rotational, vibrational, and electronic states of a reactant. No reactive scattering studies have been reported as yet which employed laser excitation to

some higher reactant electronic state. Some reactive scattering studies have employed reactants in metastable electronic states prepared by other methods. These studies have analyzed the subsequent product chemiluminescence, however, and are beyond the scope of this present chapter.

Two reactive scattering studies have successfully employed laser promoted vibrational excitation of a hydrogen halide reactant. Odiorne, *et.al.* (1971) employed a multi-line HCl laser to study the effect of HCl vibrational excitation on the magnitude of the  $K + HCl$  reaction cross reaction. Pruett and Zare (1976) employed a single line HF laser in order to assess the effect of HF vibrational excitation on the energy partitioning in the  $Ba + HF$  reaction. These studies directly measure the difference induced in the scattered spectrum upon reactant laser excitation so that their quantitative interpretation is dependent upon the fraction of the reagent gas which is excited. Pruett and Zare (1976) discuss the extent to which the uncertainty in this fraction complicates the subsequent data analysis. Its effect is not too severe because of the very large effect of HF vibrational excitation on the  $Ba + HF$  reaction dynamics.

In addition to laser excitation, alkali halide beams with very high average vibrational excitation have been prepared by a chemical activation technique. The alkali halide beam source in these "triple beam" studies consists of crossed beams of the alkali atom and halogen molecule because these reactions are known to produce a relative sharp distribution over highly excited vibrational levels. Moulton and Herschback (1966) first used this technique to observe the production of electronically excited potassium atoms in the reaction of Na with highly excited KBr. Fisk and co-workers subsequently used it to study energy transfer from highly excited KBr to a variety of collision partners; this work is discussed in Section IV.

### III.B.3. Elastic Scattering from Reactive Systems

Even for potentially reactive partners, the majority of the collisions are elastic. Experimentally, it is observed that the elastic differential cross sections are similar for reactive versus non-reactive collision partners at narrow scattering angles which correspond to relatively large collision impact parameters,  $b$ . At wider scattering angles corresponding to smaller impact parameters, however, the elastic scattering from reactive partners is observed to be attenuated relative to that observed from non-reactive partners. The probability of reaction as a function of impact parameter can be obtained from these elastic scattering measurements as

$$p(b, E) = 1 - \frac{\partial^2 \sigma / \partial^2 \omega}{(\partial^2 \sigma / \partial^2 \omega)_e} \quad (14)$$

where  $\partial^2 \sigma / \partial^2 \omega$  is the elastic differential cross section transformed into the CM system measured at a particular collision energy,  $E$ . A "reference" cross section,  $(\partial^2 \sigma / \partial^2 \omega)_e$ , obtained by fitting the  $\partial^2 \sigma / \partial^2 \omega$  narrow angle measurements, describes the wide angle scattering which would be expected in the absence of attenuation by reaction and determines the  $b \leftrightarrow \theta$  correspondence. The data symbols and solid curves shown in Fig. 9 indicate the contrasting behaviors of  $\partial^2 \sigma / \partial^2 \omega$  and  $(\partial^2 \sigma / \partial^2 \omega)_e$  which were determined for the  $K + CCl_4$  reaction in Harris and Wilson (1971).

Details of this technique are discussed and reviewed elsewhere [e.g., Fluendy and Lawley (1973); Greene, *et.al.* (1966); Greene and Ross (1968); Ross and Greene (1970); Toennies (1974)] and only a few comments are offered here. The simple treatment of the elastic scattering given in Eq. (14) has been upgraded by the development of an optical model [reviewed in Kinsey (1972)] wherein a complex potential is responsible for a



complex phase shift; the imaginary part of the phase shift accounts for the attenuation (i.e., non-unitarity) of the elastic scattering. This more formal treatment serves to define the region of validity of Eq. (14) and provides a better treatment in other cases. It also shows promise as a convenient vehicle for correlating or extrapolating reactivity measurements for a particular chemical reaction or family of reactions [Roberts and Iasonidou Nelson (1974), Roberts (1976)].

The quantitative interpretation of these measurements (e.g., Fig. 9) are somewhat hampered by difficulty in assigning the proper  $(\partial^2 \sigma / \partial \omega^2)_e$  and  $b \longleftrightarrow \theta$  correspondence; the resulting uncertainty in  $p(b, E)$  varies widely with the chemical system. Another problem is that both inelastic and reactive collisions can attenuate the elastic scattering, and the inelastic scattering can dominate in the case of an appreciable reaction threshold energy [e.g., Odiorne and Brooks (1976) and Truhlar (1971)]. In cases where both measurements exist, however, the assignment of the attenuated elastic scattering to chemical reaction appears to be a good approximation because the total reaction cross sections calculated from the inferred  $p(b, E)$  agree within experimental errors with estimates from direct measurements of the scattered product flux. Moreover, these measurements remain the only ones which provide information on the probability of reaction versus impact parameter in the collision. An alternate expression of  $p(b, E)$  in terms of probability of reaction versus distance of closest approach in the elastic trajectory is sometimes useful because it weakens or eliminates the dependence on  $E$  [e.g., Harris and Wilson (1971)].

### III.C. Dependence upon Product Quantum States

The use of an SDVS to measure the product recoil velocity spectra and thus the distribution in recoil energy was discussed in Section III A. The ability of magnetic deflection to distinguish between  $^2\Sigma$  and other electronic states of diatomic molecules was noted in Section II. This same Section noted the phenomenal resolution afforded by LIF in favorable cases, i.e. the ability to measure the distribution over product vibrational ( $v'$ ) and rotational ( $J'$ ) quantum numbers. Other beam measurements of product internal excitation have employed electric deflection. Except for the observation of a pseudo-first order Stark interaction for the  $\text{CsNO}_2$  product from  $\text{Cs} + \text{CH}_3\text{NO}_2$  reported in Maltz and Herschbach (1967), these studies have all exploited the second order Stark interaction of a product alkali halide.

For a random distribution in product  $M_j'$  states, Eqs. (2) and (12) indicate that the extent of deflection of a product alkali halide molecule varies inversely as the product rotational energy,  $E_r'$ , times the LAB recoil kinetic energy. Herm and Herschbach (1965) and Maltz and Herschbach (1967) employed deflection in a two pole field to determine  $E_r'$  for a number of reactions of alkali atoms with molecules containing halogens, although the results reported for  $E_r'$  have been revised in Maltz (1969). Grice, et. al. (1970), Mosch, et. al. (1974), and Mosch, et.al. (1975) exploited the intensity enhancement provided by a quadrupole refocussing field as well as an SDVS to eliminate the distribution in LAB product kinetic energy to determine  $E_r'$  for the  $\text{Rb} + \text{HBr}$  and  $\text{Br}_2$  reactions. The use of the SDVS should make it possible to determine the distribution over  $E_r'$  by either technique from the observed dependence of the deflection on the applied field strength. In practice, however, results thus far have been analyzed by assuming some functional form for the  $E_r'$  distribution (e.g., thermal) and determining the average product

rotational energy. Mosch, et.al. (1974) point out that a thermal  $E_r'$  distribution will usually be approximately correct in the absence of beam velocity selection, owing to the thermal reactant distributions. It should also be noted that Hill and Gallagher (1975) have described a new deflection concept using an inhomogeneous resonant deflecting field which might prove useful as a product state analyzer.

Perhaps the most elegant manifestation of the electric deflection technique is the molecular beam electric resonance spectrometer described in other chapters of this book. Here, a quadrupole field focusses a particular rotational quantum state into a region of homogeneous field strength where RF or microwave radiation may induce a transition to some other quantum state; upon leaving this homogeneous field, a second deflecting field is used to test whether a transition has taken place. The molecular dipole moment and rotation constant depends weakly on the vibrational quantum number,  $v$ , so that resonant transitions for different  $v$  levels occur at easily resolvable transition frequencies. An electric resonance spectrometer has been used to analyze the product alkali fluoride vibrational distribution for the reactions of  $\text{Cs} + \text{SF}_6$  [Freund, et. al. (1971)],  $\text{Cs} + \text{SF}_4$  and  $\text{SF}_6$  [Bennewitz, et.al. (1971)], and  $\text{Li} + \text{SF}_6$  [Mariella, et. al. (1973)]. Mariella, et. al. (1974) also used it to study the vibrational relaxation of a thermal LIF beam by a variety of molecules.

Mosch, et. al. (1975) discuss the merits of the electric resonance method as a product state analyzer. Its most critical limitation is its restriction to very low  $J'$  values ( $J' \lesssim 5$ ) because of the sensitivity loss which would be occasioned by the larger path lengths needed to refocus the higher  $J'$  levels. Since the most probable  $J'$  value from an alkali atom plus halide molecule reaction is typically  $\sim 50$ - $100$  [e.g., Maltz and Herschbach (1967)], the conclusion that the measured distribution over  $v'$  is characteristic of the

reaction is critically dependent on an assumed independence of the  $v'$  and  $J'$  distributions. Indeed, the  $J'$  values which are studied are so unrepresentative of a typical product that this question would cause serious concern even if the same vibrational distribution were measured for different  $J'$  values. In this regard, it is fortunate that the technique has thus far been applied to chemical systems where this assumed independence of the  $J'$  and  $v'$  distributions seems most plausible, i.e. a highly exothermic reaction of an atom with a large polyatomic molecule possessing thermally distributed internal excitation which appears to proceed via statistical equipartitioning of energy in a long-lived collision complex.

Angular momentum conservation in a reactive collision requires that the orbital and rotational angular momenta of reactants and products be related by

$$\vec{J} + \vec{L} = \vec{F} = \vec{J}' + \vec{L}' \quad (15)$$

Here,  $\vec{F}$  is the total rotational angular momentum of the collision intermediate, and electron or nuclear angular momenta have been ignored. Since  $\vec{L}$  must be orthogonal to  $\vec{g}$ ,  $\vec{F}$  and thus  $\vec{J}'$  will not be isotropically distributed in space in general. Conceptually, the distribution in  $\vec{F}$  can be calculated or, at least, estimated so that a measurement of the joint distribution over  $J'$  and  $M_{J'}$  determines the angular momenta coupling in the reaction. Equation (12) indicates that the second order Stark effect is dependent on  $M_{J'}$  as well as  $J'$  so that information on both parameters can be obtained from the direction and extent of deflection of a product alkali halide beam as the spatial direction of the inhomogeneous deflecting field is varied. A two pole deflecting field is the better choice for these studies because the field direction in a refocussing field is randomly distributed in the plane perpendicular to the beam axis.



The first successful observation of an anisotropic  $M_j'$  distribution in alkali halide product molecules was reported by Maltz, *et. al.* (1972) who used this two pole deflection technique. Their apparatus inadvertently included a field-free region between buffer and deflecting fields so that they had to correct for a sudden, non-adiabatic reprojecton of quantization axis. Hsu, *et. al.* (1975) describe an improved apparatus which eliminates this reprojecton correction and an improved data analysis procedure which indicate that the measurements yield  $\langle \cos^2 \chi \rangle$  and  $\langle \cos^4 \chi \rangle$ , the first two moments of the distribution over  $\cos \chi$  where  $\chi$  is the angle between  $\vec{J}'$  and  $\vec{g}$ . Results on different chemical systems are cited in Section IV. It should also be noted that polarization studies with LIF can provide information on the  $M_j'$  distribution. Although no reports of its application to reactive scattering have appeared as yet, Sinha, *et. al.* (1973) have provided an analysis of the technique and used it to measure the alignment of dimers in a supersonic nozzle beam expansion [see also Visser, *et. al.* (1977)].

#### IV. Results for Different Chemical Systems

Results obtained with the various beam techniques on inelastic and reactive scattering of alkali halides and on reactive scattering of metal atoms are listed in tables and are discussed in this section. Abbreviations used in these tables to identify the various types of beam measurements are defined in Table I. A study which combined a couple of techniques is indicated by two or more abbreviations; for example, LECT-LIF would describe the Pruett and Zare (1976) study of the  $\text{Ba} + \text{HF}(\nu) \rightarrow \text{BaF}(\nu') + \text{H}$  reaction. An entry of P(y) under results indicates a determination of the dependence of the scattering cross section upon parameter y, where y might denote E,  $E_v$ ,  $E_r$ , b,  $\Theta$ ,  $E'$ ,  $E'_v$ ,  $E'_r$ , etc. or some combination. For example, the Pruett and Zare (1976) study is denoted P( $E_v$ ;  $E'_v$ ). A  $y = K/J$  entry denotes a determination of the reaction steric effect, whereas  $y = M_J'/J'$  denotes a determination of the polarization of product rotational angular momentum. Product recoil angular and velocity measurements are denoted I( $\Theta$ ) and I( $\Theta, v$ ), respectively, rather than the entries for the corresponding CM recoil functions. This is meant to emphasize the widely varying qualities of different LAB  $\rightarrow$  CM transformation procedures. The reader may judge the quality of this procedure in any particular study in terms of the discussion given in second III. A. An entry of  $\sigma(E)$  indicates a determination of the energy dependence of relative values of the total reaction cross section in addition to recoil function measurements.

## IV.A. Scattering of Alkali Halide Molecules

### IV.A.1. Vibrational Inelasticity

Crossed molecular beam studies of vibrationally inelastic collisions of alkali halide molecules are listed in Table II. Related studies of elastic and rotationally inelastic [e.g., Toennies (1965)] collisions and of high energy collisional dissociation into ion pairs [e.g., Tully, et. al. (1971), Parks et. al. (1973a and b) and Piper, et. al. (1972)] are discussed elsewhere and aren't included here. The studies listed in table II span a wide range in  $E_{\text{int}}/E$ , the ratio of alkali halide internal excitation to relative collision energy.

Fisk and co-workers crossed beams of K and  $\text{Br}_2$  to produce a beam of KBr with a well characterized, reasonably narrow vibrational energy distribution peaked at 180 kJ/mole. They proceeded to measure  $\partial^3 \sigma / \partial \omega^2 \partial w$  differential cross sections for transfer of this very large initial vibrational excitation into recoil energy with which the collision partners separate for a wide variety of non-reactive collision partners, and reported different mechanistic behavior for different classes of collisions partners. Crim, et. al. (1973) reported total cross sections of the order of  $20 \text{Å}^2$  for transfer of large amounts of vibrational energy into translation in collision with Ne and Ar atoms and with nonpolar ( $\text{N}_2$  and  $\text{CO}_2$ ) or weakly polar (CO) small molecules. They suggested that energy transfer proceeds mainly through impulsive interactions and that long range attractive forces are relatively unimportant in these systems. Quantitative differences in observed energies transferred led them to suggest that some energy also appeared as vibrational excitation in CO and  $\text{CO}_2$ , but not in  $\text{N}_2$ . However, a more recent surprisal analysis of these

measurements reported in Crim and Fisk (1976) suggests some V-V transfer even in the case of  $\text{KBr}^\dagger + \text{N}_2$ . In contrast, Donohue, et. al. (1973) reported that attractive forces appear important in the relaxation of  $\text{KBr}^\dagger$  by small polar molecules. Inelastic collisions proceeded through a short lived energy randomizing collision complex with total cross sections as large as  $300 \text{ \AA}^2$ . However, they saw no evidence that the energy equilibrated with internal vibrational modes in these small molecules. Crim, et. al. (1976) subsequently reported that several internal modes in  $\text{CH}_3\text{NO}_2$  did participate in energy randomization in the complex formed in the  $\text{KBr}^\dagger + \text{CH}_3\text{NO}_2$  collision. Nitromethane was specifically chosen as a collision partner to demonstrate this effect because it is highly polar and also has several low frequency skeletal vibrations. KBr recoil velocity spectra recorded with  $\text{KBr}^\dagger + (\text{CH}_3)_2\text{O}$ ,  $\text{C}_2\text{H}_5\text{OH}$ , and  $\text{C}_3\text{H}_8$  showed features suggestive of both the impulsive and the collision complex energy transfer models.

At the opposite extreme of the  $E_{\text{int}}/E$  ratio range, Loesch and Herschbach (1972) crossed a  $\sim 1000^\circ\text{K}$  thermal CsI beam with an Ar beam obtained from a seeded nozzle to obtain collision energies from 34 to 106 kJ/mole. Their measured recoil velocity spectra indicated total cross sections of  $\sim 20 \text{ \AA}^2$  for transfer of  $\geq 90\%$  of this collision energy into CsI internal excitation (both rotational and vibrational excitations are probably important). They point out that completely impulsive collision could transfer a maximum



of only 40% of the collision energy for the masses of these collision partners. This indicates a qualitatively different energy transfer mechanism which they've referred to as "ballistic". They suggest that it might be due to a resonant or quasibound CsIAr complex. King, et. al.(1973) report a similar ballistic effect in Ar + CsF collisions and argue that their interpretation is not an artifact of their data analysis because the tendency of the CM  $\rightarrow$  LAB transformation Jacobian to strongly weigh low recoil events in the LAB frame of reference is offset by a density of states dependence on  $E'$ .

Armstrong, et. al. (1975) and Green, et. al. (1977) measured recoil spectra in two perpendicular planes containing the cesium halide beam for  $E_{int}/E$  ratios of order unity. They employed a velocity selected thermal cesium halide beam and reported that both excitation and deexcitation occurred with cross sections approaching that for wide angle ( $\geq 40^\circ$ ) elastic scattering. They did not observe individual peaks in the recoil velocity spectra corresponding to different vibrational transitions which indicated that both rotational and vibrational transitions were involved. Greene, et. al. (1977) suggest that a long-lived collision complex between alkali halides and rare gases may randomize the energy over degrees of freedom at low  $E + E_{int}$ . They further suggest that a statistical energy partitioning might account for all of the results listed in Table II on collisions of rare gases with alkali halides.

#### IV.A.2. Reactive Scattering of Alkali Halides

Practically no information on the gas phase reaction kinetics of alkali halide molecules existed prior to the advent of crossed molecular beam studies. Beam studies of three reaction families involving alkali halide reactants which are reviewed in Table III all produced surprising results. Although chemists had grown accustomed to discussing reactions in terms of a transition state collision complex, early molecular beam studies of

interaction mechanism, i.e. the lifetime of the collision intermediate,  $\tau_c$ , was less than its rotational period,  $\tau_r$ . The distinction between a direct ( $\tau_c < \tau_r$ ) and long-lived complex ( $\tau_c > \tau_r$ ) reaction mechanism is readily established from beam measurements because the product angular distribution must be symmetric about  $\theta = 90^\circ$  for the case of  $\tau_c \gg \tau_r$ . It would be a rare accident for a direct interaction mechanism to produce such a symmetric angular distribution. Thus, it was a refreshing contrast to these early reactive scattering results when Miller, et. al. (1967) reported a long-lived complex mechanism in the reactions of alkali atoms with alkali halide molecules. Reactions between KI and CsCl [Miller, et. al. (1972)] provided one of the rare examples of fast bimolecular reaction between two compounds in saturated valance configurations. Reactions of alkali [King and Herschbach (1973)] and alkaline earth [Freedman, et. al. (1976)] halides with halogen and hydrogen halide molecules subsequently provided an even more surprising example of this behavior. All of these reaction dynamic features have been interpreted in terms of the unique electronic structure of the alkali halides, i.e. they are well approximated as polarizable ion spheres which exhibit long-range Coulombic, inductive, and dispersive forces as well as shorter-range repulsive forces.

#### IV.A.2.a. Alkali Halides plus Alkali Atoms

Table III indicates that a variety of molecular beam techniques have been deployed in the study of the exchange reactions of alkali halides with alkali atoms. The large dipole moments of the alkali halide molecules make them especially well suited to electric deflection techniques. More significantly, however, this family of reactions has been and will continue to be important in testing predictions of statistical theories of reaction

proceeding via a long-lived complex. The recent extension to include studies of alkaline earth metals [Dagdigian and Zare (1974) and Smith and Zare (1976)] is noteworthy because the ability to deploy the LIF technique will provide better resolution of the reaction energy partitioning.

Miller, et. al. (1967) first reported that Cs and K + RbCl and their reverse reactions proceeded via formation of a long-lived complex. They observed large cross sections for formation of the complexes which they attributed to the strong long-range dipole-induced dipole forces present in these systems. The RRKM treatment of unimolecular decomposition indicates that the formation of a long-lived collision complex is ordinarily dependent upon a substantial binding energy of the complex relative to either reactants or products. Miller, et. al. (1967) plausibly attributed the formation of a long-lived complex in these reactions to the fact that the reactions are close to thermoneutral and that the known bonding in the diatomic alkali ions,  $M_2^+$ , suggests substantial binding energy in the intermediate because the complex formation can be viewed as  $M' + M^+X^- \rightarrow (M'M)^+X^-$ . This picture was reinforced by reports that Cs + TlCl and TlI [Fisk, et. al. (1967)] as well as Li + MX [Kwei, et. al. (1971); Lees and Kwei (1973)] failed to exhibit this symmetric angular distribution; a weaker complex binding energy is expected in these cases.

The K, Cs + RbCl and other early beam studies of long-lived collision complexes [Ham, et. al. (1967); Ham and Kinsey (1970)] prompted the development of statistical theories of reaction dynamics. These may take the form of a phase space theory (PST) wherein decomposition of the complex into any particular set of quantum states is judged equably probable within the constraints of conservation of energy and angular momentum. Alternatively, a transition state theory (TST) may envision a statistical distribution over degrees of freedom in an activated complex.

For example, Miller, et. al. (1967) analyzed their product angular distribution in terms of a TST patterned after the compound nucleus treatment of nuclear fission. Recently, Case and Herschbach (1976) have pointed out that a variety of directional properties (e.g. product angular distribution, product rotational polarization) of long-lived complex reactions can be calculated from PST in terms of  $\Lambda = L / (L + J)$  and  $\Lambda' = L' / (L' + J')$ . These authors also reviewed previous TST and PST treatments of these properties. In the limit that both  $\Lambda$  and  $\Lambda'$  go to unity, for example, the product differential cross section approaches the sharply peaked  $(\sin \theta)^{-1}$  whereas an isotropic distribution is obtained if either  $\Lambda$  or  $\Lambda'$  goes to zero. The rigorous PST formulation of the energy partitioning was given by Pechukas, et. al. (1966), but this can be complicated to apply. Pechukas, et. al. (1966) give formulas for the 3-atom complex, and Dagdigian, et. al. (1974) treat the 4-atom complex. For this reason, an approximate TST formulation of Safron, et. al. (1972) has commonly been employed in analyzing beam measurements because it provides simple expressions for the energy partitioning. Care must be taken in applying it, however, because it was derived only for the case of  $\Lambda \approx \Lambda' \approx 1$  [Safron, et. al. (1972); Marcus (1975)]. Moreover, it (and many other existing TST's) cannot be confidently applied to the breakup of a tight activated complex because of the neglect of possible product channel interactions [Herschbach (1973), Marcus (1973), Marcus (1975)]. Even within these limits, Holmlid and Rynefors (1977) have recently emphasized that some approximations employed in the Safron, et. al. (1972) derivation seriously restrict the permissible applications of this TST formulation.

In addition to the possibility that such statistical theories describe experimental measurements in the case of a long-lived complex mechanism, it was long recognized that they also served to define a reaction dynamic baseline, i.e. measured deviations from PST



must be due to dynamical effects. This qualitative argument was made quantitative by Bernstein and Levine (1972) who used information theory and introduced the surprisal function, i.e. the negative of the natural logarithm of the ratio of the measured distribution function to that predicted by PST. This has proven very valuable because a surprisal analysis may reduce an overwhelming quantity of reaction dynamic data to a few parameters.

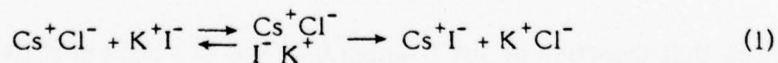
With reference to the alkali atom plus alkali halide exchange reactions, the most recent measurements [Aniansson, et. al. (1974), Stolte, et. al. (1976)] confirm the initial suggestions of Miller, et. al. (1967) that reaction proceeds via a long-lived collision complex. Product recoil angular and energy distributions are consistent with equipartitioning of reaction energy in a long-lived complex; experimental resolution is probably incapable of distinguishing between approximate TST formulations and rigorous PST. However, the measured branching ratio for decomposition of the complex into products or back into reactants clearly disagrees with statistical predictions. It has been suggested that this non-statistical branching ratio may be due to the centrifugal force produced by the relatively high angular momentum in the complex. This tends to promote a linear M'MX complex and inhibits the bending required to interchange alkali atoms.

#### IV.A.2.b. Alkali Halide plus Alkali Halide

Exchange reactions between two alkali halide molecules are especially difficult to study because of the high probability for fragmentation upon ionization. Nevertheless, Miller, et. al. (1972) managed to study the  $\text{Cs Cl} + \text{KI} \rightarrow \text{CsI} + \text{KCl}$  reaction by exploiting the kinematics of comparable masses of reactants but a large mass difference in the products which restricted the scattering of the heavy CsI product to a limited range of LAB recoil velocity space. They reported a large cross section for a reaction which

proceeded via a long-lived complex with symmetric angular distribution and product recoil energy distribution consistent with TST. As in the case of  $M + M'X$ , however, the branching ratio for reactive versus non-reactive decomposition of the complex was considerably less than that expected from TST.

These observations are generally consistent with the electronic structure of the reagents. The very strong long-range dipole-dipole forces can account for the large total reaction cross section. The formation of a long-lived complex is consistent with the known large binding energies of alkali halide dimers. The stable isomer of these dimers is known to be a cyclic, planar rhomboid. Miller, et. al. (1972) attribute the discrepancy between measured and TST branching ratio to a less stable, linear-chain isomer which might be favored for high complex angular momentum states and predominantly decompose back into reactants. Concerted four-center reactions ordinarily exhibit very large activation energies. The rapid reaction reported here at only modest energies ( $\sim 17$  kJ/mole collision energy,  $\sim 46$  kJ/mole total reactant energy) can be attributed to the special ionic nature of the bonding, i.e. the reaction proceeds by

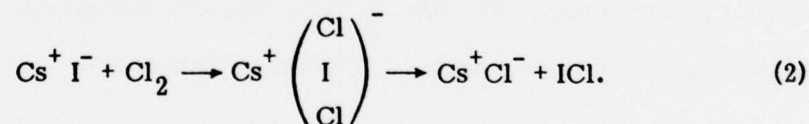


so that there is no reason to expect any significant energy barrier to formation or decay of the complex.

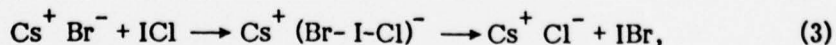
#### IV.A.2.c. Alkali Halide plus Halogen Molecule

King and Herschbach (1973) reported large cross sections for the exchange of halogen atoms in thermal energy reactions of CsI with  $\text{Cl}_2$  and CsBr with ICl. The product recoil angular and energy distributions from  $\text{CsI} + \text{Cl}_2$  were again consistent with TST. For  $\text{CsBr} + \text{ICl}$ , only  $\text{CsCl} + \text{IBr}$  products were observed. Here, the product angular distribution was asymmetric about  $\theta = 90^\circ$ , and the recoil energy distribution was inconsistent with TST.

Observation of fast reactions in these systems is much more surprising than in the case of two alkali halides where the behavior was readily understood in terms of the ionically bound complex. King and Herschbach (1973) attribute the fast reaction observed in these systems to an ion-pair intermediate as well. This can arise because the trihalide negative ions are known stable species which follow the rule that the least electronegative halogen atom is always the central atom. Thus, the  $\text{CsI} + \text{Cl}_2$  reaction is pictured as proceeding by



They argue that insertion of the  $\text{I}^-$  anion into the  $\text{Cl}_2$  bond promotes a long-lived complex mechanism. The  $\text{CsBr} + \text{ICl}$  reaction, on the other hand, involves an end-on attack of  $\text{Br}^-$  on ICl,



which apparently promotes a direct mechanism and accounts for the absence of the  $\text{CsI} + \text{BrCl}$  product channel.

Further support for this picture was provided by Freedman, et. al. (1976) who studied the thermal energy reactions of alkaline earth dihalides with  $\text{Cl}_2$  and  $\text{HCl}$ . The bonding in the heavier alkaline earth halides is also largely ionic. In order to draw the analogy to the alkali halide systems,  $\text{BaI}_2$  may be pictured as  $(\text{BaI})^+ \text{I}^-$ . Freedman, et. al. (1976) reported halogen exchange product recoil angular and energy distributions in  $\text{BaI}_2 + \text{Cl}_2$  consistent with TST, in direct analogy to the  $\text{CsI} + \text{Cl}_2$  results. They were unable to establish whether the product was  $\text{BaCl} + \text{ICl}$  or  $\text{BaCl}_2 + \text{I}_2$  because of the absence of a  $\text{BaX}_2^+$  parent ion in the EB mass spectrum. In contrast, a direct reaction mechanism was observed for  $\text{BaI}_2 + \text{HCl} \rightarrow \text{BaCl} + \text{HI}$ . This is directly analogous to  $\text{CsBr} + \text{ICl}$  because the  $\text{IHCl}^-$  anion is known to be bound with the H-atom in the center. Two additional observations also supported this ion-pair intermediate model of these reactions. Reaction was observed between  $\text{BaF}_2$  and  $\text{BCl}_3$ , where a  $(\text{BaF}^+) (\text{BCl}_3)^-$  ion-pair intermediate is quite plausible, whereas no reaction was observed for  $\text{BaI}_2 + \text{CH}_3\text{CHCl}_2$ ,  $\text{C}_2\text{H}_2\text{Cl}_2$ , or  $\text{C}_2\text{H}_3\text{Cl}$ . Furthermore, reactivity with  $\text{Cl}_2$  followed the sequence  $\text{BaI}_2 > \text{SrI}_2 \gg \text{MgI}_2$  which correlates nicely with the decreasing ionic character of the alkaline earth dihalide bonding.

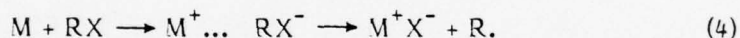
#### IV.B. Reactive Scattering of Alkali Atoms

Magee originally suggested the electron-transfer or "harpoon" model to account for the large cross sections for reactions of alkali atoms with halogen molecules. This model recognizes that the potential energy surface correlating asymptotically to neutral  $\text{M} + \text{X}_2$  reactants intersects a surface correlating to  $\text{M}^+ + \text{X}_2^-$  at an approximate reactant separation of  $r_c = e^2/\Delta$  where  $\Delta$  is the difference between the ionization potential of the alkali atom and the electron affinity of the halogen molecules. This simple model



and its refinement to include such features as the nature of the mixing of these two zeroth order electronic states in the vicinity of  $r_c$  and the inclusion of the vibrational degree of freedom in  $X_2$  is discussed in detail in another chapter of this volume.

This electron transfer model provides a convenient language for discussing the range of dynamical behaviors observed with different reagents. As often happens, the language of the model is applicable to a broader range of reactions than is suggested by its original derivation. All of the reactions discussed in this section involve the cleavage of a "covalent" bond in the RX halide reagent to form an "ionic" metal halide bond so that charge density must flow from the metal atom during the reaction, i.e.



For halogen molecules and other good electron acceptors, it is reasonable to discuss a well-developed ion-pair intermediate. For other reagents, such as  $CH_3I$ , with a small or negative electron affinity, the  $M^+ \dots RX^-$  symbol in reaction (4) simply indicates the inception of polar bonding as the reactants begin to interact. In either case, the metal atom electron density begins to flow into the lowest unfilled molecular orbital(s) (LUMO) on R-X so that the nature of this LUMO is very important in determining features of the reaction dynamics, e.g. the recoil energy of the products. Thus, it is expected and observed that the reaction dynamics vary widely for differing R-X reagents but show weaker sensitivity to the identity of the metal atom. For this reason, the discussion that follows is grouped into families of different R-X reagents. Furthermore, the review is not restricted to alkali atom reactions because it is the similarities rather than the differences which are most striking in comparing reactions of an alkali atom and a non-alkali metal atom with a particular halogen-containing reagent.

#### IV.B.1. Metal Atom plus Halogen Molecule

Molecular beam studies of the reactions of metal atoms with halogen molecules and related reagents are listed in Table IV. Related studies of bimolecular chemiluminescence [e.g., Mims and Brophy (1977)] and chemi-ionization [e.g., Diebold, et. al. (1977)] with the alkaline earth metals are not included. All of the listed studies indicate the following general features of the reactions: (1) large total reaction cross sections ( $> 100 \text{ \AA}^2$ ); (2) severe attenuation of the wide-angle elastic scattering with no rainbow angle feature present [e.g. Greene, et. al. (1969)]; (3) a direct reaction mechanism producing an asymmetric product angular distribution peaked in the forward direction [e.g., Gillen, et. al. (1971)]; and (4) a preference for low recoil energy events channelling most of the reaction exoergicity into alkali halide vibrational excitation [e.g., Gillen, et. al. (1971) for the product recoil energy distribution and Grice, et. al. (1970) which indicates only moderate alkali halide rotational excitation]. Properties (1)-(3) are all qualitatively consistent with the large  $r_c$  crossing radius and reactive collision impact parameters predicted by the electron transfer model. Since the halogen molecular negative ions are bound and have a large vertical electron affinity, the harpoon model is also qualitatively consistent with property (4) because the electron transfer transition can reach a bound region of the  $X_2^-$  ion which subsequently dissociates in the force field produced by the approaching  $M^+$ . Sholeen, et. al. (1976) and Lin, et. al. (1973) discuss weak trends in the product angular distribution with changing halogen molecule or metal atom. For a given halogen molecule, the product metal monohalide angular distribution narrows with increasing metal atom mass in both the alkali and alkaline earth families. This could be a true mass effect or it could be due to the decrease in metal atom ionization potentials in these sequences. This is a relatively weak effect, however, and only primitive product

angular distribution measurements are available for most chemical combinations so that it would be misleading to quantitatively compare features of the alkali and alkaline earth reactions in detail. Lin, et. al (1973) do observe that the product angular distributions from  $\text{Ba} + \text{Cl}_2$  and  $\text{Br}_2$  resemble more closely those of Cs, where the mass factors are comparable, than those of Li, where the metal atom ionization potentials are similar. Another weak trend in both metal atom families is observed with  $\text{Cl}_2$  producing a more sharply peaked product angular distribution than  $\text{Br}_2$ . However, the most striking aspect of the comparison of features of the different chemical systems listed in Table IV is their qualitative similarity. In unpublished work from the author's own laboratory, this similarity has been extended to include the reaction of Sn atoms with  $\text{Cl}_2$  [Parr (1977)].

Precise determinations of the product recoil velocity spectra,  $\partial^3\sigma/\partial^2\omega\partial w$ , are important for these reactions as quantitative tests of refined theories built around the electron transfer model. In view of this, the limited number of such measurements for this family of reactions is surprising. Some of the earliest product recoil velocity measurements were obtained for the  $\text{K} + \text{Br}_2$  reaction [Grosser and Bernstein (1965); Birely and Herschbach (1966); Warnock, et. al. (1967)]. Since experimental and LAB  $\rightarrow$  CM transformation techniques were still evolving during this period, these studies only determined a range of possible  $\text{K} + \text{Br}_2$  CM recoil functions. This was followed by the careful study of the  $\text{K} + \text{I}_2$  reaction by Gillen, et. al. (1971) as a function of collision energy. They reported the reaction dynamics to be relatively insensitive to collision energy, and Fig. 5 shows their composite  $\partial^3\sigma/\partial^2\omega\partial w$  derived by combining results at different energies. This illustrates the direct, asymmetric product angular distribution favoring forward scattering with only modest recoil energy. It further illustrates that there is typically appreciable breadth to the product recoil angular and energy

distributions from these reactions. Sholeen, et. al. (1976) subsequently reported  $\partial^3 \sigma / \partial^2 \omega$   $\partial \omega$  determinations for  $\text{Li} + \text{Cl}_2$  and  $\text{Br}_2$  at lower resolution than that of Gillen, et. al. (1971) because they employed crossed thermal beams. They reported a significant coupling of the recoil angular and energy distributions from  $\text{Li} + \text{Cl}_2$  with higher product recoil energies favored at lower scattering angles. However, they failed to resolve similar coupling in  $\text{K} + \text{Br}_2$ , and the higher resolution data of Gillen, et. al. (1971) show only very weak coupling in  $\text{K} + \text{I}_2$ . Sholeen, et. al. (1976) review the somewhat unsatisfactory status of existing trajectory calculations for these reactions based on potential surfaces suggested by the electron transfer model and point out that the published data and other unpublished measurements [referenced in Siska (1973) and Grice (1975)] represent a stiff test of our ultimate ability to understand the alkali atom plus halogen molecule reaction dynamics in terms of the electronic structure rearrangement embodied in the electron transfer model. In particular, it is important to understand the recoil angle-energy coupling because the contrasting behaviors of related chemical systems suggest that this reaction feature might be especially sensitive to some subtle topological feature of the potential energy hypersurface.

In general, the reactions with the interhalogens are less well characterized. Moulton and Herschbach (1966) obtained indirect evidence that both product channels are formed in the  $\text{K} + \text{ICl}$  reaction. Mims, et. al. (1973) observed both product channels in reactions of alkaline earths with  $\text{ICl}$ , and reported that  $\text{MI}$  is formed with broader product angular distributions and higher recoil energies than is  $\text{MCl}$ . Kinematic blurring of the  $\text{LAB} \rightarrow \text{CM}$  transformation of their measured primitive product angular distributions precluded a more quantitative comparison of these CM recoil functions, however.



The  $\text{NO}_2$  molecule is included in Table IV because reaction cross sections comparable to those of the halogen molecules are predicted by the electron transfer model by virtue of the high electron affinity of  $\text{NO}_2$ . In contrast to the direct alkali atom plus halogen molecule reaction mechanism, however, a long-lived collision complex mechanism for the  $\text{Li} + \text{NO}_2$  reaction is suggested by the much larger exoergicity for the association reaction to give  $\text{LiNO}_2$  than for the exchange reaction to give  $\text{LiO} + \text{NO}$ . This long-lived complex behavior is well-established in collisions of alkali atoms with other, nonreactive oxides [Ham, et. al. (1967), Ham and Kinsey (1970)]. The history of crossed beams studies of reactions of alkali atoms with  $\text{NO}_2$  is somewhat unusual. Herm and Herschbach (1970) found the differential surface ionization technique to be impractical with  $\text{NO}_2$  because of filament surface "poisoning". Product magnetic deflection-surface ionization analysis of the  $\text{Cs} + \text{NO}_2$  scattering failed to indicate formation of a "diamagnetic" species, whereas product electric deflection revealed a polar cesium-containing molecule. This led them to suggest that the ground electronic state of the alkali monoxides shifted from the  $^2\Pi$  symmetry known for  $\text{LiO}$  to  $^2\Sigma$  in the case of  $\text{CsO}$ , a suggestion which was confirmed by a matrix-isolation EPR study of Lindsay, et. al. (1974). Parrish and Herm (1971) subsequently successfully studied the  $\text{Li} + \text{NO}_2$  reaction by product magnetic deflection, and Sholeen and Herm (1976a) reported the product recoil velocity spectra shown in Fig. 6. Contrary to prior expectations of symmetry, the measured  $\text{LiO} (^2\Pi) + \text{NO}$  product angular distribution is sharply peaked forward in analogy to the halogen molecule reactions. Sholeen and Herm (1976a) suggest that this indicates reactions through the excited  $^3B_1$  as well as ground  $^1A_1$  electronic states of the  $\text{LiNO}_2$  intermediate.

#### IV.B.2. Metal Atom plus Organic Halide

The alkali atom plus methyl iodide reaction was one of the first to be studied by the crossed molecular beam technique. Indeed, these early studies [Herschbach, et. al. (1961); Herschbach (1962)] comprised the first experimental information on a CM product angular distribution. The qualitative features of the product angular distribution were correctly inferred in these very early studies, but the recoil energy distribution proved more troublesome. The initial estimate [Herschbach, et. al. (1961); Herschbach (1962)] that most of the reaction exoergicity appears as product internal excitation was in error because of a neglect of the insidious effect of the LAB  $\rightarrow$  CM Jacobian [Entemann and Herschbach (1967)]. As Fig. 7 illustrates, the experimental determination of the



recoil energy distributions has continued to be troublesome because of the awkward kinematics. The most careful study is that of Rulis and Bernstein (1972) for the  $\text{K} + \text{CH}_3\text{I}$  reaction who determined the KI recoil velocity spectra with a velocity selected K beam.

Bernstein and Rulis (1973) reviewed the experimental status of  $M + \text{CH}_3\text{I}$  studies. The variety of beam techniques applied to these reactions which are listed in Table V is impressive. In addition to simple angular distribution measurements, these include product recoil velocity spectra [Sholeen and Herm (1976b); Rulis and Bernstein (1972)], the dependence of the LAB angular distribution on collision energy [Rotzoll, et. al. (1975); Gonzalez-Urena and Bernstein (1974)], optical potential analysis of the attenuation of wide-angle elastic scattering [e.g., Harris and Wilson (1971)], product

magnetic deflection analysis [Sholeen and Herm (1976b)],  $\text{CH}_3\text{I}$  spatial orientation in a refocussing electric field to measure the steric effect [e.g. Brooks and Jones (1966); Beuhler, et. al. (1969); Marcelin and Brooks (1973)], integration over the in-plane and out-of-plane LAB product angular distribution to measure the energy dependence of the total reaction cross section [Gersch and Bernstein (1972); Litrak, et. al. (1974); Pace, et. al. (1977)], product electric deflection analysis of the rotational energy [Maltz and Herschbach (1967)] and polarization [Maltz, et. al. (1972); Hsu and Herschbach (1973)] as well as polarization-scattering angle correlation [Hsu, et. al. (1974)], and LIF determination of the product metal halide vibrational state distribution for the Ba atom reaction [Dagdigian, et. al. (1976)]. The collective reaction features of  $\text{M} + \text{CH}_3\text{I}$  have come to be described as a "rebound" mechanism wherein reaction is favored for relatively small impact parameter collisions with the iodine end of the  $\text{H}_3\text{C-I}$  bond which scatters the MI product predominately backward (e.g., Fig. 4) with a recoil velocity corresponding to a substantial fraction of the total reaction exoergicity (e.g., Figs. 4 and 7). All of these features are qualitatively consistent with the electron transfer model and the electronic structure of  $\text{CH}_3\text{I}$  whose LUMO is a strongly antibonding  $\sigma$ -orbital localized along the C-I bond. The zero or negative electron affinity of  $\text{CH}_3\text{I}$  is consistent with the smaller reactive impact parameters and total reaction cross section relative to the reactions with halogen molecules (the  $\text{M} + \text{CH}_3\text{I}$  total cross section is approximately gas kinetic) which favors backward scattering. The strongly antibonding nature of the LUMO imparts considerable C-I repulsion upon the electron transfer and accounts for the efficient conversion of reaction exoergicity into recoil energy which is observed.

The energy partitioning in these  $\text{M} + \text{I-CH}_2\text{-R}$  reactions is especially well-suited to perturbation treatments on the impulsive limit because of the repulsive energy release

character of these reactions [Parrish and Herm (1970); Harris and Herschbach (1971)]. In the two-body limit that this repulsive energy is impulsively released along the I-CH<sub>2</sub> bond, the MI CM recoil momentum would be independent of the identity of M or R in this family of reactions for a constant repulsive energy produced by the electron transfer. Figure 10 illustrates the similarity in measured alkali halide recoil momentum distributions for a series of M + I-CH<sub>2</sub>-R reactions. Herschbach (1973) has discussed the Gaussian shapes of these distributions and the weak trend with changing alkyl iodide in terms of the known alkyl iodide photodissociation spectrum [see also Pollak and Levine (1977)]. The model calculations of Parrish and Herm (1970) suggest that the degree of internal excitation of the alkyl radical product is especially sensitive to the reaction potential surface, i.e. the degree to which the actual energy partitioning deviates from the simple *impulsive limit*. Unfortunately, very little is known about this feature of the reaction energy partitioning. Bernstein and Rulis (1973) do cite indirect evidence which indicates little CH<sub>3</sub> excitation in the K + CH<sub>3</sub>I reaction. Dagidian, et. al. (1976) determined an average BaI vibrational excitation of only 18% of the Ba + CH<sub>3</sub>I reaction exoergicity by LIF. This suggests that the CH<sub>3</sub> product possesses more internal excitation than the BaI product based upon the recoil energy estimates from the primitive LAB BaI angular distribution measurements of Lin, et. al. (1973b) which are shown in Fig. 4. Since this is a surprising result of utmost importance to our understanding of the M + CH<sub>3</sub>I systems, it should be confirmed by product recoil velocity spectra measurements on Ba + CH<sub>3</sub>I. Assuming that it is true, it need not imply a corresponding high CH<sub>3</sub> excitation in the alkali atom plus CH<sub>3</sub>I reactions. The low resolution BaI LAB angular distributions reported by Lin, et. al. (1973b) are certainly similar to those observed in the alkali reactions, and unpublished product recoil velocity spectra reported in Parr (1977) for Sn + CH<sub>3</sub>I indicate similar



product recoil spectra for alkali and tin atoms plus  $\text{CH}_3\text{I}$ . Nevertheless, Dagidgian et. al. (1976) suggest that high  $\text{CH}_3$  internal excitation from  $\text{Ba} + \text{CH}_3\text{I}$  might be due to an intersection of the  $\text{BaI} + \text{CH}_3$  and  $\text{BaI}^+ + \text{CH}_3^-$  potential surfaces in the exit channel. This second electron transfer interaction is plausible for Ba (or other alkaline earth atoms) by virtue of the low ionization potential of  $\text{MI}$ , whereas it is unlikely in the alkali or tin atom systems.

The organic halides provided a particularly fruitful system for the establishment of chemical trends in total reaction rate constant measurements in the early M. Polanyi diffusion flame studies, and they have proven equally interesting in molecular beam studies in exhibiting a broad spectrum of reaction dynamic behaviors. Entemann and Kwei (1971), Entemann (1971), Goldbaum and Martin (1975), Wilson and Herschbach (1968), and Lin, et. al. (1973b) provide particularly interesting low resolution chemical studies of this type. In addition to  $\text{CH}_3\text{I}$ , the behavior of a few other reagents have proven especially interesting and are discussed below.

Di and tri-iodomethane show a strikingly different behavior from  $\text{CH}_3\text{I}$ . Only low resolution  $\text{MI}$  LAB product angular distributions are available for alkali atoms plus  $\text{CH}_2\text{I}_2$  and  $\text{CHI}_3$  [Entemann (1971); Lin, et. al. (1974b)]. These indicate that  $\text{CH}_2\text{I}_2$  behaves more like  $\text{I}_2$  than  $\text{CH}_3\text{I}$  in that forward scattering is favored, although the peaking is less sharp with  $\text{CH}_2\text{I}_2$  than with  $\text{I}_2$ . Lin, et. al. (1974b) report that  $\text{CHI}_3$  produces more sharply peaked forward product scattering than does  $\text{CH}_2\text{I}_2$ . They also point out that trends in the alkali atom plus various organic halide reaction dynamics correlate nicely with the corresponding known trends for dissociative electron attachment in these organic halides. These dissociative electron attachment studies indicate that the electron affinity increases and the repulsive energy along the carbon-halogen bond upon electron

attachment decreases as the number of halogens on the carbon increases. For a fixed number of halogens, an iodide is a better electron acceptor than a bromide which is better than a chloride. Lin, et. al. (1973b) reported LAB angular distributions of  $MI^+$  from crossed beams of Ba, Sr, or Ca and  $CH_2I_2$  obtained with an electron bombardment ionizer-quadrupole mass filter unit. They suggested that most of the  $MI^+$  signal observed arose from ionization of  $MI_2$  rather than MI product because: (1)  $MI_2$  as well as MI gives  $MI^+$  almost exclusively upon ionization; and (2) the  $MI^+$  angular distribution was only slightly broader than the calculated centroid angular distribution which suggested that the detected product was much heavier than the undetected product. This indicated that  $MI_2 + CH_2$  is an important product channel of the alkaline earth  $CH_2I_2$  reaction, although not necessarily the dominant channel since kinematic factors could render their measurements more sensitive to  $MI_2$  than MI. Dagidigian, et. al. (1976) subsequently reported the LIF spectrum of product BaI from  $Ba + CH_2I_2$ . Although they saw no LIF from  $BaI_2$  product, their results in conjunction with Lin, et. al. (1973b) suggest that  $BaI_2$  and BaI are formed in comparable yields in the  $Ba + CH_2I_2$  reaction since LIF may be insensitive to  $BaI_2$ .

The  $K + CF_3I$  reaction provided a surprising result with the report [Brooks (1969); Brooks (1973); Marcelin and Brooks (1973b), see Fig. 8] of an unusual steric effect. A strong steric effect in K [Brooks and Jones (1966); Marcelin and Brooks (1973 a and b)] and Rb [Beuhler, et. al. (1966); Beuhler, et. al. (1968); Beuhler, et. al. (1969)] +  $CH_3I$  had been established by spatial orientation of  $CH_3I$  in an electric refocussing field. For  $CH_3I$ , results agreed with intuitive expectations that reaction was strongly favored for approach of the metal atom on the iodine side of the  $H_3C-I$  molecule. In contrast,  $F_3C-I$  reacts to product KI for either orientation. Approach from the  $-I$  end scatters KI backward, whereas approach from the  $F_3C-$  end scatters KI forward. Rulis, et. al. (1974)

subsequently reported KI recoil velocity spectra which failed to show any appreciable coupling of the recoil angle and energy. This suggests that only one LUMO is important in the  $\text{CF}_3\text{I}$  case. The difference between the  $\text{F}_3\text{C-I}$  and  $\text{H}_3\text{C-I}$  cases suggests a greater delocalization of the LUMO in  $\text{F}_3\text{C-I}$  so that the electron transfer probability is less orientation dependent. Smith, et. al. (1977) have also recently reported the LIF spectrum of BaI from  $\text{Ba} + \text{CF}_3\text{I}$  which indicates a bimodal vibrational distribution with the BaI high vibrational component scattered more predominately forward. Since Rulis, et. al. (1974) report no angle-recoil energy coupling in  $\text{K} + \text{CF}_3\text{I}$ , this report suggest that the alkaline earth reaction dynamics are more complex than are the alkali; indirect evidence of Lin, et. al. (1973b) that BaIF as well as BaI is formed in the  $\text{Ba} + \text{CF}_3\text{I}$  reaction further supports this possibility. Again, the possibility of a second electron transfer in the alkaline earth atom reaction could account for this difference.

The alkali atom plus  $\text{CCl}_4$  reaction provides a classic example of a sideways peaked product angular distribution. The high symmetry of  $\text{CCl}_4$  suggests that this conical distribution could be a "rainbow" phenomenon associated with averaging the reactive trajectories over  $\text{CCl}_4$  orientations. The only published product recoil velocity data are those of Sholeen and Herm (1976b) on  $\text{Li} + \text{CCl}_4$ . Figure 7 illustrates the similar product recoil energy distributions from  $\text{Li} + \text{CH}_3\text{I}$  and  $\text{CCl}_4$ , which suggests comparable repulsive energy releases. Figure 7 indicates an average  $\text{Li} + \text{CCl}_4$  recoil energy which represents 31% of the energy available to the products of the  $\text{Li} + \text{CCl}_4$  reaction. Schmidt, et. al. (1976) recently reported the LIF spectrum of BaCl from  $\text{Ba} + \text{CCl}_4$ . They concluded that vibration (75%) and rotation (4%) of BaCl accounted for 79% of the reaction energy.

After subtracting an estimated  $\text{CCl}_3$  internal excitation, 6% of the reaction energy was left for  $\text{BaCl} + \text{CCl}_3$  recoil. Here again, these comparisons suggest different reaction mechanisms for alkali and alkaline earth atoms.

Sholeen and Herm (1976b) point out that the energy partitioning in the  $\text{Li} + \text{CH}_3\text{NO}_2 \rightarrow \text{LiNO}_2 + \text{CH}_3$  reaction shown in Fig. 7 is surprising. In contrast to  $\text{CH}_3\text{I}$  or  $\text{CCl}_4$ , the  $\text{CH}_3\text{NO}_2$  LUMO is a  $\pi^*$  ( $b_1$ ) orbital weakly antibonding along the N-O bonds in the nitro group which cannot account for any substantial repulsive energy release along the C-N bond. However, the  ${}^2B_1$   $\text{CH}_3\text{NO}_2^-$  anion state produced by an electron transfer into this LUMO dissociates adiabatically into  $\text{CH}_3$  plus the excited  $B_1$  state of  $\text{NO}_2^-$ . The next highest orbital in  $\text{CH}_3\text{NO}_2$  is probably a  $\sigma^*$  ( $a_1$ ) which is strongly antibonding along the C-N bond. An electron transfer into this orbital would produce a  ${}^2A_1$   $\text{CH}_3\text{NO}_2^-$  state correlating asymptotically with  $\text{CH}_3$  plus the ground state of  $\text{NO}_2^-$ . The observed  $\text{LiNO}_2 + \text{CH}_3$  product recoil energy indicates the participation of this  $\text{Li}^+-\text{CH}_3\text{NO}_2^-$  charge transfer state, possibly due to an internal conversion from the  ${}^2B_1$  anion state produced initially. Here again, Herm, et. al. (1973) have emphasized the contrasting dynamics of alkali and alkaline earth atom reactions with nitromethane. It is less surprising here, however, because the much stronger monoxide bond in the alkaline earth family favors the metal monoxide product channel which is energetically inaccessible in the alkali atom reactions.

#### IV.B.3. Metal Atom plus Inorganic Polyhalide

Molecular beam studies of the reactive scattering of alkali atoms from various inorganic polyhalides are listed in Table VI. The history of these studies is interesting and was recently reviewed in Behrens, et. al. (1976b). With the exceptions of  $\text{SCl}_2$ ,  $\text{PCl}_3$ , and



$\text{PBr}_3$ , the reactions listed in Table VI appear to proceed via formation of long-lived or oscillating complexes. This is particularly well established for the  $\text{Cs} + \text{SF}_6 \rightarrow \text{CsF} + \text{SF}_5$  reaction. Here PRVS show the forward-backward product angular distribution symmetry expected of a long-lived complex, and the product recoil energy distribution is consistent with an TST equipartitioning of reaction energy over degrees of freedom within the complex [Riley and Herschbach (1973)]. Product electric resonance spectra indicates a Boltzman distribution in CsF vibration levels. Both the magnitude of this CsF vibrational temperature and its variation with  $\text{SF}_6$  beam temperature also indicate a reaction energy equipartitioning within the complex [Bennewitz, et. al. (1971) and Freund, et. al. (1971)]. Similar experiments on  $\text{Li} + \text{SF}_6 \rightarrow \text{LiF} + \text{SF}_5$  also indicate a Boltzman distribution over LIF vibrational levels [Mariella, et. al. (1973)]. Here, however, both the magnitude of the LIF vibrational temperature and its insensitivity to the  $\text{SF}_6$  beam temperature are inconsistent with an equipartitioning of reaction energy. This is surprising and still not well understood since the LiF PRVS from the same reaction is consistent with a long-lived complex, TST energy-equipartitioning reaction mechanism [Behrens, et. al. (1976b)].

Alkali atom reactions with  $\text{SnCl}_4$  are interesting in that both alkali chloride (MCl) and alkali chlorostannite ( $\text{MCl} \cdot \text{SnCl}_2$ ) products apparently form. The evidence for this is strong but indirect since the surface ionization detection technique cannot distinguish between these two possible products. The possibility of both products channels was first suggested by Whitehead, et. al. (1972b). Product recoil velocity spectra measurements on K, Rb, and Cs +  $\text{SnCl}_4$  by Riley and Herschbach (1973) and subsequently on Li +  $\text{SnCl}_4$  by Behrens, et. al. (1976b) provided much stronger kinematic evidence for both product channels because the measured bimodal product recoil velocity spectra were well fit by a

long-lived, TST energy equipartitioning complex which could decompose into either product channel. Behrens, et. al. (1976b) obtained some evidence that the  $\text{LiCl} \cdot \text{SnCl}_2 + \text{Cl}$  product angular distribution is less sharply peaked than is that of the  $\text{LiCl} + \text{SnCl}_3$  product channel, although this is not established with high confidence due to severe kinematic blurring of the  $\text{LAB} \rightarrow \text{CM}$  transformation for the case of the  $\text{LiCl} \cdot \text{SnCl}_2$  product. They point out, however, that these contrasting angular distributions would correlate nicely with different plausible angular momenta couplings within the complex leading to decomposition into the alternate product channels.

#### IV.B.4. Metal Atom plus Hydrogen Halide

The status of product recoil angular and energy distribution measurements on K (the best studied metal) plus H-, D-, and T-Br has been review by Kinsey (1972), and Table VII lists the metal atom + HX studies. Grosser, et. al. (1965), Riley, et. al. (1967), and Gillen, et. al. (1969) studied the  $\text{K} + \text{HBr}$  and  $\text{K} + \text{DBr}$  reactions using velocity selection of the K-beam and velocity analysis of the  $\text{KBr}$  product. They subjected hundreds of individual LAB data points to a careful numerical  $\text{LAB} \rightarrow \text{CM}$  inversion analysis to extract the CM distributions. Owing to the extremely unfavorable kinematics, a broad range of CM functions were compatible with the data. Nevertheless, their results indicate that the  $\text{K} + \text{HBr}$  reaction favors backward scattering whereas the  $\text{K} + \text{DBr}$  reaction yields a practically isotropic angular distribution with a slight preference for forward scattering despite the fact that the  $\text{HBr}$  total reaction cross reaction is 40% larger than that of  $\text{DBr}$ . Martin and Kinsey (1967) developed a method for detecting atomic tritium (but not TBr) by adsorbing it on a molybdenum trioxide surface, and used this technique to measure the LAB angular distribution of T from  $\text{K}$  (and  $\text{Cs}$ ) + TBr. Although neither velocity selection

nor analysis was employed, the very favorable kinematics in this study clearly indicated that their measured LAB T product angular distribution implied that the K + TBr reaction favors backward scattering of the KBr. It is still not clear why these product angular distribution do not follow a simple trend in the HBr, DBr, TBr isotopic sequence. This may be due to some unusual quantum effect associated with the large zero point energies or limited number of product channel partial waves in these reactions.

Perhaps the most interesting recent studies on the alkali atom reactions are the series of papers by Odiorne and Brooks (1969), Odiorne, et. al. (1971), and Pruett, et. al. (1974 and 1975). These indicate that the K + HCl total reaction cross section is increased by increasing the reactant relative translational or vibrational energy, but that vibrational energy is more effective. Pruett, et. al. (1975) have emphasized the importance of expressing results in terms of an average state-of-state transition rate. They report that the K + HCl reaction rate constant increases monotonically as the collision energy increases from 8.8 to 50.5 kJ/mole, but that the ratio of this rate constant to the density of possible product states shows a simple exponential decay with the square root of the energy in excess of thermodynamic threshold.

Much more detailed information is potentially available on the alkaline earth atom reactions because of the ability to deploy the LIF technique. Cruse, et. al. (1973), for example, have reported LIF determination of the BaX vibrational level distributions in reactions of Ba with HF, HCl, HBr, and HI. Because of the relatively small exoergicities of these reactions, however, the implications of the results are somewhat obscured by the small uncertainties in the barium monohalide bond dissociation energies. For example, the most recent  $D_0^0$  (BaX) determination [Hildebrand (1977)] indicates that the Ba + HCl reaction is only marginally exoergic and the Ba + HBr reaction is actually endoergic.

Thus, the interpretation of the results of Cruse, et. al. (1973) is critically dependent on the energy distribution of species which react which is poorly characterized in the absence of experimental control of reactant energy. This is especially critical for the Ba + HF reaction because Cruse, et. al. (1973) report that a surprisingly low 12% of the reaction energy appears in the BaF vibration on the average. However, this is based upon a  $D_0^{\circ}$  (BaF) from chemiluminescent spectra which is 23.9 kJ/mole higher than the best high-temperature gaseous equilibrium value [Hildebrand (1968)]. Gole and Preuss (1977) have recently emphasized the need for careful temperature dependence studies in chemiluminescent bond energy determinations, and have reported an activation energy of  $\sim 17$  kJ/mole for the Sr + F<sub>2</sub> chemiluminescent reaction. Pruett and Zare (1976) have also reported a particularly striking study of the Ba + HF ( $v = 1$ ) reaction wherein an HF laser was employed for reactant excitation and LIF determined the distribution over BaF product vibrational states. They report that an average of 57% of the HF vibrational energy appears as BaF vibrational energy.

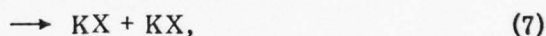
#### IV.C. Alkali Dimers plus Various Halides

Studies of reactions of the alkali dimers with halogen-containing compounds are listed in Table VIII. In contrast to the variety of beam techniques which have been applied to the study of alkali atom reactions, the alkali dimer studies have been confined to LAB product angular distribution measurements. However, the kinematic situation is better than in many of the simple primitive LAB product angular distribution measurements in the alkali atom reaction families because the alkali dimers are produced by condensation in a nozzle expansion so that the beam has a sharp speed distribution. Thus, these studies have provided semi-quantitative CM recoil functions, particularly for the product angular



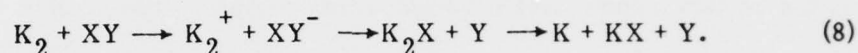
distributions, and have certainly characterized the qualitative reaction mechanisms. Most of these studies are due to R. Grice and his co-workers, and the results have been reviewed in Grice (1975).

The reactions of  $K_2$  with the halogen molecules proceed with total cross sections comparable to those of  $K + X_2$  to scatter  $KX$  predominately forward (relative to the direction of the original  $K_2$  velocity). This immediately indicates that formation of an alkali halide, alkali atom, and halogen atom (Reaction (6)) must dominate over formation of two alkali halides (Reaction (7)),



because momentum conservation would dictate symmetry about  $\theta = 90^\circ$  for reaction (7) irrespective of the reaction dynamics. Indeed, Whitehead, et. al. (1972a and 1973) have shown that the approximate K product LAB angular distribution from Reaction (6) can be obtained by comparing the sum of  $K_2$  plus K scattering with a  $K_2$  beam with the elastic scattering of a supersonic K-beam, although this technique is only practical in the case of large total reaction cross sections. For  $K_2 + Br_2$ ,  $I Br$ , and  $BrCN$ , Whitehead, et. al. (1972a and 1973) report that both the K and  $KX$  product angular distributions are peaked forward with comparable product flux intensities, but that the K-product differential cross section falls off more rapidly at wider angles. This indicates that Reaction (6) is the dominant product channel with reaction at large impact parameters producing small deflection angles, but that Reaction (7) probably occurs as well for smaller impact parameter collisions. The large reaction cross section and other similarities to the alkali atom plus halogen molecule reactions for this reaction of a singlet spin  $K_2$  molecule is no

more surprising than was the analogous behavior for the alkaline earth atoms. Here again, the electron transfer model accounts nicely for the observations by virtue of the low  $K_2$  ionization potential. Thus, the reaction mechanism may be viewed as

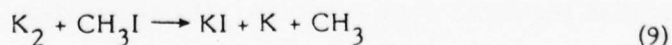


Lin, et. al. (1974a) actually report that the K-product flux in the forward direction from  $K_2 + I_2$  exceeds that of KI which suggests that, for this reaction, the  $K_2^+$  dissociates as fast or faster than the  $I_2^-$  resulting in a stripping type mechanism for the K product.

For all of the reactions listed in Table VIII, the potassium halide product peaks in the forward direction defined by the original  $K_2$  velocity. This is sometimes accompanied by a secondary peak in the backward direction indicative of an osculating complex. The reactions with the polyhalides typically convert both potassium atoms into potassium halide products. This may account for the entries in Table VIII of reactions with  $BBr_3$  and  $SiCl_4$ ; the cross sections for reactions of alkali atoms with these reagents are too small to permit beam studies. This unanimity of mechanistic behavior contrasts sharply with the broad spectrum of dynamical behaviors observed in the alkali atom reactions with this spectrum of reagents. Grice and his co-workers have pointed out the importance of a second electron transfer in all of these systems. The ionization potential of  $K_2X$  can be comparable to or less than that of  $K_2$  so that an electron transfer from  $K_2X$  to the departing radical can give rise to an attractive interaction in the product channel which is not present in the alkali atom reactions. The observation of chemiluminescence [Struve, et. al. (1975)] and, more significantly, chemi-ionization [Lin and Grice (1973), Lin, et. al. (1974c)] in some of these systems is a direct manifestation of this second electron jump.

Nevertheless, this second electron transfer doesn't seem to fully account for the difference between the  $K_2$  and K reaction behaviors. In particular, the forward scattered KI component from the  $K_2 + CH_3I$  reaction requires additional explanation. As noted earlier, the barium monohalides have ionization potentials comparable to or lower than that of a barium atom so that this second electron transfer should be operative in barium atom reactions as well. Indeed, it was noted previously that differences in the details of energy partitioning between some alkali and alkaline earth atom reactions suggested that this second electron transfer gave rise to product channel attractions in the alkaline earth systems. Again, a more direct manifestation of this effect was noted in the chemi-ionization reactions of Ca, Sr, and Ba with the halogen molecules [Diebold, et. al. (1977)]. Nevertheless, Fig. 4 illustrates that the BaI product angular distribution from  $Ba + CH_3I$  is similar to that of alkali atom reactions and favors backward scattering.

Thus, it is at least plausible that the "double rebound" mechanism depicted schematically in Fig. 11 could account for the unusual  $K_2 + CH_3I$  product angular distribution. This is drawn for collinear approach; other geometries would serve to broaden the distribution. Reaction is initiated by approach of  $K_2$  on the I- end of  $CH_3I$  in accordance with the steric effect established for the alkali reactions. The initial electron transfer ejects the methyl radical and the iodine atom (more properly  $I^-$  anion after the electron transfer) is propelled toward the  $K_2$ . However, a second rebound reaction of I with  $K_2$  causes the KI to recoil in the direction of the original  $K_2$ . Since the



reaction is only 46.2 kJ/mole exoergic, this simple double rebound picture might be overly simplistic. The true explanation might require some combination of the second electron transfer and double rebound mechanism. Nevertheless, it seems likely that this double rebound mechanism is an important component of the  $K_2 + CH_3I$  reaction dynamics because it accounts for the contrasting  $K_2$  and Ba behaviors and is nicely consistent with the results of Struve, et. al. (1975) who report a preference for reversal in halogen atom direction in the reactions of halogen atoms with  $K_2$ .



## V. Closing Remarks

Related beam studies of reactions of non-alkali metal atoms with various oxides and of other reactions of alkali dimers are listed in Tables IX and X. It seemed inappropriate to discuss these studies because they are somewhat outside the subject matter implied by the title of this volume.

It seems appropriate in closing to note some especially important studies which are needed to complete our understanding of gas-phase, thermal-energy metal atom chemistry. The various beam techniques, especially PRVS measurements, should be applied to some of the reactions of alkaline earth atoms with halogen-containing compounds in order to compliment the completely resolved MX vibrational distributions which can be and are being provided by LIF studies. It also seems important to extend these studies to other metal atoms (and semi-metals such as boron atoms) in order to assess the sensitivity or insensitivity of the reaction dynamics to the electronic structure of the metal atoms. The recent LIF studies seem to suggest significant differences between the reaction dynamics of alkali and alkaline earth atoms. In this regard, it is the author's opinion that the alkalis will prove to be representative of a typical metal atom and that the alkaline earths are unusual because of the ease of the "second electron transfer".

PRECEDING PAGE BLANK-NOT FILMED

## REFERENCES

- Ackerman, M., Greene, E. F., Moursund, A. L., and Ross, J. (1964). J. Chem. Phys. 41, 1183.
- Airey, J. R., Greene, E. F., Kodera, K., Reck, G. P., and Ross, J. (1967a). J. Chem. Phys. 46, 3287.
- Airey, J. R., Greene, E. F., Reck, G. P., and Ross, J. (1967b). J. Chem. Phys. 46, 3295.
- Aniansson, G., Creaser, R. P., Held, W. D., Holmlid, L., and Toennies, J. P. (1974). J. Chem. Phys. 61, 5381.
- Annis, B. K. and Datz, S. (1977). J. Chem. Phys. 66, 4468.
- Armstrong, W. D., Conley, R. J., Creaser, R. P., Greene, E. F., and Hall, R. B. (1975). J. Chem. Phys. 63, 3349.
- Batalli-Cosmovici, C. and Michel, K.-W. (1971). Chem. Phys. Letters 11, 245.
- Batalli-Cosmovici, C. and Michel, K. W., (1972). Chem. Phys. Letters 16, 77.
- Beck, D., Greene, E. F., and Ross, J. (1962). J. Chem. Phys. 37, 2895.
- Behrens, R., Jr., Freedman, A., Herm, R. R., and Parr, T. P. (1975). J. Chem. Phys. 63, 4622.
- Behrens, R., Jr., Freedman, A., Herm, R. R., and Parr, T. P. (1976a). J. Am. Chem. Soc. 98, 294.

PRECEDING PAGE BLANK-NOT FILMED

- Behrens, R., Jr., Herm, R. R., and Sholeen, C. M. (1976b). J. Chem. Phys. 65, 4791.
- Bennewitz, H. G., Haerten, R., and Muller, G. (1971). Chem. Phys. Letters 12, 335.
- Bernstein, R. B., and Levine, R. D. (1972). J. Chem. Phys. 57, 434.
- Bernstein, R. B. and Rulis, A. M. (1973). Faraday Disc. Chem. Soc. 55, 293.
- Beuhler, R. J., Jr. and Bernstein, R. B. (1968) Chem. Phys. Letters 2, 166.
- Beuhler, R. J. and Bernstein, R. B. (1969). J. Chem. Phys. 51, 5305.
- Beuhler, R. J., Jr., Bernstein, R. B., and Kramer, K. H. (1966). J. Amer. Chem. Soc. 88, 5331.
- Birely, J. H. and Herschbach, D. R. (1966). J. Chem. Phys. 44, 1690.
- Birely, J. H., Herm, R. R., Wilson, K. R., and Herschbach, D. R. (1967). J. Chem. Phys. 47, 993.
- Birely, J. H., Entemann, E. A., Herm, R. R., and Wilson, K. R. (1969). J. Chem. Phys. 51, 5461.
- Bromberg, E. E. A., Proctor, A. E., and Bernstein, R. B. (1975). J. Chem. Phys. 63, 3287.
- Brooks, P. R. (1969). J. Chem. Phys. 50, 5031.
- Brooks, P. R. (1973). Faraday Disc. Chem. Soc. 55, 299.
- Brooks, P. R. and Jones, E. M. (1966). J. Chem. Phys. 45, 3449.

- Brooks, P. R., Jones, E. M., and Smith, K. (1969). *J. Chem. Phys.* 51, 3073.
- Bull, T. H. and Moon, P. B. (1954). *Disc. Faraday Soc.* 17, 54.
- Bullitt, M. K., Fischer, C. H., and Kinsey, J. L. (1974). *J. Chem. Phys.* 60, 478.
- Case, D. A. and Herschbach, D. R. (1976). *J. Chem. Phys.* 64, 4212.
- Cosmovici, C. B., D'Anna, E., D'Innocenzo, A., Leggieri, G., Perrone, A., and Dirscherl, R. (1977). *Chem. Phys. Letters* 47, 241.
- Crim, E. F., and Fisk, G. A. (1976). *J. Chem. Phys.* 65, 2480.
- Crim, E. F., Chou, M. S., and Fisk, G. A. (1973). *Chem. Phys.* 2, 283.
- Crim, E. F., Bente, H. B., and Fisk, G. A. (1974). *J. Phys. Chem.* 78, 2438.
- Cruse, H. W., Dagdigian, P. J., and Zare, R. N. (1973). *Faraday Disc. Chem. Soc.* 55, 277.
- Dagdigian, P. J. and Zare, R. N. (1974). *J. Chem. Phys.* 61, 2464.
- Dagdigian, P. J., Cruse, H. W., Schultz, A., and Zare, R. N. (1974). *J. Chem. Phys.* 61, 4451.
- Dagdigian, P. J., Cruse, H. W., and Zare, R. N. (1975). *J. Chem. Phys.* 62, 1824.
- Dagdigian, P. J., Cruse, H. W., and Zare, R. N. (1976). *Chem. Phys.* 15, 249.
- Datz, S., and Taylor, E. H. (1956). *J. Chem. Phys.* 25, 389, 395.
- Datz, S. and Mintrun, R. E. (1964). *J. Chem. Phys.* 41, 1153.



Datz, S., Herschbach, D. R., and Taylor, E. H. (1961). J. Chem. Phys. 35, 1549.

Diebold, G. J., Engelke, F., Lee, H. U., Whitehead, J. C., and Zare, R. N. (1977). Chem. Phys. 30, 265.

Dirscherl, R. and Michel, K. W. (1976). Chem. Phys. Letters 43, 547.

Donohue, T., Chou, M. S., and Fisk, G. A. (1972). J. Chem. Phys. 57, 2210.

Donohue, T., Chou, M. S., and Fisk, G. A. (1973). Chem. Phys. 2, 271.

Entemann, E. A. (1971). J. Chem. Phys. 55, 4872.

Entemann, E. A. and Herschbach, D. R. (1967). Disc. Faraday Soc. 44, 289.

Entemann, E. A. and Kwei, G. H. (1971). J. Chem. Phys. 55, 4879.

Farrar, J. M. and Lee, Y. T. (1974). Ann. Rev. Phys. Chem. 25, 357.

Fisk, G. A., McDonald, J. D., and Herschbach, D. R. (1967). Disc. Faraday Soc. 44, 228.

Flueudy, M. A. D. and Lawley, K. P. (1973). Chemical Applications of Molecular Beam Scattering (Chapman and Hall, London).

Foreman, P. B., Kendall, G. M., and Grice, R. (1972a) Mol. Phys. 23, 117 .

Foreman, P. B., Kendall, G. M., and Grice, R. (1972b). Mol. Phys. 23, 127.

Foreman, P. B., Kendall, G. M., and Grice, R. (1973a). Mol. Phys. 25, 529.

Foreman, P. B., Kendall, G. M., and Grice, R. (1973b). Mol. Phys. 25, 551.

- Fraser, R. G. J. (1937). Molecular Beams (Methuen and Company Ltd., London).
- Freedman, A., Behrens, R., Jr., Parr, T. P., and Herm, R. R. (1976). J. Chem. Phys. 65, 4739.
- Freund, S. M., Fisk, G. A., Herschbach, D. R., and Klemperer, W. (1971). J. Chem. Phys. 54, 2510.
- Gersh, M. E. and Bernstein, R. B. (1971). J. Chem. Phys. 55, 4661.
- Gersh, M. E. and Bernstein, R. B. (1972). J. Chem. Phys. 56, 6131.
- Gillen, K. T. and Bernstein, R. B. (1970). Chem. Phys. Letters 5, 275.
- Gillen, K. T., Riley, C., and Bernstein, R. B. (1969). J. Chem. Phys. 50, 4019.
- Gillen, K. T., Rulis, A. M., and Bernstein, R. B. (1971). J. Chem. Phys. 54, 2831.
- Goldbaum, R. H. and Martin, L. R. (1975). J. Chem. Phys. 62, 1181.
- Gole, J. L. and Preuss, D. R. (1977). J. Chem. Phys. 66, 3000.
- Gonzalez Urena, A. and Bernstein, R. B. (1974). J. Chem. Phys. 61, 4101.
- Gonzalez Urena, A., Bernstein, R. B., and Phillips, G. R. (1975). J. Chem. Phys. 62, 1818.
- Gordon, R. J., Herm, R. R., and Herschbach, D. R. (1968). J. Chem. Phys. 49, 2684.
- Gowenlock, B. G., Johnson, C. A. F., and Parker, J. E. (1976). Comprehensive Chemical Kinetics, C. H. Bamford and C. F. H. Tipper, Eds. (Elsevier Scientific Publishing Company, New York), Chap. 4.

Greene, E. F. and Ross, J. (1968). *Science* 159, 587.

Greene, E. F., Roberts, R. W., and Ross, J. (1960). *J. Chem. Phys.* 32, 940.

Greene, E. F., Moursund, A. L., and Ross, J. (1966). *Adv. Chem. Phys.* 10, 135.

Greene, E. F., Hoffman, L. F., Lee, M. W., Ross, J., and Young, C. E. (1969). *J. Chem. Phys.* 50, 3450.

Greene, E. F., Hall, R. B. and Sondergaard, N. A. (1977). *J. Chem. Phys.* 66, 3171.

Grice, R. (1975). *Adv. Chem. Phys.* 30, 247.

Grice, R. and Empedocles, P. B. (1968). *J. Chem. Phys.* 48, 5352.

Grice, R., Cosandey, M. R., and Herschbach, D. R. (1968). *Ber. Bunsenges. Phys. Chem.* 72, 975.

Grice, R., Mosch, J. E., Safron, S. A., and Toennies, J. P. (1970). *J. Chem. Phys.* 53, 3376.

Grosser, A. E. (1967). *Rev. Sci. Instr.* 38, 257.

Grosser, A. E. and Bernstein, R. B. (1965). *J. Chem Phys.* 43, 1140.

Grosser, A. E., Blythe, A. R., and Bernstein, R. B. (1965). *J. Chem. Phys.* 42, 1268.

Haberman, J. A., Anlauf, K. G., Bernstein, R. B., and Van Itallie, F. J. (1972). *Chem. Phys. Letters* 16, 442.

Ham, D. O. and Kinsey, J. L. (1970). *J. Chem. Phys.* 53, 285.

- Ham, D. O., Kinsey, J. L., and Klein, F. S. (1967). *Disc. Faraday Soc.* 44, 174.
- Hardin, D. R., Woodall, K. B., and Grice, R. (1973a). *Mol. Phys.* 26, 1057.
- Hardin, D. R., Woodall, K. B., and Grice, R. (1973b) *Mol. Phys.* 26, 1073.
- Harris, R. M. and Herschbach, D. R. (1971). *J. Chem. Phys.* 54, 3652.
- Harris, R. M. and Wilson, J. F. (1971). *J. Chem. Phys.* 54, 2088.
- Helbing, R. K. B. and Rothe, E. W. (1968). *J. Chem. Phys.* 48, 3945.
- Herm, R. R. and Herschbach, D. R. (1965). *J. Chem. Phys.* 43, 2139.
- Herm, R. R. and Herschbach, D. R. (1970). *J. Chem. Phys.* 52, 5783.
- Herm, R. R., Gordon, R., and Herschbach, D. R. (1964). *J. Chem. Phys.* 41, 2218.
- Herm, R. R., Lin, S.-M., and Mims, C. A. (1973). *J. Phys. Chem* 77, 2931.
- Herschbach, D. R. (1960). *J. Chem. Phys.* 33, 1870.
- Herschbach, D. (1961). *The Vortex* 22, 348.
- Herschbach, D. R. (1962). *Disc. Faraday Soc.* 33, 149.
- Herschbach, D. R. (1965). *Appl. Optics, Suppl. 2 (Chemical Lasers)*, 128.
- Herschbach, D. R. (1966). *Adv. Chem. Phys.* 10, 319.
- Herschbach, D. R. (1973). *Faraday Disc. Chem. Soc.* 55, 233.



Herschbach, D. R., Kwei, G. H., and Norris, J. A. (1961). *J. Chem. Phys.* 34, 1842.

Hildebrand, D. L. (1968). *J. Chem. Phys.* 48, 3657.

Hildebrand, D. L. (1977). *J. Chem. Phys.* 66, 3526.

Hill, R. M. and Gallagher, T. F. (1975). *Phys. Rev. A* 12, 451.

Holmlid, L. and Rynefors, K. (1977). *Chem. Phys.* 19, 261.

Hostettler, S. U. and Bernstein, R. B. (1960). *Rev. Sci. Instr.* 31, 872.

Hsu, D. S. Y. and Herschbach, D. R. (1973). *Faraday Disc. Chem. Soc.* 55, 116.

Hsu, D. S. Y., McClelland, G. M., and Herschbach, D. R., (1974). *J. Chem. Phys.* 61, 4927.

Hsu, D. S. Y., Weinstein, N. D., and Herschbach, D. R. (1975). *Mol. Phys.* 29, 257.

Jones, E. M. and Brooks, P. R. (1970). *J. Chem. Phys.* 53, 55.

King, D. L. and Herschbach, D. R. (1973). *Faraday Disc. Chem. Soc.* 55, 331.

King, D. L., Loesch, H. J., and Herschbach, D. R. (1973). *Faraday Disc. Chem. Soc.* 55, 222.

Kinsey, J. L. (1966). *Rev. Sci. Instr.* 37, 61.

Kinsey, J. L. (1972). *MTP International Review of Science*, (Butterworths, London), Physical Chemistry, Series One, Vol. 9, Chap. 6.

Kiney, J. L. (1977). *J. Chem. Phys.* 66, 2621.

- Kinesey, J. L., Kwei, G. H., and Herschbach, D. R. (1976). *J. Chem. Phys.* 64, 1914.
- Kwei, G. H. and Herschbach, D. R. (1969). *J. Chem. Phys.* 51, 1742.
- Kwei, G. H., Norris, J. A., and Herschbach, D. R. (1970). *J. Chem. Phys.* 52, 1317.
- Kwei, G. H., Lees, A. B., and Silver, J. A. (1971). *J. Chem. Phys.* 55, 4561.
- Langmuir, I. and Kingdom, K. H. (1925). *Proc. Roy. Soc. (London)* A107, 61.
- Lee, Y. T., McDonald, J. D., LeBreton, P. R., and Herschbach, D. R. (1969). *Rev. Sci. Instr.* 40, 1402.
- Lee, Y. T., Gordon, R. J., and Herschbach, D. R. (1971). *J. Chem. Phys.* 54, 2410.
- Lees, A. B. and Kwei, G. H. (1973). *J. Chem. Phys.* 58, 1710.
- Lin, S.-M. and Grice, R. (1973). *Faraday Disc. Chem. Soc.* 55, 370.
- Lin, S.-M., Mims, C. A., and Herm, R. R. (1973a) *J. Chem. Phys.* 58, 327.
- Lin, S.-M., Mims, C. A., and Herm, R. R. (1973b). *J. Phys. Chem.* 77, 569.
- Lin, S.-M., Mascord, D. J., and Grice, R. (1974a). *Mol. Phys.* 28, 957.
- Lin, S.-M., Mascord, D. J., and Grice, R. (1974b). *Mol. Phys* 28, 975.
- Lin, S.-M., Whitehead, J. C., and Grice, R. (1974c). *Mol. Phys.* 27, 741.
- Lindsay, D. M., Herschbach, D. R., and Kwiram, A. L. (1974). *J. Chem. Phys.* 60, 315.

Litvak, H. E., Gonzalez Urena, A., and Bernstein, R. B. (1974). J. Chem. Phys. 61, 738, 4091.

Loesch, H. J. and Herschbach, D. R. (1972). J. Chem. Phys. 57, 2038.

Maltz, C. (1969). Ph.D. thesis, Harvard University.

Maltz, C. and Herschbach, D. R. (1967). Disc. Faraday Soc. 44, 176.

Maltz, C., Weinstein, N. D., and Herschbach, D. R. (1972). Mol. Phys. 24, 133.

Marcelin, G. and Brooks, P. R. (1973a). Faraday Disc. Chem. Soc. 55, 318.

Marcelin, G. and Brooks, P. R. (1973b). J. Amer. Chem. Soc. 95, 7885.

Marcus, R. A. (1973). Disc. Faraday Soc. 55, 379, 381.

Marcus, R. A. (1975). J. Chem. Phys. 62, 1372.

Mariella, R. P., Jr., Herschbach, D. R., and Klemperer, W. (1973). J. Chem. Phys. 58, 3785.

Mariella, R. P., Jr., Herschbach, D. R., and Klemperer, W. (1974). J. Chem. Phys. 61, 4575.

Martin, L. R. and Kinsey, J. L. (1967). J. Chem. Phys. 46, 4834.

Mascord, D. J., Cruse, H. W., and Grice, R. (1976). Mol. Phys. 32, 131.

Miller, W. B., Safron, S. A., and Herschbach, D. R. (1967). Disc. Faraday Soc. 44, 108, 292.

- Miller, W. B., Safron, S. A., and Herschbach, D. R. (1972). *J. Chem. Phys.* 56, 3581.
- Mims, C. A. and Brophy, J. H. (1977). *J. Chem. Phys.* 66, 1378.
- Mims, C. A., Lin, S.-M., and Herm, R. R. (1972). *J. Chem. Phys.* 57, 3099.
- Mims, C. A., Lin, S.-M., and Herm, R. R. (1973). *J. Chem. Phys.* 58, 1983.
- Minturn, R. E., Datz, S., and Becker, R. L. (1966). *J. Chem. Phys.* 44, 1149.
- Mosch, J. E., Safron, S. A., and Toennies, J. P. (1974). *Chem. Phys. Letters* 29, 7.
- Mosch, J. E., Safron, S. A., and Toennies, J. P. (1975). *Chem. Phys.* 8, 304.
- Moulton, M. C. and Herschbach, D. R. (1966). *J. Chem. Phys.* 44, 3010.
- Odiorne, T. J. and Brooks, P. R. (1969). *J. Chem. Phys.* 51, 4676.
- Odiorne, T. J. Brooks, P. R., and Kasper, J. V. V. (1971). *J. Chem. Phys.* 55, 1980.
- Pace, S. A., Pang, H. F., and Bernstein, R. B. (1977). *J. Chem. Phys.* 66, 3635.
- Parks, E. K., Hansen, N. J., and Wexler, S. (1973a). *J. Chem. Phys.* 58, 5489.
- Parks, E. K., Wagner, A., and Wexler, S. (1973b). *J. Chem. Phys.* 58, 5502.
- Parr, T. P. (1977). Ph. D. thesis, University of California, Berkely.
- Parrish, D. D. and Herm, R. R. (1968). *J. Chem. Phys.* 49, 5544.
- Parrish, D. D. and Herm, R. R. (1969). *J. Chem. Phys.* 51, 5467.



- Parrish, D. D. and Herm, R. R. (1970). J. Chem. Phys. 53, 2431.
- Parrish, D. D. and Herm, R. R. (1971). J. Chem. Phys. 54, 2518.
- Pasternack, L. and Dagdigian, P. J. (1976). J. Chem. Phys. 65, 1320.
- Pechukas, P., Light, J. C., and Rankin, C. (1966). J. Chem. Phys. 44, 794.
- Piper, L. G., Hellemans, L., Sloan, J., and Ross, J. (1972). J. Chem. Phys. 57, 4742.
- Polanyi, J. C. (1972). Accts. Chem. Research 5, 161.
- Pollak, E. and Levine, R. D. (1977). Chem. Phys. 21, 61.
- Pruett, J. G. and Zare, R. N. (1976). J. Chem. Phys. 64, 1774.
- Pruett, J. G., Grabiner, F. R., and Brooks, P. R. (1974). J. Chem. Phys. 60, 3335.
- Pruett, J. G., Grabiner, F. R., and Brooks, P. R. (1975). J. Chem. Phys. 63, 1173.
- Ramsey, N. F. (1956). Molecular Beams (Oxford University Press, London).
- Reck, G. P., Mathur, B. P., and Rothe, E. W. (1977). J. Chem. Phys. 66, 3847.
- Riley, C., Gillen, K.T., and Bernstein, R. B. (1967). J. Chem. Phys. 47, 3672.
- Riley, S. J. and Herschbach, D. R. (1973). J. Chem Phys. 58, 27.
- Roberts, R. E. (1976). J. Chem. Phys. 64, 3311.
- Roberts, R. E. and Iasonidou Nelson, C. (1974). Chem. Phys. Letters 25, 278.

- Rommel, M. and Schultz, A. (1977). Ber. Bunsen. Ges. Phys. Chem. 81, 139.
- Ross, J. and Greene, E. F. (1970). Molecular Beams and Reaction Kinetics, Ch. Schlier, Ed. (Academic Press, New York), p. 86.
- Rothe, E. W. and Fenstermaker, R. W. (1971). J. Chem. Phys. 54, 4520.
- Rotzoll, G., Viard, R., and Schugerl, K. (1975). Chem. Phys. Letters 35, 353.
- Rulis, A. M. and Bernstein, R. B. (1972). J. Chem. Phys. 57, 5497.
- Rulis, A. M., Wilcomb, B. E., and Bernstein, R. B. (1974). J. Chem. Phys. 60, 2822.
- Safron, S. A., Weinstein, N. D., Herschbach, D. R., and Tully, J.C. (1972). Chem. Phys. Letters 12, 564.
- Schmidt, W., Siegel, A. and Schultz, A. (1976). Chem. Phys. 16, 161.
- Schultz, A., Cruse, H. W., and Zare, R. N. (1972). J. Chem. Phys. 57, 1354.
- Sholeen, C. M. and Herm, R. R. (1976a). J. Chem. Phys. 64, 5261.
- Sholeen, C. M. and Herm, R. R. (1976b). J. Chem. Phys. 65, 5398.
- Sholeen, C. M., Gundel, L. A., and Herm, R. R. (1976). J. Chem. Phys. 65, 3223.
- Sinha, M. P., Schultz, A., and Zare, R. N. (1973). J. Chem. Phys. 58, 549.
- Siska, P. E. (1973). J. Chem. Phys. 59, 6052.
- Sloane, T. M., Tang, S. Y. and Ross, J. (1972). J. Chem. Phys. 57, 2745.

- Smith, G. P. and Zare, R. N. (1975). J. Amer. Chem. Soc. 97, 1985.
- Smith, G. P. and Zare, R. N. (1976). J. Chem. Phys. 64, 2632.
- Smith, G. P., Whitehead, J. C., and Zare, R. N. (1977). Preprint to be published.
- Steinfeld, J. I. and Kinsey, J. L. (1970). Progress Reaction Kinetics 5, 1.
- Stolte, S., Proctor, A. E., and Bernstein, R. B. (1974). J. Chem. Phys. 61, 3855.
- Stolte, S., Proctor, A. E., and Bernstein, R. B. (1975). J. Chem. Phys. 62, 2506.
- Stolte, S., Proctor, A. E., and Bernstein, R. B. (1976). J. Chem. Phys. 65, 4990.
- Struve, W. S., Krenos, J. R., McFadden, D. L., and Herschbach, D. R. (1975). J. Chem. Phys. 62, 404.
- Taylor, E. H. and Datz, S. (1955). J. Chem. Phys. 23, 1711.
- Toennies, J. P. (1965). Z. Phys. 182, 257.
- Toennies, J. P. (1974). Physical Chemistry, An Advanced Treatise, Kinetics of Gas Reactions, W. Jost, Ed. (Academic Press, New York) 4: Chap. 6.
- Touw, T. R. and Trischka, J. W. (1963). J. Appl. Phys. 34, 3635.
- Truhlar, D. G. (1971). J. Chem. Phys. 54, 2635.
- Tully, F. P., Lee, Y. T., and Berry, R. S. (1971). Chem. Phys. Letters 9, 80.
- van der Meulen, A., Rulis, A. M., and deVries, A. E. (1975). Chem. Phys. 7, 1.

Visser, A. G., Bekooy, J. P., van der Meij, L. K., DeVreugd, C., and Korving, J. (1977). Chem. Phys. 20, 391.

Warnock, T. T. and Bernstein, R. B. (1968). J. Chem. Phys. 49, 1878.

Warnock, T. T., Bernstein, R. B., and Grosser, A. E. (1967). J. Chem. Phys. 46, 1685.

Whitehead, J. C. and Grice, R. (1973). Faraday Disc. Chem. Soc. 55, 320, 374.

Whitehead, J. C., Hardin, D. R., and Grice, R. (1972a) Chem. Phys. Letters 13, 319.

Whitehead, J. C., Hardin, D. R., and Grice, R. (1972b). Mol. Phys. 23, 787.

Whitehead, J. C., Hardin, D. R., and Grice, R. (1973). Mol. Phys. 25, 515.

Wilson, K. R. and Herschbach, D. R. (1968). J. Chem. Phys. 49, 2676.

Wilson, K. R., Kwei, G. H., Norris, J. A., Herm, R. R., Birely, J. H., and Herschbach, D. R. (1964). J. Chem. Phys. 41, 1154.

Zare, R. N. (1974). Ber. Bunsenges. Phys. Chem. 78, 153.

Zare, R. N. and Dagdigian, P. J. (1974). Science 185, 739.



Table I. Abbreviations of Different Experimental Techniques

<u>Abbreviation</u>	<u>Technique</u>
ANGD	product angular distribution without velocity selection of either beam or scattered species
OPANGD	product angular distribution out of reactant beams plane
CEANGD	product angular distribution with collision energy defined via SDVS or nozzle beam
PRVS	product recoil velocity spectra
CEPRVS	product recoil velocity spectra for well-defined collision energy
LECT	laser excitation of some reactant internal state
CHMACT	chemical activation of high product internal excitation
RMAGDF	magnetic deflection of a reactant beam (e.g., to prepare a beam of alkali dimers)
REDORT	orientation of a symmetric top reactant by electric deflection
REDJS	selection of a particular reactant rotational quantum number by electric deflection
ELASOP	optical potential analysis of attenuation of wide angle elastic scattering
PMAGDF	magnetic deflection of a scattered beam (e.g., to confirm differential surface ionization)

PEDTP	electric deflection of a scattered beam in a two-pole field
PEDRF	electric deflection of a scattered beam in a quadrupole refocussing field
PERA	electric resonance analysis of product vibrational distribution
LIF	laser induced fluorescence analysis of product vibrational (and possibly rotational) states.

---

---

Table II. Vibrationally Inelastic Collisions of Alkali Halides.

Collision Partners	Technique	Result	Reference
LiF + Ar, Xe, N <sub>2</sub> , O <sub>2</sub> , NO, CO, HF, HCl CO <sub>2</sub> , H <sub>2</sub> O, NH <sub>3</sub> , ND <sub>3</sub> , CHFCl <sub>2</sub> , SF <sub>6</sub>	PERA	P(E <sub>v</sub> ')	Mariella, et. al. (1974)
KBr + Ne, Ar, N <sub>2</sub> , CO, CO <sub>2</sub>	CHMACT-PRVS	I(⊙,v)	Crim, et. al. (1973)
KBr + H <sub>2</sub> O, NH <sub>3</sub> , CH <sub>3</sub> OH	CHMACT-PRVS	I(⊙,v)	Donohue, et. al. (1973)
KBr + CH <sub>3</sub> OH	CHMACT-PRVS	I(⊙,v)	Donohue, et. al. (1972)
KBr + CH <sub>3</sub> NO <sub>2</sub> , C <sub>2</sub> H <sub>5</sub> OH, (CH <sub>3</sub> ) <sub>2</sub> O, C <sub>3</sub> H <sub>8</sub>	CHMACT-PRVS	I(⊙,v)	Crim, et. al. (1974)
CsF + Ar	CEPRVS	I(⊙,v)	King, et. al. (1973)
CsCl, CsI + Ar, Xe	CEPRVS	I(⊙,v;E)	Armstrong, et. al. (1975) <sup>a</sup>
CsI + Ar	CEPRVS	I(⊙,v;E)	Loesch and Herschbach (1972)
CsI + Ar, Xe	CEPRVS	I(⊙,v;E)	Greene, et. al. (1977)

<sup>a</sup>Armstrong, et. al. (1975) didn't actually study the CsCl + Xe combination. However, this subtle distinction is not made here or in entries in other tables in order to save space.

Table III. Reactive Scattering of Alkali Halides.

Reactants	Technique	Results	Reference
<u>Alkali Halide + Alkali Atom</u>			
LiCl + Ba	ANGD-LIF	$P(E_v'; \odot)$	Dagdikian and Zare (1974)
KF, KBr + Li	ANGD	I( $\odot$ )	Kwei, et. al. (1971)
KF, KCl, KBr, KI, CsF, CsCl CsBr, CsI + Li	ANGD	I( $\odot$ )	Lees and Kwei (1973)
KCl + Rb, RbCl + K	ANGD	I( $\odot$ )	Miller, et. al. (1967)
KCl + Ba	ANGD-LIF	$P(E_v'; \odot)$	Smith and Zare (1976)
RbF, CsF + K	CEANGD	$\sigma(E)$	Stolte, et. al. (1974)
RbF, CsF + K	CEANGD	$\sigma(E)$	Stolte, et. al. (1976)
RbCl + K	ANGD	I( $\odot$ )	Aniansson, et. al. (1974) <sup>a</sup>
RbCl + Cs, CsCl + Rb	ANGD, PRVS	I( $\odot, v$ )	Miller, et. al. (1967)
CsF + K	REDJS-CEANGD	$P(E_p)$	Stolte, et. al. (1975)
TlCl, TlI + Cs	ANGD	I( $\odot$ )	Fisk, et. al. (1967)



Alkali Halide + Alkali Halide

KI + CsCl	PRVS	I(⊕,v)	Miller, et. al. (1967)
KI + CsCl	PRVS	I(⊕,v)	Miller, et. al. (1972)

Alkali Halide + Halogen Molecules

CsBr + ICl	ANGD	I(⊕)	King and Herchbach (1973)
CsI + Cl <sub>2</sub>	PRVS	I(⊕,v)	King and Herschbach (1973)
SrI <sub>2</sub> , BaI <sub>2</sub> + Cl <sub>2</sub> , BaI <sub>2</sub> + HCl	PRVS	I(⊕,v)	Freedman, et. al. (1976)

---

---

<sup>a</sup>Aniansson, et. al. (1974) report the absolute total reaction cross sections.

Table IV. Metal Atoms plus Halogen Molecules.

Reactants	Technique	Result	Reference
<u>Alkali Atoms</u>			
Li + Cl <sub>2</sub> , Br <sub>2</sub> , ICl	ANGD-PMAGDF	I(⊙)	Parrish and Herm (1968)
Li + Cl <sub>2</sub> , Br <sub>2</sub> , ICl	ANGD-PMAGDF	I(⊙)	Parrish and Herm (1969)
Li + Cl <sub>2</sub> , Br <sub>2</sub>	PRVS-PMAGDF	I(⊙,v)	Sholeen, et. al. (1976)
Li + NO <sub>2</sub>	ANGD-PMAGDF	I(⊙)	Parrish and Herm (1971)
Li + NO <sub>2</sub>	PRVS-PMAGDF	(I(⊙,v)	Sholeen and Herm (1976a)
Na + Br <sub>2</sub> , ICl	ANGD	I(⊙)	Birely, et. al. (1969)
Na, Cs + NO <sub>2</sub>	PMAGDF & PEDTP		Herm and Herschbach (1970) <sup>a</sup>
K, Rb, Cs + Cl <sub>2</sub>	ANGD	I(⊙)	Grice and Empedocles (1968)
K + Cl <sub>2</sub> , Br <sub>2</sub> , I <sub>2</sub> , ICl	ELASOP	σ(E)	Greene, et. al. (1969)
K, Cs + Br <sub>2</sub> , I <sub>2</sub> , ICl, IBr	ANGD	I(⊙)	Wilson, et. al. (1964)
K + Br <sub>2</sub> , ICl	PMAGDF		Herm, et. al. (1964) <sup>b</sup>
K + Br <sub>2</sub>	PEDTP	P(E <sub>r</sub> )	Herm and Herschbach (1965)
K + Br <sub>2</sub>	CEPRVS	I(⊙,v;E)	Grosser and Bernstein (1965)
K, Cs + Br <sub>2</sub> , I <sub>2</sub>	CEANGD-ELASOP	I(⊙;E)	Minturn, et. al. (1966)

K + Br <sub>2</sub>	PRVS	I(⊙,v)	Birely and Herschbach (1966)
K + Br <sub>2</sub>	CEPRVS		Warnock, et. al. (1967) <sup>c</sup>
K, Rb, Cs + Br <sub>2</sub> , I <sub>2</sub>	ANGD	I(⊙)	Birely, et. al. (1967)
K, Cs + Br <sub>2</sub>	PEDTP	P(E <sub>r</sub> ')	Maltz and Herschbach (1967)
K + Br <sub>2</sub> , BrCN	CEANGD	I(⊙)	Whitehead, et. al. (1972b)
K, Cs + Br <sub>2</sub>	PEDTP	P(M <sub>J</sub> '/J')	Hsu and Herschbach (1973)
K + Br <sub>2</sub>	CEANGD	I(⊙;E)	van der Meulen, et. al. (1975)
K + I <sub>2</sub>	CEPRVS	I(⊙,v;E)	Gillen, et. al. (1971)
K + I <sub>2</sub> , IBr	CEANGD	I(⊙)	Lin, et. al. (1974b)
K + ICl	ANGD		Moulton and Herschbach (1966) <sup>d</sup>
K,Rb, Cs + ICl, IBr	ANGD	I(⊙)	Kwei and Herschbach (1969)
K, Rb, Cs + BrCN, ICN, NOCl	ANGD	I(⊙)	Grice, et. al. (1968)
Rb + Br <sub>2</sub>	PEDRF	P(E <sub>r</sub> ')	Grice, et. al. (1970)
Rb + Br <sub>2</sub>	PEDRF	P(E <sub>r</sub> ')	Mosch, et. al. (1975)
Rb + IBr	CEANGD	I(⊙,E)	Minturn, et. al. (1966)
Cs + Br <sub>2</sub>	CEANGD	I(⊙,E)	Datz and Minturn (1964)
Cs + Br <sub>2</sub>	PMAGDF		Gordon, et. al. (1968) <sup>b</sup>

Cs + Br <sub>2</sub>	PEDTP	P(M <sub>J</sub> '/J')	Maltz, et. al. (1972)
<u>Alkaline Earth Atoms</u>			
Mg, Ca, Sr, Ba + Cl <sub>2</sub> , Br <sub>2</sub>	ANGD	I(⊕)	Lin, et. al. (1973a)
Mg, Ca, Sr, Ba + ICl	ANGD	I(⊕)	Mims, et. al. (1973) <sup>e</sup>
Ca, Sr, Ba + BrCN	LIF	P(E <sub>v</sub> ')	Pasternack and Dagdigian (1976) <sup>e</sup>
Ca, Sr + NO <sub>2</sub>	ANGD	I(⊕)	Herm, et. al. (1973)
Ba + Cl <sub>2</sub> , NO <sub>2</sub>	ANGD	I(⊕)	Haberman, et. al. (1972)
Ba + BrCN	ANGD	I(⊕)	Mims, et. al. (1973) <sup>e</sup>

<sup>a</sup>Reported a <sup>2</sup>Σ CsO ground state.

<sup>b</sup>Confirmed differential surface ionization results

<sup>c</sup>LAB → CM transformation of K + Br<sub>2</sub> data.

<sup>d</sup>Partial resolution of KI versus KCl product channels

<sup>e</sup>Data on both product channels



AD-A048 230

AEROSPACE CORP EL SEGUNDO CALIF CHEMISTRY AND PHYSICS LAB F/G 20/7  
REACTIVE SINGLE COLLISION STUDIES WITH METAL ATOMS OR METAL HAL--ETC(U)  
NOV 77 R R HERM F04701-77-C-0078

UNCLASSIFIED

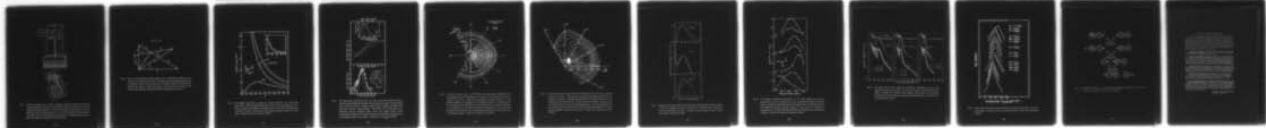
TR-0078(3970-10)-2

SAMSO-TR-77-209

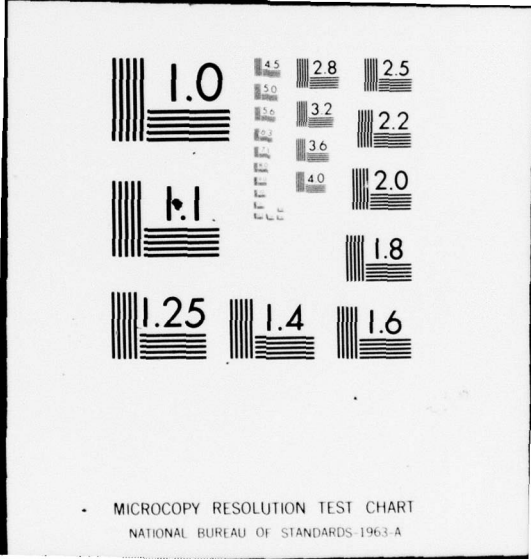
NL

2 of 2

ADA048 230



END  
DATE  
FILMED  
1-78  
DDC



MICROCOPY RESOLUTION TEST CHART  
NATIONAL BUREAU OF STANDARDS-1963-A

Table V. Metal Atoms plus Organic Halides.

Reactants	Technique	Results	Reference
<u>Alkali Atoms</u>			
Li + CH <sub>3</sub> I, CCl <sub>4</sub> , CH <sub>3</sub> NO <sub>2</sub>	ANGD-PMAGDF	I(⊙)	Parrish and Herm (1971)
Li + CH <sub>3</sub> I, CCl <sub>4</sub> , CH <sub>3</sub> NO <sub>2</sub>	PRVS-PMAGDF	I(⊙,v)	Sholeen and Herm (1976b)
Na, K, Cs + CH <sub>3</sub> I, CHCl <sub>3</sub> , CCl <sub>4</sub>	PMAGDF		Gordon, et. al. (1968) <sup>a</sup>
Na + CH <sub>3</sub> I	ANGD	I(⊙)	Birely, et. al. (1969)
Na, K, Cs + CH <sub>3</sub> NO <sub>2</sub> , C <sub>2</sub> H <sub>5</sub> ONO <sub>2</sub> , C <sub>5</sub> H <sub>11</sub> ONO	ANGD, PMAGDF, PEDTP	I(⊙)	Herm and Herschbach (1970)
K + CH <sub>3</sub> I	ANGD	I(⊙)	Herschbach, et. al. (1961)
K, Rb, Cs + CH <sub>3</sub> I	ANGD	I(⊙)	Herschbach (1962)
K + CH <sub>3</sub> I	PMAGDF		Herm, et. al. (1964) <sup>a</sup>
K + CH <sub>3</sub> I	REDORT	P(K/J;⊙)	Brooks and Jones (1966)
K + CH <sub>3</sub> I, CCl <sub>4</sub>	ELASOP	P(b,E)	Airey, et. al. (1967b)
K + CH <sub>3</sub> I, C <sub>2</sub> H <sub>5</sub> I, C <sub>3</sub> H <sub>7</sub> I, (CH <sub>3</sub> ) <sub>2</sub> CHI, C <sub>4</sub> H <sub>9</sub> I, (CH <sub>3</sub> ) <sub>2</sub> CHCH <sub>2</sub> I, (CH <sub>3</sub> )(C <sub>2</sub> H <sub>5</sub> )CHI, (CH <sub>3</sub> ) <sub>3</sub> CI, C <sub>5</sub> H <sub>11</sub> I, C <sub>7</sub> H <sub>15</sub> I	OPANGD	I(⊙,Φ)	Kwei, et. al. (1970)
K, Rb, Cs + CH <sub>3</sub> I, CCl <sub>4</sub>	ELASOP	P(b,E)	Harris and Wilson (1971)

K + CH <sub>3</sub> I	CE-OPANGD	σ(E)	Gersch and Bernstein (1971)
K + CH <sub>3</sub> I, CCl <sub>4</sub>	CEANGD	I(⊙)	Whitehead, et. al. (1972b)
K + CH <sub>3</sub> I	CE-OPANGD	σ(E)	Gersch and Bernstein (1972)
K + CH <sub>3</sub> I	CEPRVS	I(⊙,v;E)	Rulis and Bernstein (1972)
K + CH <sub>3</sub> I	CEPRVS	I(⊙,v;E)	Bernstein and Rulis (1973)
K + CH <sub>3</sub> I, CHCl <sub>3</sub>	REDORT	P(K/J;⊙)	Marcelin and Brooks (1973a)
K + CH <sub>3</sub> I, C <sub>4</sub> H <sub>7</sub> I, CF <sub>3</sub> I, CHCl <sub>3</sub>	REDORT	P(K/J;⊙)	Marcelin and Brooks (1973b)
K + CH <sub>3</sub> I	CEANGD	I(⊙;E)	Rotzoll, et. al. (1975)
K, Rb + (CH <sub>3</sub> I) <sub>n</sub>	ANGD		Gonzalez-Urena and Bernstein (1975)
K, Cs + CH <sub>2</sub> CHI, CH <sub>2</sub> CHCH <sub>2</sub> I, C <sub>6</sub> H <sub>5</sub> I, CH <sub>2</sub> CHCH <sub>2</sub> Br	ANGD	I(⊙)	Entemann and Kwei (1971)
K + CF <sub>3</sub> I	REDORT	P(K/J;⊙)	Brooks (1969)
K + CF <sub>3</sub> I	REDORT	P(K/J;⊙)	Brooks (1973)
K + CF <sub>3</sub> I	CEPRVS	I(⊙,v)	Rulis, et. al. (1974)
K + CH <sub>3</sub> COI, CH <sub>3</sub> Br, CH <sub>3</sub> COBr, CH <sub>3</sub> COCl, CH <sub>3</sub> CN, CH <sub>3</sub> NC, CH <sub>2</sub> CHCH <sub>2</sub> CN, CH <sub>2</sub> CHCH <sub>2</sub> NC, CH <sub>3</sub> COCN	ANGD	I(⊙)	Goldbaum and Martin (1975)
K, Cs + CH <sub>2</sub> I <sub>2</sub> , CH <sub>2</sub> Br <sub>2</sub> , CH <sub>3</sub> CHBr <sub>2</sub> , (CH <sub>3</sub> ) <sub>2</sub> CBr <sub>2</sub> , CH <sub>2</sub> Cl <sub>2</sub>	ANGD	I(⊙)	Entemann (1971)



K + CH <sub>2</sub> I <sub>2</sub> , CHI <sub>3</sub> , CBr <sub>4</sub>	CEANGD	I(⊙)	Lin, et. al. (1974b)
K + CH <sub>3</sub> Br, CBr <sub>4</sub>	ELASOP	P(b,E)	Green, et. al. (1966)
K + (CH <sub>3</sub> ) <sub>3</sub> CBr, C <sub>2</sub> (CN) <sub>4</sub>	ELASOP	P(b,E)	Green, et. al. (1969)
K, Rb, Cs + CBr <sub>4</sub> , CHCl <sub>3</sub> , CCl <sub>4</sub>	ANGD	I(⊙)	Wilson and Herschbach (1968)
K + CCl <sub>4</sub>	ELASOP	P(b,E)	Sloane, et. al. (1972)
Rb + CH <sub>3</sub> I	REDORT	P(K/J;⊙)	Beuhler, et. al. (1966)
Rb + CH <sub>3</sub> I	REDORT	P(K/J;⊙)	Beuhler, et. al. (1968)
Rb + CH <sub>3</sub> I	REDORT	P(K,J;⊙)	Beuhler, et. al. (1969)
Rb + CH <sub>3</sub> I	CE-OPANGD	σ(E)	Litvak, et. al. (1974)
Rb + CH <sub>3</sub> I	CE-ANGD	I(⊙;E)	Gonzalez Urena and Bernstein (1974)
Rb, Cs + CH <sub>3</sub> I, C <sub>2</sub> H <sub>5</sub> I, C <sub>3</sub> H <sub>7</sub> I, (CH <sub>3</sub> ) <sub>2</sub> CHI, C <sub>4</sub> H <sub>9</sub> I, C <sub>5</sub> H <sub>11</sub> I	OPANGD	I(⊙,Φ)	Kinsey, et. al. (1976)
Rb + CH <sub>3</sub> I	CE-OPANGD	σ(E)	Pace, et. al. (1977)
Cs + CH <sub>3</sub> I, CCl <sub>4</sub> , CH <sub>3</sub> NO <sub>2</sub>	PEDTP	P(E <sub>r</sub> ' )	Maltz, and Herschbach (1967)
Cs + CH <sub>3</sub> I, CCl <sub>4</sub>	PEDTP	P(M <sub>J</sub> '/J')	Maltz, et. al. (1972)
Cs + CH <sub>3</sub> I, CF <sub>3</sub> I, CCl <sub>4</sub>	PEDTP	P(M <sub>J</sub> '/J')	Hsu and Herschbach (1973)
Cs + CH <sub>3</sub> I	PEDTP	P(M <sub>J</sub> '/J';⊙)	Hsu, et. al. (1974)

Cs + CCl<sub>4</sub>

CE

Bull and Moon (1954)<sup>b</sup>

Alkaline Earth Atoms

Ca, Sr, Ba + CH<sub>3</sub>I, CF<sub>3</sub>I, CH<sub>2</sub>I<sub>2</sub>, CCl<sub>4</sub>

ANGD

I(⊙)

Lin, et. al. (1973b)

Ca, Sr, Ba + CCl<sub>3</sub>NO<sub>2</sub>, (CH<sub>3</sub>)<sub>2</sub>CHNO<sub>2</sub>

ANGD

I(⊙)

Herm, et. al. (1973)

Ba + CH<sub>3</sub>I, CH<sub>2</sub>I<sub>2</sub>

LIF

P(E<sub>v</sub>')

Dagdigian, et. al. (1976)

Ba + CF<sub>3</sub>I

ANGD-LIF

P(E<sub>v</sub>';⊙)

Smith, et. al. (1977)

Ba + CH<sub>3</sub>Br, CH<sub>2</sub>Br<sub>2</sub>, CHBr<sub>3</sub>, CBr<sub>4</sub>

LIF

P(E<sub>v</sub>')

Rommel and Schultz (1977)

Ba + CCl<sub>4</sub>

LIF

P(E<sub>v</sub>')

Schmidt, et. al. (1976)

<sup>a</sup>Confirmed differential surface ionization results.

<sup>b</sup>First observation of a reactive scattering signal.

Table VI. Metal Atoms plus Inorganic Polyhalides

Reactants	Technique	Results	Reference
<u>Alkali Atoms</u>			
Li + PCl <sub>3</sub> , SnCl <sub>4</sub>	ANGD-PMAGDF	I(⊙)	Parrish and Herm (1968)
Li + PCl <sub>3</sub> , SnCl <sub>4</sub>	ANGD-PMAGDF	I(⊙)	Parrish and Herm (1969)
Li + PCl <sub>3</sub> , SnCl <sub>4</sub> , SF <sub>6</sub>	PRVS-PMAGDF	I(⊙,v)	Behrens, et. al. (1976b)
Li + SF <sub>6</sub>	ANGD-PMAGDF	I(⊙)	Parrish and Herm (1971)
Li + SF <sub>6</sub>	PERA	P(E <sub>v</sub> ')	Mariella, et. al. (1973) <sup>a</sup>
K, Rb, Cs + SCl <sub>2</sub>	ANGD	I(⊙)	Grice, et. al. (1968)
K + SCl <sub>2</sub>	ANGD	I(⊙)	Goldbaum and Martin (1975)
K + ZnCl <sub>2</sub> , ZnI <sub>2</sub> , CdI <sub>2</sub> , HgBr <sub>2</sub> , HgI <sub>2</sub>	PRVS	I(⊙,v)	Bullitt, et. al. (1974)
K + HgCl <sub>2</sub> , HgBr <sub>2</sub> , HgI <sub>2</sub>	CEANGD	I(⊙)	Hardin, et. al. (1973b)
K + PCl <sub>3</sub> , SnCl <sub>4</sub>	CEANGD	I(⊙)	Whitehead, et. al. (1972b)
K + SiCl <sub>4</sub> , SnCl <sub>4</sub> , SF <sub>6</sub>	ELASOP	P(b,E)	Airey, et. al. (1967b)
K, Rb, Cs + SnCl <sub>4</sub>	ELASOP		Harris and Wilson (1971)
K + SnCl <sub>4</sub> , SF <sub>6</sub>	ELASOP	P(b,E)	Sloane, et. al. (1972) <sup>a</sup>

K, Rb, Cs + SnCl <sub>4</sub> , SF <sub>6</sub>	PRVS	I(⊙,v)	Riley and Herschbach (1973)
K, Cs + SeF <sub>6</sub> , TeF <sub>6</sub> , MoF <sub>6</sub> , WF <sub>6</sub> , UF <sub>6</sub>	ANGD	I(⊙)	Annis and Datz (1977)
Rb, Cs + PCl <sub>3</sub> , PBr <sub>3</sub> , SnCl <sub>4</sub>	ANGD	I(⊙)	Wilson and Herschbach (1968)
Cs + SnCl <sub>4</sub>	PMAGDF		Gordon, et. al. (1968) <sup>b</sup>
Cs + SF <sub>4</sub> , SF <sub>6</sub>	PERA	P(E <sub>v</sub> ')	Bennewitz, et. al. (1971) <sup>a</sup>
Cs + SF <sub>4</sub> , SF <sub>6</sub>	PEDTP	P(M' <sub>J</sub> /J')	Hsu and Herschbach (1973)
Cs + SF <sub>6</sub>	PERA	P(E <sub>v</sub> ')	Freund, et. al. (1971) <sup>a</sup>

Alkaline Earth Atoms

Sr, Ba + PCl <sub>3</sub> , SF <sub>6</sub>	ANGD	I(⊙)	Herm, et. al. (1973)
---	------	------	----------------------

---

<sup>a</sup>Varied the beam temperature to gain information on the importance of reactant internal energy.

<sup>b</sup>Confirmed differential surface ionization results.



Table VII. Metal atoms plus Hydrogen Halides.

Reactants	Technique	Results	Reference
<u>Alkali Atoms</u>			
K + HCl, HI	ELASOP	P(b,E)	Ackerman, et. al. (1964)
K + HCl	ANGD	$\sigma(E)$	Odiorne and Brooks (1969)
K + HCl	LECT-ANGD	$P(E_{\nu})$	Odiorne, et. al. (1971)
K + HCl	CEANGD	$\sigma(E)$	Pruett, et. al. (1974) Pruett, et. al. (1975)
K + HBr	ANGD		Taylor and Datz (1955)
K + HBr	CEANGD		Greene, et. al. (1960) Herschbach (1960)
K + HBr	CEANGD-ELASOP	P(b,E)	Beck, et. al. (1962)
K + HBr	CEPRVS	$I(\Theta, \nu; E)$	Grosser, et. al. (1965)
K + HBr, DBr	ELASOP	P(b,E)	Airey, et. al. (1967a)
K + HBr, DBr	CEPRVS	$I(\Theta, \nu)$	Riley, et. al. (1967)
K, Cs + TBr	ANGD	$I(\Theta)$	Martin and Kinsey (1967) <sup>a</sup>
K, Cs + HBr	PEDTP	$P(E_r')$	Maltz and Herschbach (1967)
K + HBr, DBr	CEPRVS	$I(\Theta, \nu)$	Gillen, et. al. (1969)

K, Cs + HBr, HI	PEDTP	$P(M_J'/J')$ Maltz, et. al. (1972)
K, Cs + HBr, HI	PEDTP	$P(M_J'/J')$ Hsu and Herschbach (1973)
K, Cs + HBr, HI	PEDTP	$P(M_J'/J')$ Hus, et. al. (1975)
Rb + HBr	PEDRF	$P(E_r')$ Mosch, et. al. (1974)
Cs + HBr	PEDTP	$P(E_r')$ Herm and Herschbach (1965)
Cs + HBr	ELASOP	$P(b,E)$ Greene, et. al. (1969)

Alkaline Earth Atoms

Ca, Sr, Ba + HI	ANGD	$\sigma(E)$ Mims, et. al. (1972)
Ba + HF, HCl, HBr, HI	LIF	$P(E_v')$ Cruse, et. al. (1973)
Ba + HF	LECT-LIF	$P(E_v'; E_v')$ Pruett and Zare (1976)

<sup>a</sup>Angular distribution of the T product from M + TBr

Table VIII. Alkali Dimers plus various Halides.<sup>a</sup>

Reactants	Technique	Results	Reference
<u>Halogen Atoms</u>			
$K_2 + Cl, Br$	RMAGDF-ANGD	I(⊙)	Struve, et. al. (1975) <sup>b</sup>
<u>Halogen Molecules</u>			
$K_2 + Cl_2, Br_2$	RMAGDF-ANGD	I(⊙)	Struve, et. al. (1975) <sup>b</sup>
$K_2 + Br_2, ICl, IBr, BrCN$	RMAGD-ANGD	I(⊙)	Foreman, et. al. (1972b)
$K_2 + Br_2, BrCN$	RMAGDF-ANGD	I(⊙)	Whitehead, et. al. (1972a) <sup>c</sup>
$K_2 + Br_2, IBr, BrCN$	RMAGDF-ANGD	I(⊙)	Whitehead, et. al. (1973) <sup>c</sup>
$K_2 + I_2$	RMAGDF-ANGD	I(⊙)	Lin, et. al. (1974a) <sup>c</sup>
<u>Organic Halides</u>			
$K_2 + CH_3I, C_2H_5I, C_3H_5I,$ $C_2H_5Br$	RMAGDF-ANGD	I(⊙)	Foreman, et. al. (1973b)
$K_2 + CH_2Br_2, CCl_4$	RMAGDF-ANGD	I(⊙)	Foreman, et. al. (1973a)
$K_2 + CBr_4, CH_2I_2, CHI_3$	RMAGDF-ANGD	I(⊙)	Lin, et. al. (1974a)

Inorganic Halides

$K_2 + HgCl_2, HgBr_2, HgI_2$	RMAGDF-ANGD	I(⊙)	Hardin, et. al. (1973a)
$K_2 + BBr_3, PCl_3, PBr_3, SiCl_4,$ $SnCl_4$	RMAGDF-ANGD	I(⊙)	Foreman, et. al. (1973a)
$K_2 + SnCl_4$	RMAGDF-ANGD	I(⊙)	Whithead, et. al. (1973)

---

<sup>a</sup>All of these experiments employ a nozzle expansion to enhance dimer formation. This also produces improved collision energy definition relative to two crossed thermal beams.

<sup>b</sup>Chemiluminescence also studied.

<sup>c</sup>Approximate K product angular distribution reported.



Table IX. Non-alkali Metals plus various Oxides.

Reactants	Technique	Results	Reference
Sr + O <sub>2</sub>	CEANGD	$\sigma(E)$	Batalli-Cosmovici and Michel (1972)
Ba + O <sub>2</sub>	ANGD	I(⊙)	Batalli-Cosmovici and Michel (1971)
Ba + O <sub>2</sub>	LIF	P(E <sub>v</sub> ', E <sub>r</sub> ')	Schultz, et. al. (1972)
Ba + O <sub>2</sub> , CO <sub>2</sub>	LIF	P(E <sub>v</sub> ', E <sub>r</sub> ')	Dagdikian, et. al. (1974)
Ba + SO <sub>2</sub>	LIF	P(E <sub>v</sub> ', E <sub>r</sub> ')	Smith and Zare (1975)
Ba + SO <sub>2</sub>	CEANGD	I(⊙)	Behrens, et. al. (1976a)
Al + O <sub>2</sub> , O <sub>3</sub>	LIF	P(E <sub>v</sub> ', E <sub>r</sub> ')	Zare (1974)
Al + O <sub>2</sub>	LIF	P(E <sub>v</sub> ', E <sub>r</sub> ')	Dagdikian, et. al. (1975)
Eu + O <sub>2</sub>	CEANGD	$\sigma(E)$	Dirscherl and Michel (1976)
Yb + O <sub>2</sub>	CEANGD	$\sigma(E)$	Cosmovici, et. al. (1977)

Table X. Miscellaneous Alkali Dimer Reactions.

Reactants	Techniques	Results	Reference
<u>Hydrogen Atom Reactant</u>			
$K_2, Rb_2, Cs_2 + H, D$	ANGD	I(⊙)	Lee, et. al. (1971)
<u>Alkali Atom Reactant</u>			
$K_2, Rb_2, Cs_2 + Na$ $Rb_2 + K$	ANGD	I(⊙)	Whitehead and Grice (1973)
$Rb_2 + Na$	PRVS	I(⊙,v)	Mascord, et. al. (1976)

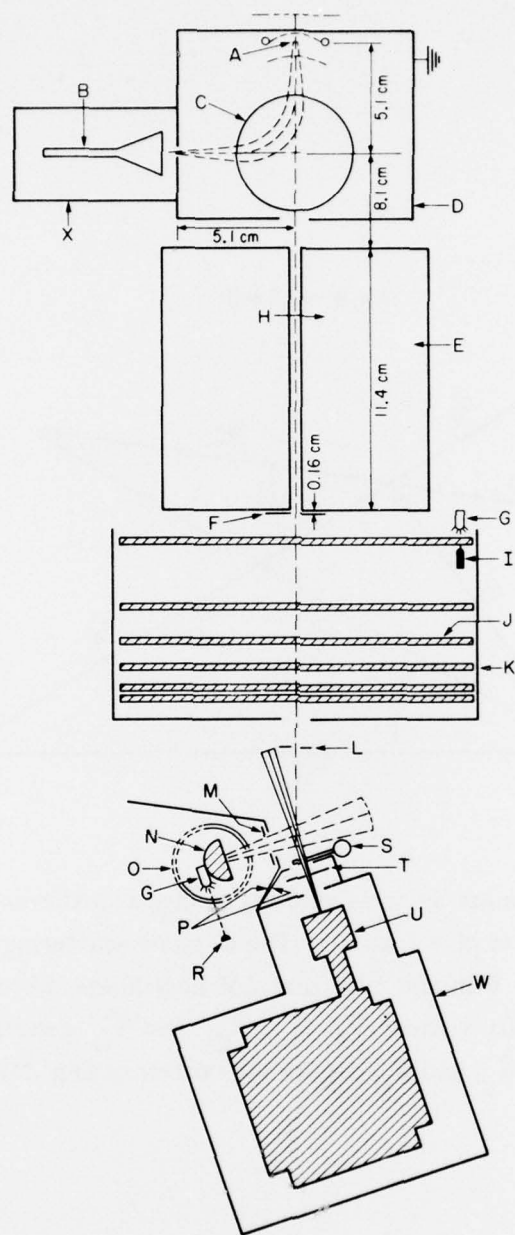


Fig. 1. Schematic diagram of a product magnetic deflection slotted disk velocity analysis apparatus (viewed from above) used to study reactions of Li atoms with halogen-containing compounds. Items not identified in text include: Li (U) and halide (N) sources, collimating slits (T, M, L, and F), shields (W, P, K, D, and X), and a light cell (G) and photodiode (I) to monitor the rotational frequency of the SDVA (J). [Taken from Sholeen and Herm (1976a)].

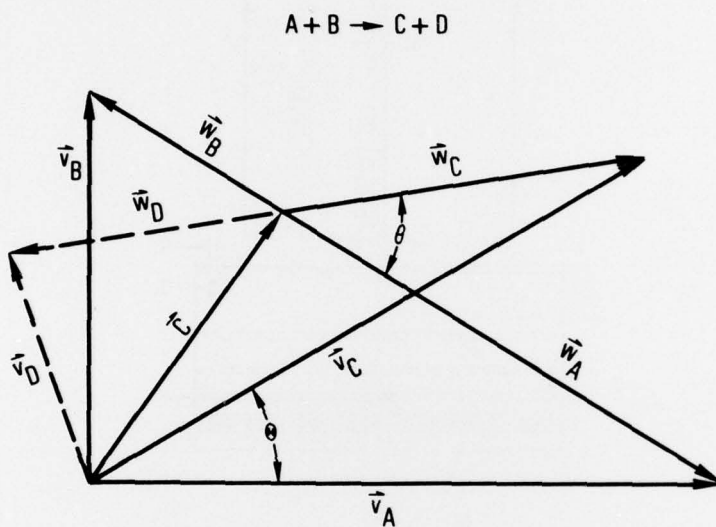


Fig. 2. LAB  $\leftrightarrow$  CM coordinate systems velocity vector transformation diagram for the collision of A and B to give C and D. The in-plane scattering angles of particle C are denoted  $\Theta$  and  $\theta$  in the LAB and CM coordinate systems, respectively;  $\vec{C}$  denotes the centroid vector;  $\vec{v}_A$ ,  $\vec{v}_B$ ,  $\vec{v}_C$ , and  $\vec{v}_D$  denote the particle LAB velocities;  $\vec{w}_A$ ,  $\vec{w}_B$ ,  $\vec{w}_C$ , and  $\vec{w}_D$  denote the corresponding CM velocities.



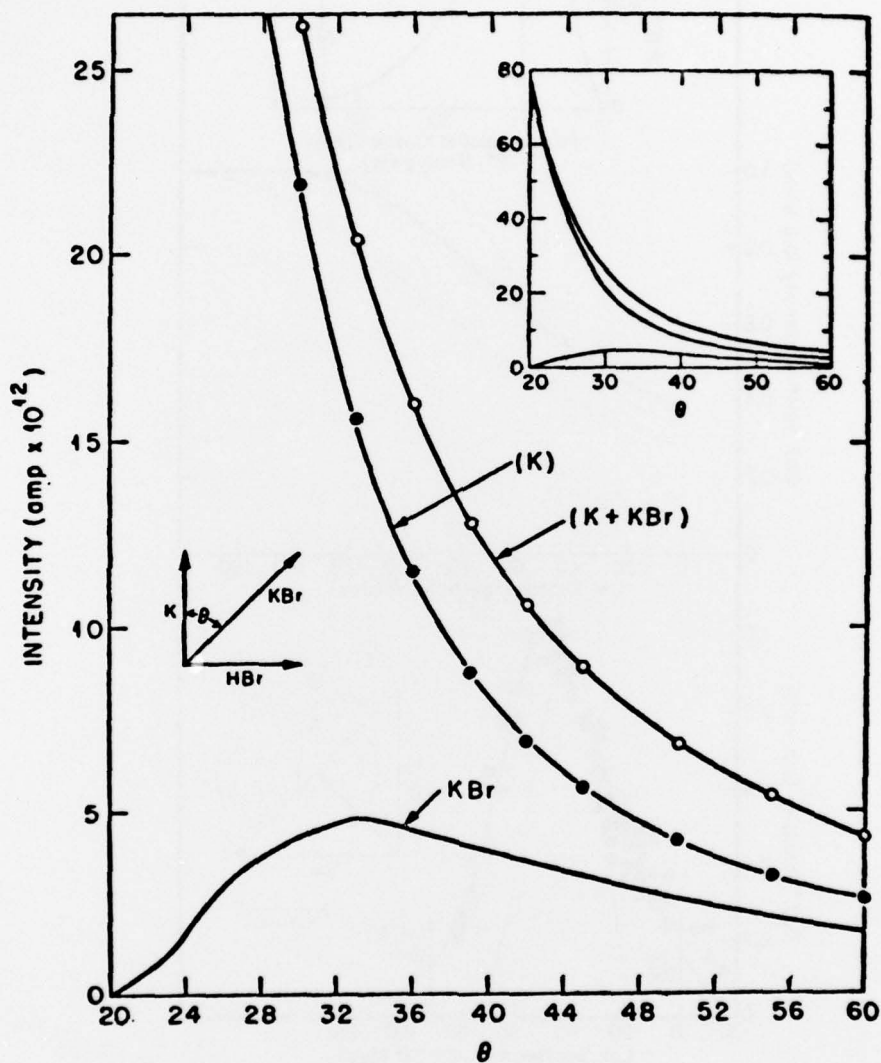


Fig. 3. LAB angular distributions measured by surface ionization with a sensitized filament (K + KBr) and desensitized filament (K) for the scattering of K from HBr. The product KBr angular distribution shown was obtained as the difference of these two curves. Note that the LAB scattering angle is denoted  $\theta$  in this figure. [Taken from Taylor and Datz (1955)].

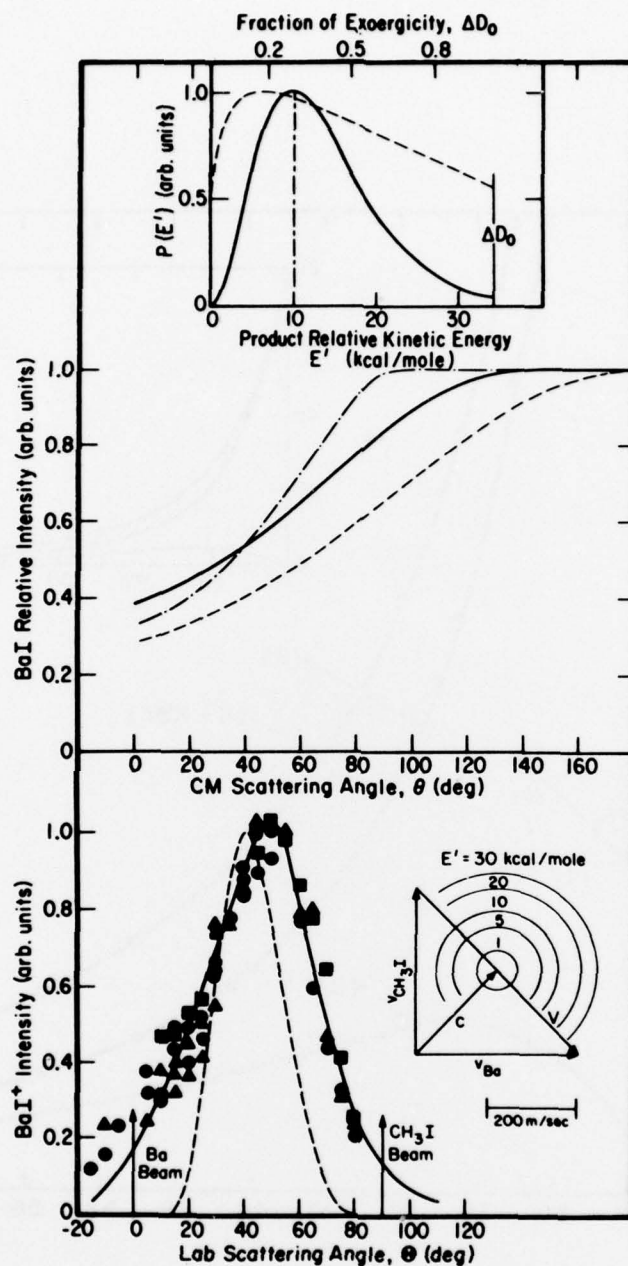


Fig. 4. The upper panel shows three sets (i.e., dash, solid, and dot-dash curves) of collision-energy-independent product recoil angle and energy CM distributions which fit (solid curve) the measured LAB BaI product angular distribution data points from the Ba + CH<sub>3</sub>I reaction. Also shown in the lower panel are a calculated centroid distribution (dash curve) and nominal velocity vector transformation diagram which depicts circles of constant BaI recoil velocity for some possible product recoil energies. [Taken from Lin, *et al.* (1973b)].

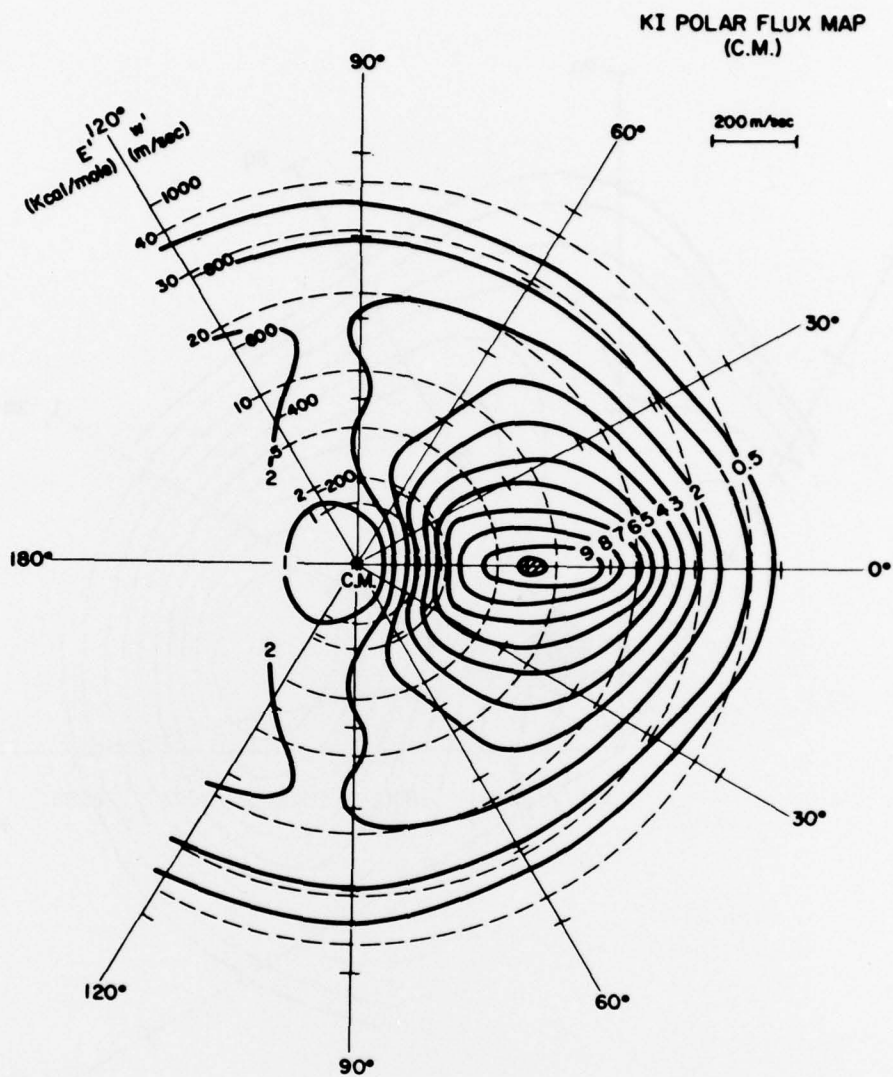


Fig. 5. CM polar contour map of  $\partial^3 \sigma / \partial^2 \omega \partial w$  (assumed energy independent) for scattering for KI from crossed beams of K and  $I_2$ . Heavy lines show contours of constant  $\partial^3 \sigma / \partial^2 \omega \partial w$  arbitrarily normalized to a peak value of 10. CM scattering angle,  $\theta$ , is measured from the original K direction. Symmetry about  $\theta = 0^\circ$  is forced in the data analysis, i.e. the bottom half of the map is redundant. A cut along any  $\theta = \text{constant}$  line gives the distribution in KI recoil speed (denoted  $w'$  in this figure). The corresponding distribution in  $E'$  would require use of the proper Jacobian. [Taken from Gillen, et. al. (1971)].

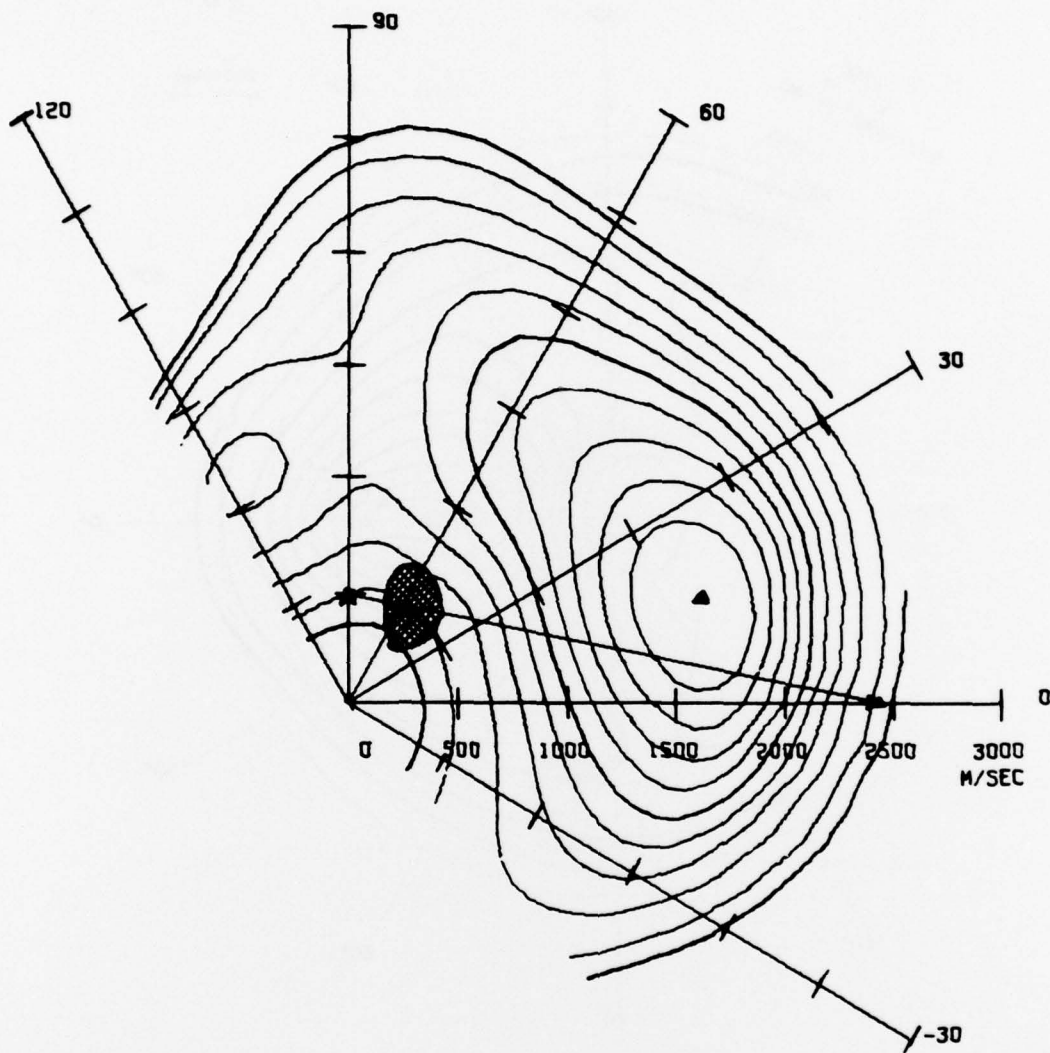


Fig. 6. Contours show plots of constant LiO ( $X^2\Pi$ ) product flux in the LAB coordinate system from the  $\text{Li} + \text{NO}_2$  reaction (LAB scattering angle measured from the original Li direction). The black triangle denotes on arbitrary intensity of 100, and 90, 80, 70, 60, 50, 40, 30, 20, 10, and 5 contours are shown. Fifty percent of the centroid vectors lie within the cross hatched area. This centroid distribution was calculated from the broad "quasi-thermal" beam speed distributions for an energy independent reaction cross section. [Taken from Sholeen and Herm (1976a)].



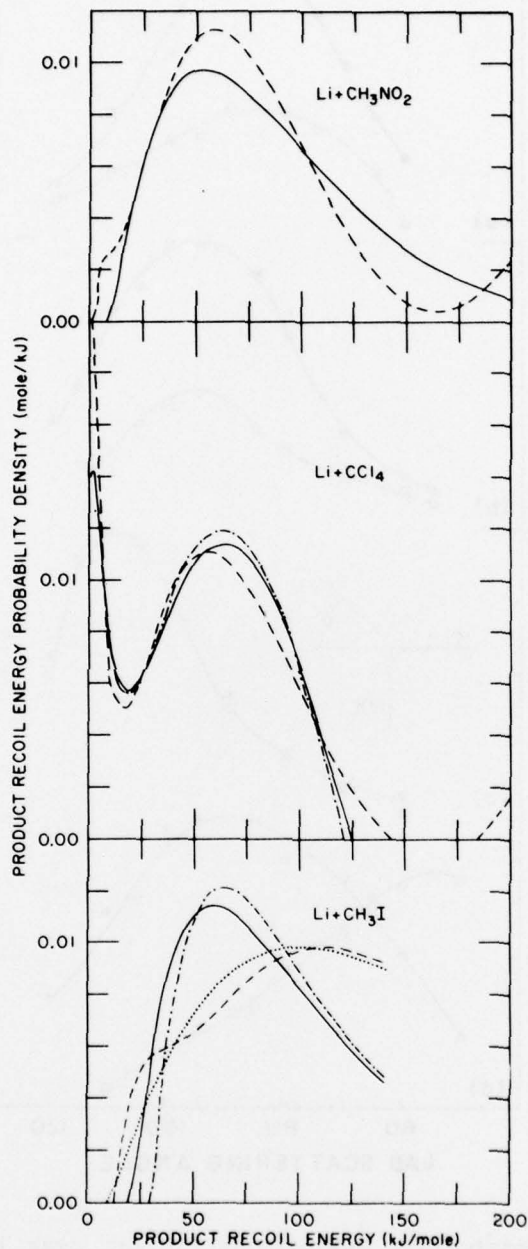


Fig. 7. Different curves show  $P(E')$  functions [from Eq. (9)] obtained by fitting different  $\partial^3 \sigma / \partial^2 \omega \partial w$  expansion functions via Eq. (5) to LiX product LAB recoil velocity spectra measurements for the Li + CH<sub>3</sub>NO<sub>2</sub>, CCl<sub>4</sub>, and CH<sub>3</sub>I reactions. [Taken from Sholeen and Herm (1976b)].

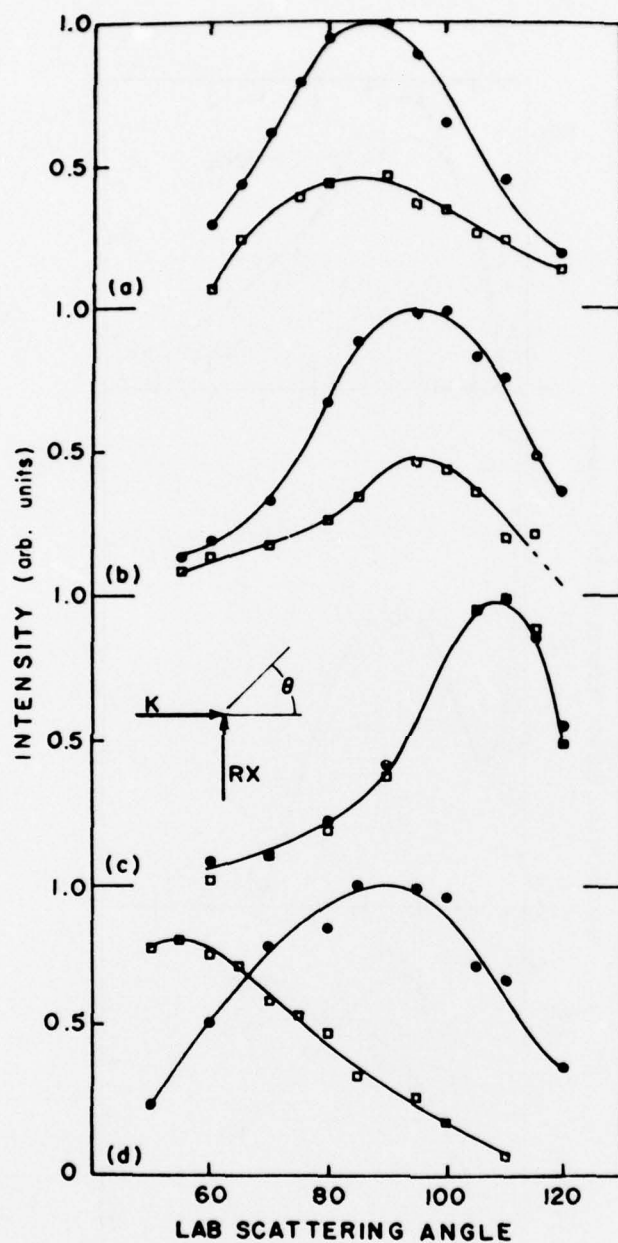


Fig. 8. LAB angular distributions (normalized to unit peak heights) of reactively scattered KI or KCl for reactions of K with orientated (a)  $\text{CH}_3\text{I}$ , (b)  $t\text{-BuI}$ , (c)  $\text{CHCl}_3$ , and (d)  $\text{CF}_3\text{I}$ . Darkened and open data points refer to orientation wherein the transferred halogen pointed toward or away from the incoming K, respectively. In all cases, intermediate behavior was observed with unorientated molecules. [Taken from Marcelin and Brooks (1973b)].

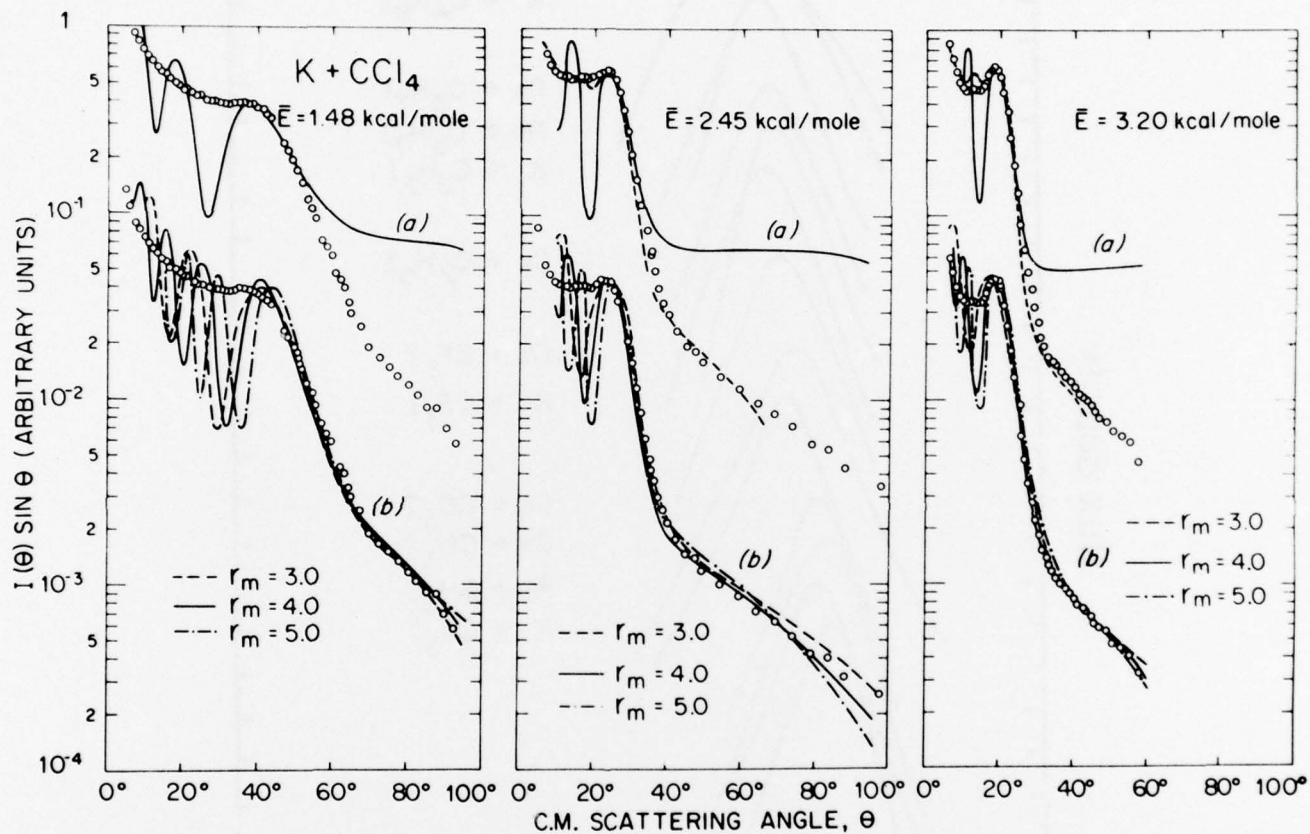


Fig. 9. The open circles show measured non-reactive scattering of K for  $\text{CCl}_4$  transformed into the CM system. The curves in (a) show optical model fits for  $p(b,E) = 0$  (solid) and its optimal values (dashed). Optical model fits in (b) show the insensitivity of the data to the potential range parameter,  $r_m$ . [Taken from Harris and Wilson (1971)].

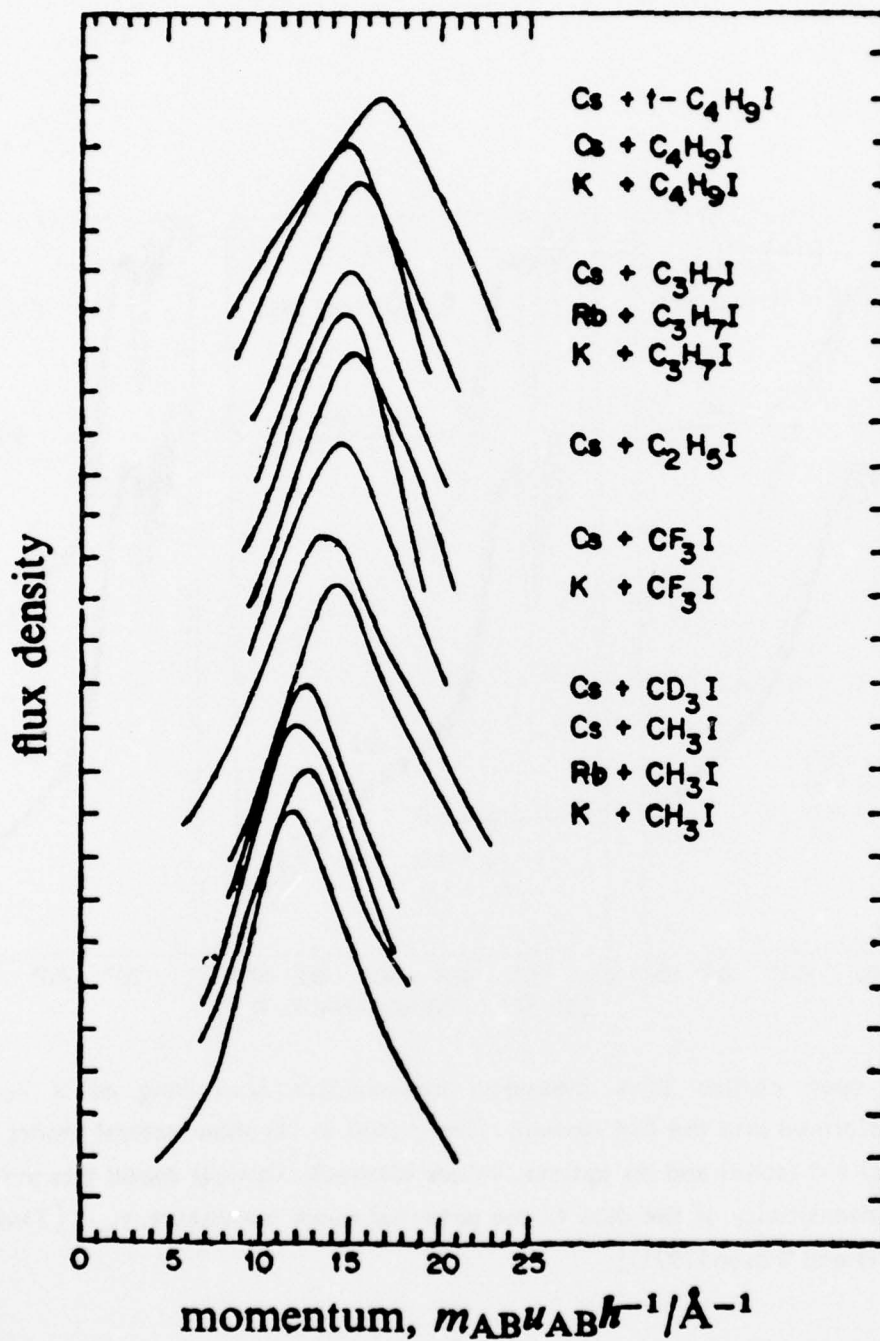


Fig.10. Alkali iodide CM product recoil momentum distributions normalized to the same peak heights. Successive curves are displaced upward. [Taken from Herschbach (1973)].



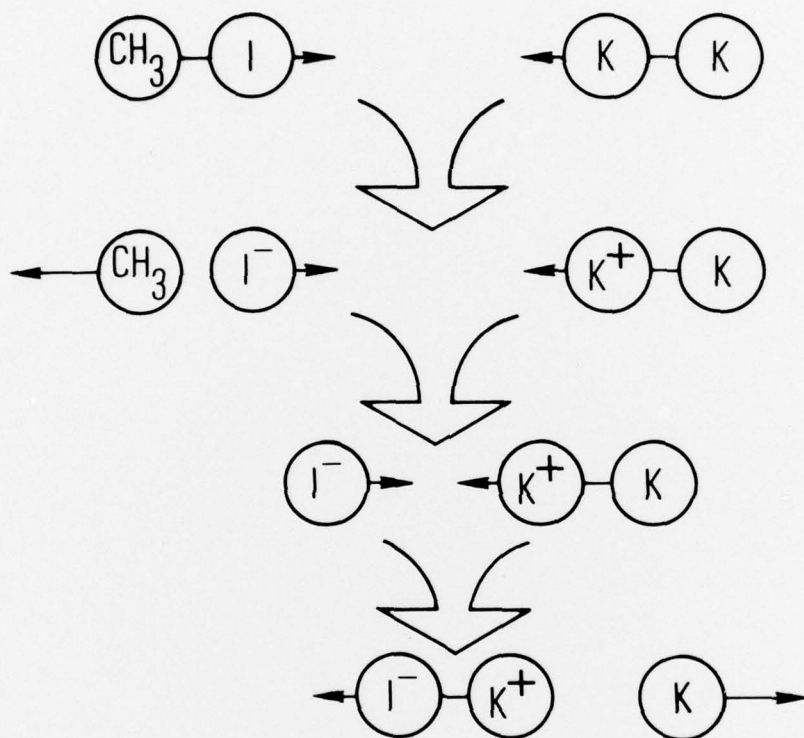


Fig.11. Schematic depiction of a possible "double rebound" mechanism to account for forward KI scattering in the  $K_2 + CH_3I$  reaction.

## THE IVAN A. GETTING LABORATORIES

The Laboratory Operations of The Aerospace Corporation is conducting experimental and theoretical investigations necessary for the evaluation and application of scientific advances to new military concepts and systems. Versatility and flexibility have been developed to a high degree by the laboratory personnel in dealing with the many problems encountered in the nation's rapidly developing space and missile systems. Expertise in the latest scientific developments is vital to the accomplishment of tasks related to these problems. The laboratories that contribute to this research are:

Aerophysics Laboratory: Launch and reentry aerodynamics, heat transfer, reentry physics, chemical kinetics, structural mechanics, flight dynamics, atmospheric pollution, and high-power gas lasers.

Chemistry and Physics Laboratory: Atmospheric reactions and atmospheric optics, chemical reactions in polluted atmospheres, chemical reactions of excited species in rocket plumes, chemical thermodynamics, plasma and laser-induced reactions, laser chemistry, propulsion chemistry, space vacuum and radiation effects on materials, lubrication and surface phenomena, photosensitive materials and sensors, high precision laser ranging, and the application of physics and chemistry to problems of law enforcement and biomedicine.

Electronics Research Laboratory: Electromagnetic theory, devices, and propagation phenomena, including plasma electromagnetics; quantum electronics, lasers, and electro-optics; communication sciences, applied electronics, semi-conducting, superconducting, and crystal device physics, optical and acoustical imaging; atmospheric pollution; millimeter wave and far-infrared technology.

Materials Sciences Laboratory: Development of new materials; metal matrix composites and new forms of carbon; test and evaluation of graphite and ceramics in reentry; spacecraft materials and electronic components in nuclear weapons environment; application of fracture mechanics to stress corrosion and fatigue-induced fractures in structural metals.

Space Sciences Laboratory: Atmospheric and ionospheric physics, radiation from the atmosphere, density and composition of the atmosphere, aurorae and airglow; magnetospheric physics, cosmic rays, generation and propagation of plasma waves in the magnetosphere; solar physics, studies of solar magnetic fields; space astronomy, x-ray astronomy; the effects of nuclear explosions, magnetic storms, and solar activity on the earth's atmosphere, ionosphere, and magnetosphere; the effects of optical, electromagnetic, and particulate radiations in space on space systems.

THE AEROSPACE CORPORATION  
El Segundo, California